

GROWTH OF FACE-HOMOGENEOUS TESSELLATIONS

STEPHEN J. GRAVES AND MARK E. WATKINS

ABSTRACT. A tessellation of the plane is *face-homogeneous* if for some integer $k \geq 3$ there exists a cyclic sequence $\sigma = [p_0, p_1, \dots, p_{k-1}]$ of integers ≥ 3 such that, for every face f of the tessellation, the valences of the vertices incident with f are given by the terms of σ in either clockwise or counter-clockwise order. When a given cyclic sequence σ is realizable in this way, it may determine a unique tessellation (up to isomorphism), in which case σ is called *monomorphic*, or it may be the valence sequence of two or more non-isomorphic tessellations (*polymorphic*). A tessellation whose faces are uniformly bounded in the hyperbolic plane but not uniformly bounded in the Euclidean plane is called a *hyperbolic tessellation*. Such tessellations are well-known to have exponential growth. We seek the face-homogeneous hyperbolic tessellation(s) of slowest growth and show that the least growth rate of such monomorphic tessellations is the “golden mean,” $\gamma = (1 + \sqrt{5})/2$, attained by the sequences $[4, 6, 14]$ and $[3, 4, 7, 4]$. A polymorphic sequence may yield non-isomorphic tessellations with different growth rates. However, all such tessellations found thus far grow at rates greater than γ .

0. INTRODUCTION

It has long been known that there are finitely many homogeneous tessellations of the Euclidean plane; they all have quadratic growth. However, in the hyperbolic plane, for various definitions of “homogeneity,” infinitely many homogeneous tessellations are realizable, and their growth, if not quadratic, is always exponential. Presently we will give a rigorous definition of growth rate, but for now one should think of this parameter intuitively as the asymptotic rate at which additional tiles (or faces) accrue with respect to some chosen center of a tessellation. In this schema, all Euclidean tessellations have growth rate equal to 1, and hyperbolic tessellations have growth rate strictly greater than 1. The first author has shown by construction in [5] that, given any $\epsilon > 0$, there exists a tessellation of the hyperbolic plane with growth rate exactly $1 + \epsilon$. In general, these latter tessellations have few if any combinatorial or geometric symmetries. The question then becomes one of determining the growth rates of hyperbolic tessellations when some sort of homogeneity is imposed. In particular, subject to a homogeneity constraint, how small can the gap be between quadratic and exponential growth?

Date: 29 June 2017.

2010 *Mathematics Subject Classification.* Primary 05B45, 05C63; Secondary 05C10, 05C12.

Key words and phrases. face-homogeneous, tessellation, growth rate, valence sequence, exponential growth, transition matrix, Bilinski diagram, hyperbolic plane.

Much of the material in this work comes from the doctoral dissertation [4] of the first author written under the supervision of the second author.

The second author was partially supported by a grant from the Simons Foundation (#209803 to Mark E. Watkins).

In a seminal work [8], Grünbaum and Shephard defined a graph to be *edge-homogeneous with edge-symbol* $\langle p, q; k, \ell \rangle$ if every edge is incident with vertices of valence p and q and faces of covalence k and ℓ . They proved that the parameters of an edge-symbol uniquely determine an edge-homogeneous tessellation up to isomorphism.

The notion of homogeneity was extended by Moran [10]. She defined a tessellation to be *face-homogeneous with valence sequence* $[p_0, \dots, p_{k-1}]$ if every face is a k -gon incident with vertices of valences p_0, \dots, p_{k-1} in either clockwise or counterclockwise consecutive order. Unfortunately, no uniqueness property analogous to the Grünbaum-Shephard result holds in general for face-homogeneous tessellations.

Moran's work on growth rates of face-homogeneous tessellations led the authors (together with T. Pisanski) to return to edge-homogeneous tessellations and conclusively determine their growth rates. In [6] they determined the growth rate of any edge-homogeneous tessellation as a function of its edge-symbol and proved that the least growth rate for an exponentially-growing, edge-homogeneous tessellation is $\frac{1}{2}(3 + \sqrt{5}) \approx 2.618$.

The goal of this article is to obtain an analogous result for face-homogeneous tessellations. Our main result is that if a face-homogeneous tessellation with exponential growth is determined up to isomorphism by its valence sequence, then its growth rate is at least $\frac{1}{2}(1 + \sqrt{5})$, namely the “golden mean.” Moreover, we determine exactly the valence sequences for which this golden mean is realized. A significant by-product of our investigation is an abundance of machinery for computing the growth rates of many classes of face-homogeneous planar tessellations.

Section 1 consists of six sections. Following some general definitions concerning infinite graphs in the plane, we present (**Section 1.2**) a system for labeling sets of vertices and sets of faces of a tessellation; such a labeling is called a “Bilinski diagram.” **Section 1.3** presents the notion of face-homogeneity and associated notation. Polynomial and exponential growth, defined on the one hand with respect to the standard graph-theoretic metric, and on the other hand with respect to the notion of angle excess, appear in **Section 1.4**. **Section 1.5** presents a rigorous theoretical treatment of growth rate with respect to regional distance in a Bilinski diagram. **Section 1.6** concludes the Preliminaries with a review of the completely resolved case of edge-homogeneous tessellations, summarizing results from [8] and [6].

In **Section 2.1** we lay out our method for filling in the formulas obtained in **Section 1.5** while introducing the notion of a transition matrix. Analogous to a Markov process, this matrix encodes for given $n \geq 1$ how many faces of each possible configuration are “begotten” at regional distance $n + 1$ from the root of a Bilinski diagram by a face at regional distance n from the root. The maximum modulus of the eigenvalues of the transition matrix are key to the growth rate of T .

Section 2.2 applies the machinery of **Section 2.1** to the significant class of valence sequences that are *monomorphic*, i.e., that are uniquely realizable as a face-homogeneous tessellation and whose Bilinski diagrams are in a certain sense well-behaved, called *uniformly concentric*. It is shown in **Theorem 2.7** that for such valence sequences, the partial order defined in **Section 1.3** is preserved by their growth rates. The six classes of monomorphic sequences of lengths 3, 4, and 5 whose Bilinski diagrams are not uniformly concentric are identified in **Section 2.3**, where it is proved that they are indeed monomorphic. The exhaustive proof that this list

is complete is contained in the Appendix [7]. Finally, we present in Section 2.4 the main result of the paper, that the least growth rate of a face-homogeneous tessellation with monomorphic valence sequence is the golden mean $\frac{1}{2}(1 + \sqrt{5})$.

Those valence sequences (described as *polymorphic*) which admit multiple non-isomorphic tessellations are alive and well in Section 3.1. A general sufficient condition for polymorphism is given. The difficulties posed by polymorphism are illustrated by an example; the polymorphic sequence [4, 4, 6, 8] is considered in some depth in Section 3.2. In particular, we see by this example that two different tessellations having the same (polymorphic) valence sequence may well have different growth rates. We conclude the chapter with some conjectures in Section 3.3.

The appendix [7] alluded to above is to be found with this article on the arXiv. All references therein are to results in the present paper.

1. PRELIMINARIES

1.1. Tessellations. For a graph Γ , the symbol $V(\Gamma)$ denotes the vertex set of Γ . If M is a planar embedding of Γ , we call M a *plane map* and denote by $F(M)$ the set of faces of M .

A graph Γ is *infinite* if its vertex set $V(\Gamma)$ is infinite; Γ is *locally finite* if every vertex has finite valence. A graph is *3-connected* if there is no set of fewer than three vertices whose removal disconnects the graph. It is well known that if the underlying graph Γ of a plane map M is 3-connected (as is generally the case in this work), then every automorphism of Γ induces a permutation of $F(M)$ that preserves face-vertex incidence and can be extended to a homeomorphism of the plane. Thus we tend to abuse language and speak of “the faces of Γ .” When a plane map is 3-connected, every edge is incident with exactly two distinct faces. In this case, the number of edges (and hence of vertices) incident with a given face is its *covalence*. A map is *locally cofinite* if the covalence of every face is finite.

An *accumulation point* of an infinite plane map M is a point x in the plane such that every open disk of positive radius (in either the Euclidean or hyperbolic metric) containing x intersects infinitely many map objects, be they faces, edges, or vertices. A map is *1-ended* when the deletion of any finite submap leaves exactly one infinite component.

Definition 1.1. A *tessellation* is an infinite plane map that is 3-connected, locally finite, locally cofinite, 1-ended, and also admits no accumulation point.

In the terminology of Grünbaum and Shepherd’s exhaustive work [9] on tilings of the plane, a tessellation T is *normal* if there is an embedding of T in the plane and radii $0 < r < R$ under a specific metric such that the boundary of each face lies within some annulus with inner radius r and outer radius R . A *Euclidean tessellation* is tessellation that is normal with respect to the Euclidean metric, and a *hyperbolic tessellation* is one that is normal with respect to the hyperbolic metric but not with respect the Euclidean metric.

1.2. Bilinski diagrams. A very useful tool for computing “growth rate” is what we have called a *Bilinski diagram*, because these diagrams were first used by Stanko Bilinski in his dissertation [1, 2].

Definition 1.2. Let M be a map that is rooted at some vertex x . Define a sequence of sets $\{U_n : n \geq 0\}$ of vertices and a sequence of sets $\{F_n : n \geq 0\}$ of faces of M

inductively as follows.

- Let $U_0 = \{x\}$ and let $F_0 = \emptyset$.
- For $n \geq 1$, let F_n denote the set of faces of M not in F_{n-1} that are incident with some vertex in U_{n-1} .
- For $n \geq 1$, let U_n denote the set of vertices of M not in U_{n-1} that are incident with some face in F_n .

The stratification of M determined by the set-sequences $\{U_n\}$ and $\{F_n\}$ is called *the Bilinski diagram of M rooted at x* . In a similar way one can define a Bilinski diagram of M rooted at a face f . In this case $U_0 = \emptyset$ and $F_0 = \{f\}$. Given a Bilinski diagram of T , the induced submap $\langle F_n \rangle$ of T is its n^{th} *corona*.

A Bilinski diagram is *concentric* if each subgraph $\langle U_n \rangle$ induced by U_n ($n \geq 1$) is a cycle; otherwise the Bilinski diagram is *non-concentric*. If a plane map yields a concentric Bilinski diagram regardless of which vertex or face is designated as its root, then the map is *uniformly concentric*; analogously a map which for every designated root yields a non-concentric Bilinski diagram is *uniformly non-concentric*.

To answer the question as to which tessellations are uniformly concentric we state a sufficient condition and a necessary condition. Let $\mathcal{G}_{a,b}$ denote the class of tessellations all of whose vertices have valence at least a and all of whose faces have covalence at least b . Let $\mathcal{G}_{a+,b}$ be the subclass of $\mathcal{G}_{a,b}$ of tessellations with no adjacent a -valent vertices.

Proposition 1.3 ([3] Corollary 4.2; [11] Theorem 3.2). *Every tessellation $T \in \mathcal{G}_{3,6} \cup \mathcal{G}_{3+,5} \cup \mathcal{G}_{4,4}$ is uniformly concentric, and in every Bilinski diagram of T , for all $n \geq 1$, every face in F_n is incident with at most two edges in $\langle U_{n-1} \rangle$.*

Proposition 1.4 ([3] Theorem 5.1). *If an infinite planar map admits any of the following configurations, then the map is not uniformly concentric:*

- (1) a 3-valent vertex incident with a 3-covalent face;
- (2) a 4-valent vertex incident with two nonadjacent 3-covalent faces;
- (3) a 4-covalent face incident with two nonadjacent 3-valent vertices;
- (4) an edge incident with two 3-valent vertices and two 4-covalent faces;
- (5) an edge incident with two 4-valent vertices and two 3-covalent faces.

1.3. Face-homogeneity and realizability. Let $k \geq 3$ be an integer and let an equivalence relation be defined on the set of ordered k -tuples $(p_0, p_1, \dots, p_{k-1})$ of positive integers whereby

- $(p_0, p_1, \dots, p_{k-1}) \equiv (p_1, p_2, \dots, p_{k-1}, p_0)$, and
- $(p_0, p_1, \dots, p_{k-1}) \equiv (p_{k-1}, p_{k-2}, \dots, p_0)$.

The equivalence class of which (p_0, \dots, p_{k-1}) is a member is the *cyclic sequence* $[p_0, \dots, p_{k-1}]$, and k is its *length*. There is a natural partial order \leq on the set of cyclic sequences:

$$[p_0, \dots, p_{k-1}] \leq [q_0, \dots, q_{\ell-1}]$$

if and only if $k \leq \ell$ and there exists a cyclic subsequence $q_{i_0}, q_{i_1}, \dots, q_{i_{k-1}}$ occurring in either order in $[q_0, q_1, \dots, q_{\ell-1}]$ such that $p_j \leq q_{i_j}$ for each $j \in \{0, \dots, k-1\}$. We write $\sigma_1 < \sigma_2$ if $\sigma_1 \leq \sigma_2$ but $\sigma_1 \neq \sigma_2$, where σ_1 and σ_2 are cyclic sequences.

Example 1.5. Let $\sigma_1 = [4, 6, 8, 10]$, $\sigma_2 = [6, 8, 12, 4]$, and $\sigma_3 = [10, 8, 12, 6, 4]$. Then $\sigma_1 < \sigma_2$ and $\sigma_1 < \sigma_3$, but σ_2 and σ_3 are not comparable.

Definition 1.6. Let $\sigma = [p_0, p_1, \dots, p_{k-1}]$ be a cyclic sequence of integers ≥ 3 . Then σ is the *valence sequence* of a k -covalent face f of a tessellation T if the valences of vertices incident with f in clockwise or counter-clockwise order are p_0, p_1, \dots, p_{k-1} . If every face of T has the same valence sequence σ , then T is *face-homogeneous* and σ is the *valence sequence of T* . Thus, to say briefly that a tessellation T has valence sequence σ implies that T is face-homogeneous.

Definition 1.7. Let the cyclic sequence σ be realizable as the valence sequence of a tessellation. If every tessellation having valence sequence σ is uniformly concentric, then we say that σ is *uniformly concentric*. Otherwise σ is *non-concentric*. If every tessellation having valence sequence σ is non-concentric, then σ is *uniformly non-concentric*.

Notation. By convention, when distinct letters are used to represent terms in a cyclic sequence (e.g. $[p, p, q, r, q]$), the values corresponding to distinct letters are all presumed to be distinct; that is, $p \neq q \neq r \neq p$. Moreover, if some term in the cyclic sequence is given as an integer (usually 3 or 4), then the terms given by letters are presumed to be greater than that integer. For example, if $\sigma = [4, p, q]$, then we understand that $p, q > 4$ and $p \neq q$. When using subscripts in the general form $[p_0, \dots, p_{k-1}]$, we do not make this assumption.

Remark 1.8. Not all cyclic sequences are realizable as vertex sequences of face-homogeneous tessellations of the plane. For instance, the map with valence sequence $[3, 3, 3]$ (the tetrahedron) is a tessellation of the sphere but not of the plane. More importantly, there are many cyclic sequences for which no face-homogeneous map exists at all. For instance, the valence sequence $[4, 5, 6, p]$ for any $p \geq 3$ is not realizable, because in any such map the valences of the neighbors of a 5-valent vertex in cyclic order would have to alternate between 4 and 6. However, this does not generalize to all cyclic sequences containing a subsequence $[p, q, r]$ where q is odd and $p \neq r$; for instance, $[5, 4, 5, 6, 5, 8]$ is realizable.

Conjecture 1.9. *Suppose σ is the valence sequence of a face-homogeneous tessellation and that σ contains $[p, q, r]$ as a subsequence, with q odd and $p \neq r$. Then σ must contain at least three terms equal to q .*

1.4. Polynomial versus exponential growth. Let x be a vertex of a connected graph Γ . For each nonnegative integer n , the *ball of radius n about x* is the set of vertices of Γ at distance $\leq n$ from x , written

$$(1) \quad B_n(x) = \{v \in V(\Gamma) : d(x, v) \leq n\},$$

where $d(-, -)$ is the *standard graph-theoretic metric*, that is, $d(u, v)$ is the length of a shortest path with terminal vertices u and v .

Definition 1.10. An infinite, locally finite, connected graph Γ has *exponential growth* if for some vertex $x \in V(\Gamma)$ there exist real numbers $\alpha > 1$ and $C > 0$ such that, for all $n > 0$, one has $|B_n(x)| > C\alpha^n$; otherwise Γ has *subexponential growth*. We say that Γ has *polynomial growth* of degree $d \in \mathbb{N}$ if there exist positive constants C_1 and C_2 such that $C_1 n^d \leq |B_n(x)| \leq C_2 n^d$ for all but finitely many n .

For example, the graph underlying the square lattice in the plane has quadratic growth ($d = 2$). If x is any vertex, then $|B_n(x)| = 2n^2 + 2n + 1$ for all $n \geq 1$, and one can set $C_1 = 2$ and $C_2 = 3$.

Continuing the notation of [Equation \(1\)](#) and [Definition 1.10](#), we consider the generating function

$$(2) \quad \beta_x(z) = \sum_{n=0}^{\infty} |B_n(x)| z^n$$

We denote the radius of convergence of $\beta_x(z)$ by R_B and define the *ball-growth rate* of Γ about x to be the reciprocal of R_B .

If Γ has exponential growth, then we have

$$(3) \quad \beta_x(z) \geq \sum_{n=0}^{\infty} C\alpha^n z^n = \frac{C}{1 - \alpha z},$$

where $\alpha > 1$ is the supremum of values for which the series of [Equation \(2\)](#) converges. The convergence is absolute if and only if $|z| < 1/\alpha < 1$. If Γ has polynomial growth of degree d , then

$$C_1 \sum_{n=0}^{\infty} n^d z^n \leq \sum_{n=0}^{\infty} |B_n(x)| z^n \leq C_2 \sum_{n=0}^{\infty} n^d z^n.$$

By the ‘‘ratio test,’’ the first and third series converge if and only if $|z| < 1$. These computations yield the following.

Proposition 1.11. *Let R_B denote the radius of convergence of the generating function of [Equation \(2\)](#). Then $R_B < 1$ if and only if Γ has exponential growth, and $R_B = 1$ if and only if Γ has polynomial growth. Moreover, R_B is independent of the vertex x about which $|B_n(x)|$ is determined.*

It will be seen in the next subsection (see [Theorem 1.16](#)) that the value of R_B is independent of the choice of the root vertex x .

It is well known (for example, see [\[9\]](#)) that there exist exactly eleven face-homogeneous Euclidean tessellations, namely the Laves nets. Their valence sequences $[p_0, \dots, p_{k-1}]$ correspond to integer solutions of the equation

$$\sum_{i=0}^{k-1} \frac{1}{p_i} = \frac{k-2}{2}.$$

A necessary condition for the existence of a face-homogeneous hyperbolic tessellation with valence sequence $[p_0, \dots, p_{k-1}]$ is that the inequality

$$(4) \quad \sum_{i=0}^{k-1} \frac{1}{p_i} < \frac{k-2}{2}$$

hold. This condition is not sufficient, because as we have seen, not every such integer solution is realizable as a valence sequence.

Definition 1.12. The *angle excess* of a cyclic sequence $\sigma = [p_0, \dots, p_{k-1}]$ is given by

$$\eta(\sigma) = \left(\sum_{i=0}^{k-1} \frac{p_i - 2}{p_i} \right) - 2.$$

Motivation for this definition comes from Descartes’ notion of angular defect in the Euclidean plane. When $\eta(\sigma) > 0$, there are too many faces incident at a vertex for the faces to be regular k -gons in the Euclidean plane.

Proposition 1.13. *For a cyclic sequence $\sigma = [p_0, \dots, p_{k-1}]$, inequality (4) is equivalent to*

$$(5) \quad \eta(\sigma) > 0$$

and is a necessary condition for σ to be a valence sequence of a face-homogeneous hyperbolic tessellation.

Angle excess provides a quick gauge of the growth behavior of a tessellation with valence sequence σ . If $\eta(\sigma) < 0$, the tessellation is finite. If $\eta(\sigma) = 0$, the tessellation is one of the Laves nets and has polynomial growth of degree 2. If $\eta(\sigma) > 0$, the tessellation has exponential growth. Additionally, we have the following comparison result.

Proposition 1.14. *Let σ_1 and σ_2 be cyclic sequences that are comparable in the partial order. Then $\sigma_1 < \sigma_2$ if and only if $\eta(\sigma_1) < \eta(\sigma_2)$.*

Proof. Suppose that $\sigma_1 < \sigma_2$, where $\sigma_1 = [p_0, \dots, p_{k-1}]$ and $\sigma_2 = [q_0, \dots, q_{\ell-1}]$. By definition there exist $q_{i_0}, \dots, q_{i_{k-1}}$ with $p_j \leq q_{i_j}$ for all $j = 0, \dots, k-1$. So

$$(6) \quad \eta(\sigma_1) = \sum_{j=0}^{k-1} \frac{p_j - 2}{p_j} \leq \sum_{j=0}^{k-1} \frac{q_{i_j} - 2}{q_{i_j}} \leq \sum_{i=0}^{\ell-1} \frac{q_i - 2}{q_i} = \eta(\sigma_2).$$

If $k = \ell$, then $p_j < q_{i_j}$ for some j and the first inequality in (6) is strict. If $k < \ell$, the second inequality in (6) is strict. Since $\sigma_1 \neq \sigma_2$, at least one such strict inequality must hold. \square

1.5. Growth formulas. In Definition 1.10, the standard graph-theoretical metric was used to define polynomial and exponential growth of a connected graph. However, to measure growth rates of tessellations, it is more convenient to use the notion of “regional distance;” we will count the number of graph objects in the n^{th} corona of a Bilinski diagram centered at a given vertex x , and our working definition of “growth rate” will be the following.

Definition 1.15. Let T be a tessellation labeled as a Bilinski diagram rooted at a vertex x . Let R be the radius of convergence of the power series

$$(7) \quad \varphi_x(z) = \sum_{i=1}^{\infty} |F_i| z^i.$$

When $0 < R < \infty$, we define the *growth rate* of T (with respect to x) to be $\gamma(T) = 1/R$.

Although it was shown in [6] (see pages 3–4) that, for any connected planar map with bounded covalences, the above definition of growth rate is equivalent to the growth rate with respect to the standard graph-theoretic metric, we need to show that said growth rate is independent of the root of the Bilinski diagram in question.

Theorem 1.16. *The growth rate $\gamma(T)$ of a face-homogeneous tessellation T computed by means of a Bilinski diagram is invariant under the choice of the root of the diagram.*

Proof. Choose an arbitrary vertex x of T and consider a Bilinski diagram rooted at x . Recall that the sequences $\{U_n(x) : 0 \leq n \in \mathbb{Z}\}$ and $\{F_n(x) : 1 \leq n \in \mathbb{Z}\}$ constitute the conventional labeling of T as a Bilinski diagram with root vertex x . As T is face-homogeneous, all faces are k -covalent for some $k \geq 3$. Hence for any $n \geq 1$ and any vertex $v \in U_{n+1}(x)$ there exists a vertex $u \in U_n$ such that $d(u, v) \leq \lfloor \frac{k}{2} \rfloor$. By induction on n , we obtain $d(x, v) \leq (n+1) \lfloor \frac{k}{2} \rfloor$, yielding

$$(8) \quad \bigcup_{i=0}^n U_i(x) \subseteq B_{n \lfloor k/2 \rfloor}(x)$$

and similarly,

$$(9) \quad B_n(x) \subseteq \bigcup_{i=0}^n U_i(x).$$

In addition to the power series $\varphi_x(z)$ of [Definition 1.15](#) with radius of convergence R_F , we require the power series $v_x(z) = \sum |U_n(x)| z^n$ with radius of convergence R_U . Writing

$$\Upsilon_x(z) = \frac{v_x(z)}{1-z} = \sum_{n=0}^{\infty} \left(\sum_{i=0}^n |U_i(x)| \right) z^n = \sum_{n=0}^{\infty} \left| \bigcup_{i=0}^n U_i(x) \right| z^n,$$

we have that the radius of convergence of $\Upsilon_x(z)$ equals $\min\{R_U, 1\} \leq R_B$ by [Equation \(8\)](#) (where R_B is as in [Proposition 1.11](#)). But similarly by [Equation \(9\)](#) we have that $R_B \leq \min\{R_U, 1\}$. Hence the radii of convergence of $\Upsilon_x(z)$ and $\beta_x(z)$ are equal, for any choice of root vertex x .

If p is the maximum valence of the vertices in T , each vertex is also incident with at most p faces, while each face is incident with k vertices, giving

$$|U_n(x)| \leq k |F_{n+1}(x)| \leq pk |U_{n+1}(x)|$$

for each $n \geq 0$, or equivalently,

$$\frac{1}{k} |U_n(x)| \leq |F_{n+1}(x)| \leq \frac{p}{k} |U_{n+1}(x)|.$$

Hence the radii of convergence of $v_x(z)$ and $\varphi_x(z)$ are equal, and more importantly, $R_F = R_B$; that is, the rate of ball-growth equals the rate of growth when the Bilinski diagram is labeled from a vertex x .

Finally, it follows from [Proposition 1.11](#) that ball-growth rates computed about distinct vertices are asymptotically equal in locally finite, connected, infinite graphs. Hence the radii of convergence of $\varphi_x(z)$, $\beta_x(z)$, $\beta_y(z)$, and $\varphi_y(z)$ are equal for all $x, y \in V$. That is to say, the growth rate of the graph is independent of the choice of root vertex. \square

Notation. The subscript on the symbol φ of [Definition 1.15](#) has now been shown to be superfluous and will henceforth be suppressed.

Consider the function $\tau : \mathbb{N}_0 \rightarrow \mathbb{N}_0$, (where $\mathbb{N}_0 = \{0, 1, 2, \dots\}$) given by

$$\tau(n) = \sum_{i=1}^n |F_i|.$$

The quantity

$$(10) \quad \lim_{n \rightarrow \infty} \frac{\tau(n+1)}{\tau(n)}.$$

was the definition of the growth rate of a face-homogeneous tessellation used by Moran [10] provided that this limit exists, in which case she called the tessellation *balanced*. Moran's limit fails to converge only when there exist subsequences of the sequence $\left\{ \frac{\tau(n+1)}{\tau(n)} \right\}_{n=1}^{\infty}$ with distinct limits.

The following proposition shows that the parameters of a face-homogeneous tessellation determine an upper bound for the limit in Equation (10).

Theorem 1.17. *Let T be a face-homogeneous tessellation with valence sequence $[p_0, \dots, p_{k-1}]$, labeled as a Bilinski diagram. Then*

$$\limsup_{n \rightarrow \infty} \frac{\tau(n+1)}{\tau(n)} \leq 1 + \sum_{i=0}^{k-1} p_i - 2k < \infty.$$

Proof. By hypothesis, each face of the tessellation shares an incident vertex with exactly

$$\sum_{i=0}^{k-1} (p_i - 2) = \sum_{i=0}^{k-1} p_i - 2k$$

other faces. So for $n > 0$,

$$|F_{n+1}| \leq |F_n| \left(\sum_{i=0}^{k-1} p_i - 2k \right),$$

which in turn gives that for all $n > 0$,

$$\begin{aligned} \frac{\tau(n+1)}{\tau(n)} &\leq 1 + \frac{|F_n|}{\sum_{i=0}^n |F_i|} \left(\sum_{i=0}^{k-1} p_i - 2k \right) \\ &\leq 1 + \sum_{i=0}^{k-1} p_i - 2k < \infty, \end{aligned}$$

since T is locally finite. □

By the ‘‘ratio test’’ of elementary calculus, the above proof implies that in the case of a ‘‘balanced’’ tessellation, Moran's definition of growth rate concurs with Definition 1.15, and

$$\frac{1}{R} = \limsup_{n \rightarrow \infty} \frac{\tau(n+1)}{\tau(n)} = \lim_{n \rightarrow \infty} \frac{\tau(n+1)}{\tau(n)}.$$

The definition of growth rate in terms of the radius of convergence of a power series also allows us to prove the following result, which is essential in many comparisons of growth rates of various tessellations.

Lemma 1.18 (Comparison Lemma). *Let T_1 and T_2 be tessellations, and for $i = 1, 2$ let $|F_{i,n}|$ be the number of faces in the n^{th} corona of a Bilinski diagram of T_i . Suppose that for some $N \in \mathbb{N}$, we have $|F_{1,n}| \leq |F_{2,n}|$ for all $n \geq N$. Then $\gamma(T_1) \leq \gamma(T_2)$.*

Proof. Let

$$\phi_1(z) = \sum_{n=0}^{\infty} |F_{1,n}| z^n, \quad \phi_2(z) = \sum_{n=0}^{\infty} |F_{2,n}| z^n,$$

and for $i \in \{1, 2\}$, let R_i be the radius of convergence of $\phi_i(z)$ about 0. Then since $|F_{1,n}| \leq |F_{2,n}|$ for sufficiently large n , and

$$\limsup_{n \rightarrow \infty} \sqrt[n]{|F_{i,n}|} = \frac{1}{R_i} = \gamma(T_i),$$

we have $\gamma(T_1) \leq \gamma(T_2)$. \square

1.6. The edge-homogeneous case. We conclude our presentation of preliminary material with a quick review of what is known about growth rates of edge-homogeneous tessellations, as this case has been completely resolved and its consequences turn out to be useful here and there in attacking the present problem. The point of departure here is the following classification theorem of Grünbaum and Shephard. (Edge-symbols were defined in [Section 0](#).)

Proposition 1.19 ([8] Theorem 1). *Let $p, q, k, \ell \geq 3$ be integers. There exists an edge-homogeneous, 3-connected, finite or 1-ended map with edge-symbol $\langle p, q; k, \ell \rangle$ if and only if exactly one of the following holds:*

- (1) all of p, q, k, ℓ are even;
- (2) $k = \ell$ is even and at least one of p, q is odd;
- (3) $p = q$ is even and at least one of k, ℓ is odd;
- (4) $p = q, k = \ell$, and all are odd.

Such a tessellation is edge-transitive, and the parameters p, q, k, ℓ determine the tessellation uniquely up to homeomorphism of the plane. If $p = q$, then the tessellation is vertex-transitive. If $k = \ell$, then it is face-transitive.

Following up on the Grünbaum-Shephard result, the authors together with T. Pisanski completely determined the growth rates of all edge-homogeneous tessellations. Their main result is the following.

Proposition 1.20 ([6] Theorem 4.1). *Let the function*

$$g : \{t \in \mathbb{N} : t \geq 4\} \rightarrow [1, \infty)$$

be given by

$$(11) \quad g(t) = \frac{1}{2} \left(t - 2 + \sqrt{(t-2)^2 - 4} \right).$$

Let T be an edge-homogeneous tessellation with edge-symbol $\langle p, q; k, \ell \rangle$, and let

$$(12) \quad t = \left(\frac{p+q}{2} - 2 \right) \left(\frac{k+\ell}{2} - 2 \right).$$

Then exactly one of the following holds:

- (1) the growth rate of T is $\gamma(T) = g(t)$; or
- (2) the edge-symbol of T or its planar dual is $\langle 3, p; 4, 4 \rangle$ with $p \geq 6$, and the growth rate of T is $\gamma(T) = g(t-1)$.

Observe that each value of $t \geq 4$ corresponds to only finitely many edge-homogeneous tessellations and that pairs of planar duals correspond to the same value of t . As the growth rates of edge-homogeneous tessellations are determined by an increasing function in one variable, the following is immediate.

Corollary 1.21. *The least growth rate of an edge-homogeneous hyperbolic tessellation is $(3+\sqrt{5})/2$. This value is attained only by the tessellations with edge-symbols $\langle 3, 3; 7, 7 \rangle$, $\langle 4, 4; 4, 5 \rangle$, $\langle 3, 7; 4, 4 \rangle$, and their planar duals.*

Remark. It is evident from [Proposition 1.19](#) that if a tessellation is both edge- and face-homogeneous, then its edge-symbol and valence sequence have, respectively, either the forms $\langle p, p; k, k \rangle$ and $[p, p, \dots, p]$ or the forms $\langle p, q; k, k \rangle$ and $[p, q, \dots, p, q]$, the latter pair being possible only when k is even.

We mention that, by an argument similar to the proof of [Theorem 1.17](#), one easily obtains the following upper bound for the growth rate of an edge-homogeneous tessellation.

Proposition 1.22. *Let T be an edge-homogeneous tessellation with edge-symbol $\langle p, q; k, \ell \rangle$. Then for any labeling of T as a Bilinski diagram, one has*

$$\lim_{n \rightarrow \infty} \frac{\tau(n+1)}{\tau(n)} \leq 1 + \max\{pk, qk, p\ell, q\ell\}.$$

2. ACCRETION AND MONOMORPHIC VALENCE SEQUENCES

2.1. Accretion. Given an arbitrary face-homogeneous tessellation T with valence sequence $\sigma = [p_0, p_1, \dots, p_{k-1}]$, we wish to apply [Definition 1.15](#) to determine its growth rate. Letting T be labeled as a Bilinski diagram, we require a means to evaluate $|F_n|$ for all $n \in \mathbb{N}$. This is done inductively; each face $f \in F_n$ “begets” a certain number of facial “offspring” in F_{n+1} , and that number is determined by the configuration of f within $\langle F_n \rangle$, that is, what the valences are of the vertices incident with f (in the rotational order of σ) that belong, respectively, to U_{n-1} and more importantly to U_n .

A class of identically configured faces (in any corona) is a *face type*, and is denoted by \mathbf{f}_i for some range of $i = 1, \dots, r$. The benefit of using face types is that we can define an r -dimensional column vector \vec{v}_n , called the n^{th} *distribution vector*, which lists the frequency with which each face type occurs in the n^{th} corona. Thus, if \vec{j} is the r -dimensional vector of 1s, then $|F_n| = \vec{j} \cdot \vec{v}_n$ via the standard dot product.

[Figure 1](#) depicts a face $f \in F_n$ of some tessellation and the faces in F_{n+1} which are determined by the face type of f . These faces are called the *offspring* of f , and the figure is accordingly called the *offspring diagram* for f . As the vertex labeled p_j is incident with both faces f and $f' \in F_n$, one-half of those faces in F_{n+1} labeled as A in the figure count as offspring of f , and one-half are counted as offspring of f' . Similarly, half of the faces labeled by B count as offspring of f and half as offspring of f'' . All those faces between labels A and B in [Figure 1](#) are wholly offspring of f . Those faces which are offspring of f , or offspring of offspring of f , and so on, are called collectively *descendants* of f .

Definition 2.1. With respect to the labeling of a Bilinski diagram, each vertex incident with a face $f \in F_n$ lies in U_{n-1} or U_n . The pattern of valences of vertices in U_{n-1} and in U_n determines the *face type* of f . The three face types occurring most routinely are called *wedges*, *bricks*, and *notched bricks*. A face f in F_n is a *wedge* if it is incident with exactly one vertex in U_{n-1} . The face f is a *brick* if it is incident with exactly two adjacent vertices in U_{n-1} and at least two vertices in U_n . Finally, f is a *notched brick* if it is incident with three consecutive vertices of U_{n-1} , of which the middle vertex is 3-valent, and f is incident with two or more vertices in U_n . For a given labeling of a tessellation T as a Bilinski diagram, the face types

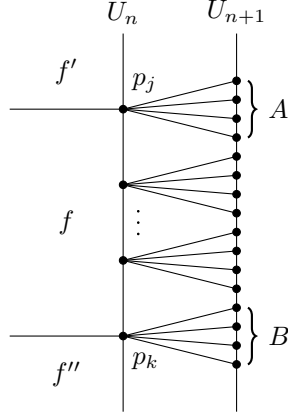


FIGURE 1. A face f in F_n of a tessellation T , along with the offspring of f in F_{n+1} .

of T are indexed $\mathbf{f}_1, \dots, \mathbf{f}_r$ for some $r \in \mathbb{N}$; we explain the method by which indices are assigned after the statement of [Theorem 2.7](#).

An algorithm by which one can describe the faces, corona by corona, of a tessellation labeled as a Bilinski diagram is called an *accretion rule*. Often some homogeneous system of recurrence relations determines such an accretion rule. In this case, the n^{th} distribution vector \vec{v}_n defined above has the property that the j^{th} component of \vec{v}_n is the number of faces of type \mathbf{f}_j in the n^{th} corona. We then encode the system of recurrences into a *transition matrix* M such that $\vec{v}_{n+1} = M\vec{v}_n$ holds for all $n \geq 1$. When $M = [m_{i,j}]$ is such a matrix, the entry $m_{i,j}$ is the number of faces of type \mathbf{f}_j that are offspring of a face of type \mathbf{f}_i . We require the following result from [\[6\]](#).

Proposition 2.2 ([\[6\]](#), Theorem 3.1). *Let T be a tessellation labeled as a Bilinski diagram with accretion rule specified by the transition matrix M and first distribution vector \vec{v}_1 . Then the ordinary generating function for the sequence $\{|F_n|\}_{n=1}^{\infty}$ is*

$$(13) \quad \varphi(z) = |F_0| + z \left(\vec{j} \cdot (I - zM)^{-1} \vec{v}_1 \right),$$

where I is the identity matrix and \vec{j} is the vector of 1s.

By using [Definition 1.15](#), we can prove the following more directly than we did in Theorem 3.4 of [\[6\]](#).

Theorem 2.3. *If M is the transition matrix of a tessellation T and Λ is the maximum modulus of an eigenvalue of M , then $\gamma(T) = \Lambda$.*

Proof. We can write the generating function $\varphi(z)$ of [Proposition 2.2](#) as a rational function $u(z)/v(z)$, with $v(z)$ determined entirely by $(I - zM)^{-1}$. Specifically, using

Cramer's rule where r denotes the order of M , we have

$$\begin{aligned}
 (I - zM)^{-1} &= \frac{1}{\det(I - zM)} \operatorname{adj}(I - zM) \\
 (14) \qquad &= \frac{1}{(-z)^r \det(M - \frac{1}{z}I)} \operatorname{adj}(I - zM) \\
 &= \frac{1}{(-z)^r \chi(\frac{1}{z})} \operatorname{adj}(I - zM)
 \end{aligned}$$

where $\chi(\frac{1}{z})$ is the characteristic polynomial (in $\frac{1}{z}$) of M . Entries of the adjoint $\operatorname{adj}(I - zM)$ are polynomials in z of degree at most $r - 1$, and so $v(z) = (-z)^r \chi(\frac{1}{z})$. As $\chi(\frac{1}{z})$ is a polynomial in $\frac{1}{z}$ of degree exactly r , $v(z)$ has a nonzero constant term and the roots of v occur precisely at the roots of $\chi(\frac{1}{z})$. These are precisely the reciprocals of the eigenvalues of M . Thus the minimum modulus of a pole of $\varphi(z)$ is $1/\Lambda$. As this is the definition of the radius of convergence of a power series expanded about 0, we have $\gamma(T) = \Lambda$. \square

2.2. Monomorphic, Uniformly Concentric Sequences. As we have already remarked, valence sequences of face-homogeneous tessellations are unlike edge-symbols of edge-homogeneous tessellations in two significant ways: (i) the requirements for realizability of an edge-symbol are simpler and less stringent than the realizability criteria for a cyclic sequence, and (ii) two or more non-isomorphic face-homogeneous tessellations may share a common valence sequence. This latter property motivates the following definition.

Definition 2.4. Let σ be a cyclic sequence. If there exists (up to isomorphism) a unique face-homogeneous tessellation with valence sequence σ , then we say that σ is *monomorphic*. If there exist at least two (non-isomorphic) tessellations with valence sequence σ , then σ is *polymorphic*.

Proposition 2.5 (Moran [10]). *All realizable cyclic sequences of length 3 are monomorphic.*

A second property of interest is whether a given valence sequence is uniformly concentric. These two properties thus yield four classes of valence sequences. Not surprisingly, the class most amenable to an elegant and simple accretion rule consists of those that are both monomorphic and uniformly concentric.

One can find in [13] a complete classification of cyclic sequences of length k for $3 \leq k \leq 5$ in terms of Definition 2.4 which will help us to narrow our investigation. (It is actually the equivalent dual problem that is treated in [13], and the term "covalence sequence" is used. In the present work we have opted to follow Moran [10], speaking rather in terms of "valence sequences.")

We now turn to considering the relative growth rates of tessellations with monomorphic valence sequences. The ideal condition would be to have that the partial order on cyclic sequences is mirrored by the natural order on growth rates: that is, if T_1 and T_2 are tessellations with valence sequences $\sigma_1 \leq \sigma_2$, then $\gamma(T_1) \leq \gamma(T_2)$. For monomorphic, uniformly concentric valence sequences, this is precisely the case, as stated below in Theorem 2.7. In order to prove the theorem, we now demonstrate the necessary machinery via the following example, which can be readily generalized.

Example 2.6. Consider T_1 and T_2 to be face-homogeneous tessellations with monomorphic valence sequences $\sigma_1 = [4, 5, 4, 5]$ and $\sigma_2 = [4, 6, 6, 4, 5]$, respectively, both labeled as face-rooted Bilinski diagrams. Note that $\sigma_1 < \sigma_2$. We continue the convention that $F_{i,n}$ denotes the set of faces of the n^{th} corona of T_i . (The reader may follow Figures 2 through 7.) Starting with T_1 , we construct by induction a sequence $\{T'_j : j \in \mathbb{N}\}$ of tessellations such that:

- (1) $T'_0 = T_1$ as a base for the induction,
- (2) if we denote by $F'_{j,n}$ the set of faces in the n^{th} corona of T'_j , then for each $j \in \mathbb{N}$, the unions of the first n coronas of T'_j satisfy

$$\left\langle \bigcup_{n=1}^j F'_{j,n} \right\rangle \cong \left\langle \bigcup_{n=1}^j F_{2,n} \right\rangle$$

as induced subgraphs, and

- (3) $|F_{1,n}| \leq |F'_{j,n}|$ for all $n \in \mathbb{N}$.

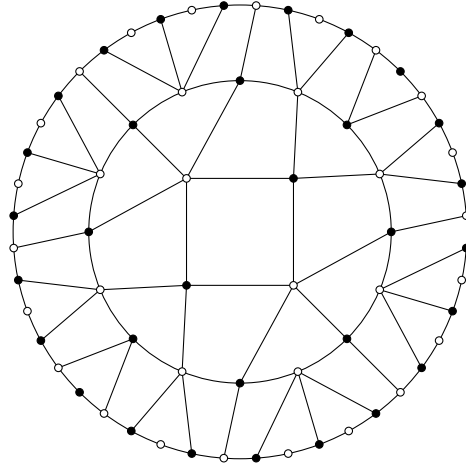


FIGURE 2. The first three coronas of T_1

To construct T'_1 from T'_0 , the valence sequence of the root face of T'_0 must change from σ_1 to σ_2 . To do so, we augment the valence of a 5-valent vertex $v \in U_1$ to 6-valent and then subdivide an edge of $\langle U_1 \rangle$ incident with v by inserting a 6-valent vertex. Augmentation and interpolation are both performed via the insertion of an infinite “cone” as follows. We choose a sequence of edges e_2, e_3, e_4, \dots , with $e_i \in \langle U_i \rangle$, such that e_2 and v are incident with a common face in F_1 , and for each $i \geq 2$, e_i and e_{i+1} are incident with a common face in F_i . On each of these edges we interpolate vertices, and we insert edges connecting vertices between U_i and U_{i+1} ensuring that every face so created has covalence 5. Furthermore, if a created face is incident only with interpolated vertices, then its valence sequence is σ_2 . This insertion is well-defined precisely because σ_2 is monomorphic, i.e., the vertices and edges may be inserted in exactly one way.

The resulting tessellation after the procedure just described is denoted by T'_1 . Faces of T'_1 fall into three classes: first, there are faces which have valence sequence

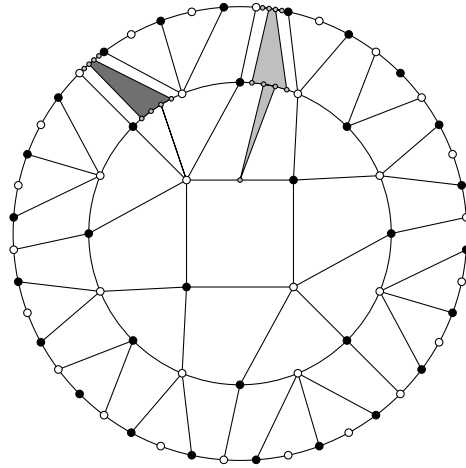


FIGURE 3. The first three coronas of T'_1 . The dark gray region is a subgraph inserted by augmentation of the valence of a vertex from 5 to 6; the light gray region is a subgraph inserted while interpolating a 6-valent vertex along an incident edge. These insertions continue throughout all coronas of T'_1 .

σ_1 and in T'_0 were not incident with any part of the inserted cone; second, there are those faces with valence sequence σ_2 that have been inserted; finally, there are faces which are incident with newly inserted edges but which have neither valence sequence σ_1 nor σ_2 . A face f in this third class has covalence equal to the length of σ_2 , but some vertices incident with f have valences from σ_1 . These faces may occur in all coronas outward from the first corona.

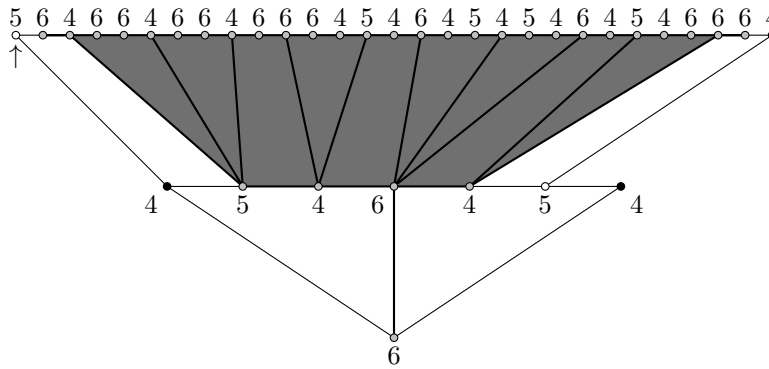


FIGURE 4. An expanded view of the subgraph inserted when increasing the valence of a 5-valent vertex to 6-valent. Note that the 5-valent vertex in the upper left, marked by the arrow, is disrupting the valence sequence of the white face with which it is incident; if the marked vertex were 6-valent, that face would have valence sequence $\sigma_2 = [4, 6, 6, 4, 5]$.

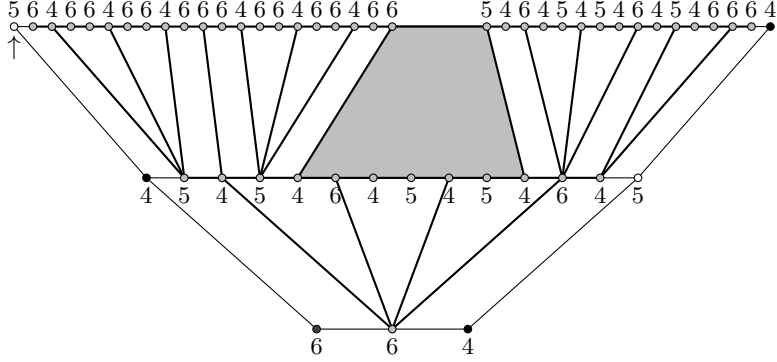


FIGURE 5. An expanded view of the subgraph inserted when interpolating a 6-valent vertex along an edge incident to the root. Again note the marked 5-valent vertex in the upper left. (The large shaded region represents a number of faces of valence sequence $[4, 6, 6, 4, 5]$ which are too dense to draw nicely in the Euclidean plane.)

We compare now the tessellations T_1 , T'_1 , and T_2 . In each case, the 0^{th} corona contains only the root face. So from our construction,

$$|F_{1,0}| = |F'_{1,0}| = |F_{2,0}|, \text{ and for all } n \in \mathbb{N}_0, |F_{1,n}| \leq |F'_{1,n}|,$$

as we have inserted faces into every corona outward from the first.

We construct T'_2 from T'_1 just as we created T'_1 from $T'_0 = T_1$; there is, however, one additional type of interpolation which may occur. Specifically, a vertex must be interpolated in an edge incident with two adjacent faces in $F'_{1,1}$. In [Figure 6](#), an example of such an edge is marked with an arrow. This obstacle proves to be minor, as the necessary interpolation is shown in [Figure 7](#) – rather than interpolating a vertex on an edge incident with vertices in both U_1 and U_2 , the vertex and its two neighbors are interpolated in U_2 , replacing a $(5, 4, 5)$ -path in $\langle U_2 \rangle$ with a $(5, 4, 6, 4, 5)$ -path.

We continue by induction; suppose a tessellation T'_j has been created by this process. Then in the j^{th} corona, there are finitely many faces which require a finite number of vertices to have their valences increased and a finite number of edges along which we must interpolate a vertex. This creates T'_{j+1} such that

$$|F_{1,n}| \leq |F'_{j+1,n}| = |F_{2,n}|$$

for $n < j+1$, as the first j coronas are comprised only of faces with valence sequence σ_2 . Furthermore,

$$|F_{1,n}| \leq |F'_{j+1,n}|$$

for all $n \in \mathbb{N}$. In this manner we can construct an infinite sequence of tessellations, namely $\{T'_j : j \in \mathbb{N}\}$, with the properties that $|F_{1,n}| \leq |F'_{j,n}|$ for any $j, n \in \mathbb{N}_0$, and $|F'_{j,n}| = |F_{2,n}|$ whenever $j > n$.

In the previous example, we constructed the sequence in the process of transforming T_1 with valence sequence $[4, 5, 4, 5]$ into T_2 with valence sequence $[4, 6, 6, 4, 5]$; however, the process of creating $\{T'_j : j \in \mathbb{N}_0\}$ is identical in any case where T_1

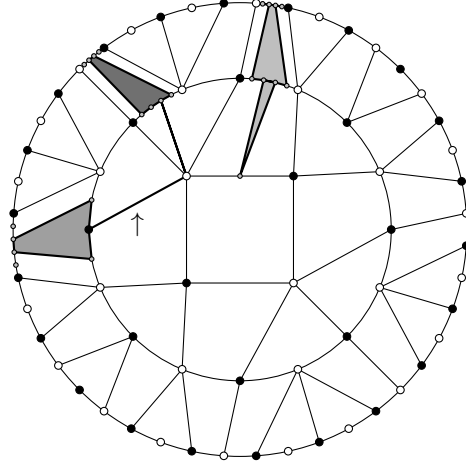


FIGURE 6. Beginning the construction of T'_2 from T'_1 .

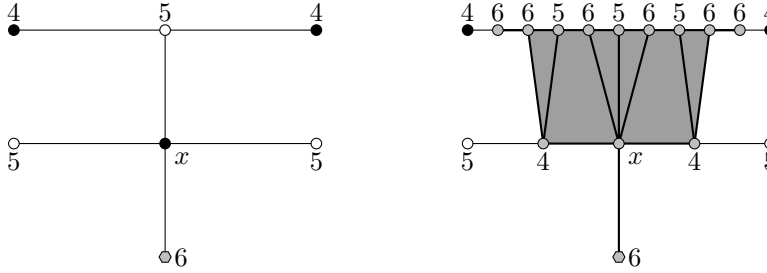


FIGURE 7. In the diagram to the left, the $(4, 6)$ -edge at the bottom must have a 6-valent vertex interpolated, along with the attendant subgraph. However, we wish to avoid non-concentricity; hence the single 4-valent vertex x is expanded to a $(4, 6, 4)$ -path as in the diagram on the right.

and T_2 are face-homogeneous and uniformly concentric with monomorphic valence sequences σ_1 and σ_2 , respectively, where $\sigma_1 < \sigma_2$. Thus by [Lemma 1.18](#), we obtain the following result.

Theorem 2.7 (Growth Comparison Theorem). *Let σ_1 and σ_2 be monomorphic valence sequences realized by tessellations $T_1, T_2 \in \mathcal{G}_{4,4} \cup \mathcal{G}_{3+,5} \cup \mathcal{G}_{3,6}$, with $\sigma_1 < \sigma_2$. Then $\gamma(T_1) \leq \gamma(T_2)$.*

Our convention is to index the face types $(\mathbf{f}_1, \dots, \mathbf{f}_r$ for some r) in the following order: first wedges, then bricks, then notched bricks, and finally, other face types if any. A wedge in F_n with face type \mathbf{f}_i is incident with a p_{i-1} -valent vertex in U_{n-1} , for $i = 1, \dots, k$. Similarly, the indices of face types of bricks begin with a brick in F_n incident with a p_0 -valent vertex and a p_{k-1} -valent vertex in U_{n-1} . A new index \mathbf{f}_j is not introduced if there is some \mathbf{f}_i for $i < j$ with the same configuration of vertices in U_{n-1} and U_n , up to orientation. For example, the valence sequence

[4, 6, 8, 8, 6, 4] yields seven face types $\mathbf{f}_1, \dots, \mathbf{f}_7$, of which $\mathbf{f}_1, \mathbf{f}_2$, and \mathbf{f}_3 are wedge types and \mathbf{f}_4 through \mathbf{f}_7 are brick types.

When a monomorphic sequence $[p_0, \dots, p_{k-1}]$ is realized by a tessellation in $\mathcal{G}_{4,4} \cup \mathcal{G}_{3+,5} \cup \mathcal{G}_{3,6}$, then every face, with respect to *any* Bilinski diagram, can be only a wedge, a brick, or a notched brick. The indexing of face types when $p_i \neq p_j$ for $i \neq j$ allows a stricter labeling which we can use in several other cases. A face f in F_n is a wedge of type \mathbf{w}_i when the vertex incident with f in U_{n-1} corresponds to valence p_{i-1} in σ . If instead f is a brick with incident vertices in U_{n-1} corresponding to valences p_{i-1} and p_{i-2} (indices here taken modulo k), then f has face type \mathbf{b}_i . Finally, if f a notched brick whose incident vertices in U_{n-1} have valences $p_i, p_{i-1} = 3$, and p_{i-2} , then f has face type \mathbf{n}_i . It is important to note that if $p_{i-1} \neq 3$, then faces of type \mathbf{n}_i never occur as offspring. This stricter labeling is used explicitly only for the few theorems which follow, by which we determine the number of offspring of each instance of these general face types. Furthermore, we demonstrate a first application of the accretion rules and half-counting of faces that were introduced in [Section 2.1](#).

Notation: Let T be a face-homogeneous tessellation with valence sequence σ , labeled as a Bilinski diagram. We denote by $\Omega(\mathbf{f})$ the number of faces in F_{n+1} that are counted as offspring of a single face of face type \mathbf{f} in F_n , for any $n > 0$. For $T \in \mathcal{G}_{4,4} \cup \mathcal{G}_{3+,5} \cup \mathcal{G}_{3,6}$ we let $\Omega(\mathbf{w}_i)$, $\Omega(\mathbf{b}_i)$, and $\Omega(\mathbf{n}_i)$ denote the number of offspring of a single wedge, brick, or notched brick of , respectively, of the given type.

Lemma 2.8. *For a face-homogeneous tessellation in $\mathcal{G}_{4,4} \cup \mathcal{G}_{3+,5} \cup \mathcal{G}_{3,6}$ with monomorphic valence sequence $\sigma = [p_0, \dots, p_{k-1}]$, one has for $i \in \{1, \dots, k\}$,*

$$(15) \quad \Omega(\mathbf{w}_i) = \frac{p_{i-2} + p_i}{2} - 2k + 3 + \sum_{j \notin I_1} p_j, \text{ and}$$

$$(16) \quad \Omega(\mathbf{b}_i) = \frac{p_{i-3} + p_i}{2} - 2k + 5 + \sum_{j \notin I_2} p_j,$$

where $I_1 = \{i-2, i-1, i\}$ and $I_2 = \{i-3, i-2, i-1, i\}$. Also, when $p_{i-1} = 3$,

$$(17) \quad \Omega(\mathbf{n}_i) = \frac{p_{i-3} + p_{i+1}}{2} - 2k + 7 + \sum_{j \notin I_3} p_j$$

with $I_3 = \{i-3, i-2, i-1, i, i+1\}$.

Proof. The reader is referred to the three offspring diagrams shown in [Figure 8](#).

Letting $i \in \{1, \dots, k\}$, the first diagram applies when $p_{i-1} \geq 4$. If also $p_{i-2}, p_i \geq 4$ as in the diagram, then we have

$$\begin{aligned} \Omega(\mathbf{w}_i) &= \frac{p_{i-2} - 4}{2} + \frac{p_i - 4}{2} + k - 2 + \sum_{j \notin I_1} (p_j - 3) \\ &= \frac{p_{i-2} + p_i}{2} - 2k + 3 + \sum_{j \notin I_1} p_j. \end{aligned}$$

If instead $p_{i-2} = 3$, then the number of wedge offspring of \mathbf{w}_i is

$$\frac{p_i - 4}{2} + \sum_{j \notin I_1} (p_j - 3),$$

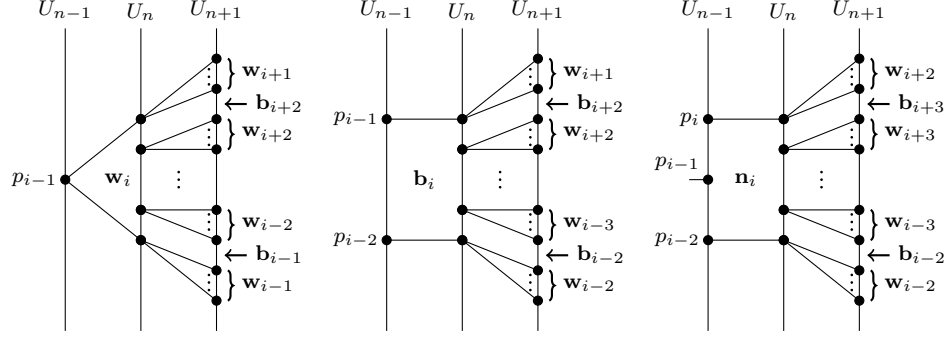


FIGURE 8. Offspring diagrams for the three general face types (respectively wedges, bricks, and notched bricks) of a tessellation with monomorphic, uniformly concentric valence sequence $[p_0, \dots, p_{k-1}]$.

the number of brick offspring is $k - 3$, and the number of notched brick offspring is $\frac{1}{2}$. Thus when $p_{i-2} = 3$,

$$\begin{aligned} \Omega(\mathbf{w}_i) &= \frac{1}{2} + \frac{p_i - 4}{2} + k - 3 + \sum_{j \notin I_1} (p_j - 3) \\ &= -\frac{1}{2} + \frac{p_i - 4}{2} + k - 2 + \sum_{j \notin I_1} (p_j - 3) \\ &= \frac{p_{i-2} - 4}{2} + \frac{p_i - 4}{2} + k - 2 + \sum_{j \notin I_1} (p_j - 3) \end{aligned}$$

as before; likewise when $p_i = 3$. Analogous arguments hold for the offspring of bricks and notched bricks. \square

The process of establishing an accretion rule and accompanying transition matrices is considerably simplified for tessellations in $\mathcal{G}_{4,4}$ by virtue of the absence of notched bricks. By applying the following lemma and [Theorem 2.3](#), one can then compute the growth rate explicitly of any monomorphic valence sequence realizable in $\mathcal{G}_{4,4}$. Recall that by [Proposition 1.3](#), all such valence sequences are uniformly concentric.

Lemma 2.9. *Let $[p_0, \dots, p_{k-1}]$ be the monomorphic valence sequence for a tessellation $T \in \mathcal{G}_{4,4}$. Then T has an accretion rule which admits the block transition matrix*

$$M = \begin{bmatrix} A & B \\ C & D \end{bmatrix},$$

with $A = (a_{i,j})$, $B = (b_{i,j})$, $C = (c_{i,j})$, and $D = (d_{i,j})$ given by

$$(18) \quad a_{i,j} = \begin{cases} 0 & j - i = 0 \\ \frac{1}{2}(p_{i-1} - 4) & j - i \in \{1, k-1\} \pmod{k} \\ p_{i-1} - 3 & \text{otherwise,} \end{cases}$$

$$(19) \quad b_{i,j} = \begin{cases} 0 & j - i \in \{0, 1\} \pmod{k} \\ \frac{1}{2}(p_{i-1} - 4) & j - i \in \{2, k-1\} \pmod{k} \\ p_{i-1} - 3 & \text{otherwise,} \end{cases}$$

$$(20) \quad c_{i,j} = \begin{cases} 0 & j - i \in \{0, 1\} \pmod{k} \\ 1 & \text{otherwise,} \end{cases}$$

$$(21) \quad d_{i,j} = \begin{cases} 0 & j - i \in \{0, 1, k-1\} \pmod{k} \\ 1 & \text{otherwise,} \end{cases}$$

for $i, j \in \{1, \dots, k\}$.

Proof. Since all general face types are wedges or bricks, we need demonstrate only that the entries $a_{i,j}$ and $c_{i,j}$ correspond to numbers of offspring of the k face types in wedge configurations and that the entries $b_{i,j}$ and $d_{i,j}$ correspond to numbers of offspring of the k face types in brick configurations.

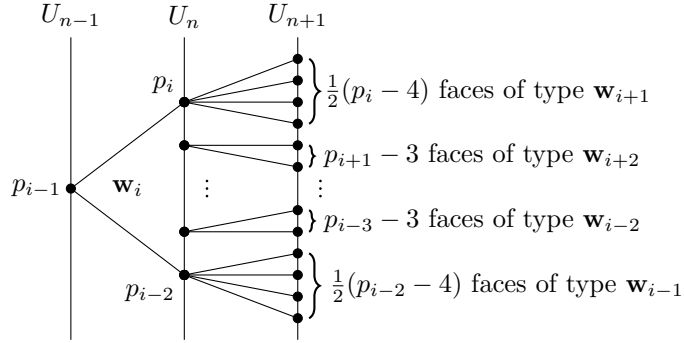


FIGURE 9. Offspring of a \mathbf{w}_i face in a tessellation $T \in \mathcal{G}_{4,4}$, where $i \in \{1, \dots, k\}$.

The offspring of wedges of type \mathbf{w}_i are shown in [Figure 9](#), and the offspring of a brick of type \mathbf{b}_i is shown in [Figure 10](#). The ordering of face types is $\mathbf{w}_1, \mathbf{w}_2, \dots, \mathbf{w}_k, \mathbf{b}_1, \dots, \mathbf{b}_k$. Recalling that the (i, j) -entry of a transition matrix M is the number of faces of the i^{th} indexed type which are produced in F_{n+1} as offspring of a face of the j^{th} indexed type in F_n , it is straightforward to verify from these two offspring diagrams that the entries of M are correct. \square

Remark 2.10. We emphasize the breadth of this class of monomorphic, uniformly concentric valence sequences. In addition to the many monomorphic face-homogeneous tessellations in $\mathcal{G}_{3,6} \cup \mathcal{G}_{3+,5} \cup \mathcal{G}_{4,4}$, there are many with covalence 3 (cf. [Proposition 2.5](#)). By [Proposition 1.19](#), all edge-transitive tessellations of constant covalence are included, except for those of the with valence sequence $[3, p, 3, p]$

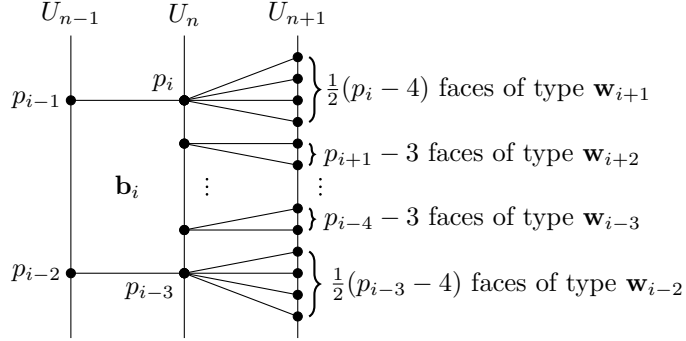


FIGURE 10. Offspring of a \mathbf{b}_i face in a tessellation $T \in \mathcal{G}_{4,4}$, where $i \in \{1, \dots, k\}$.

(edge-symbol $\langle 3, p; 4, 4 \rangle$), as they are not uniformly concentric. By [Proposition 1.3](#), a k -covalent tessellation T is uniformly concentric whenever $k \geq 6$. If $k \geq 7$ and if σ is monomorphic, then $\sigma \geq [3, 3, 3, 3, 3, 3, 3]$. In that case, [Theorem 2.7](#) and [Proposition 1.20](#) tell us that σ has growth rate at least $\gamma([3, 3, 3, 3, 3, 3, 3]) = \frac{1}{2}(3 + \sqrt{5})$.

2.3. Monomorphic Non-Concentric Sequences. The purpose of this section is to characterize the six forms of monomorphic, non-concentric valence sequences with positive angle excess. These sequences give rise to face types other than wedges, bricks, and notched bricks, and so the foregoing methods cannot be applied to compute their growth rates.

An interesting situation arises when a tessellation is not *uniformly* concentric but nonetheless, by prudent selection of the root, admits *some* Bilinski diagram that *is* concentric. To illustrate this point, we examine sequences of the form $[4, p, q]$.

Example 2.11. Consider the valence sequence $\sigma = [4, p, q]$ with $4 < p < q$, where $\frac{1}{p} + \frac{1}{q} < \frac{1}{4}$, and let T be a face-homogeneous tessellation with valence sequence σ . For σ to be realizable, clearly p and q must be even. Note as well that the inequality [\(4\)](#) is satisfied. While σ is monomorphic and admits a concentric Bilinski diagram, σ is not uniformly concentric (cf. the second case of [Proposition 1.4](#)).

When a Bilinski diagram of T admits a 4-valent vertex $v_0 \in U_n$ (for some n) adjacent to the vertices $u_1, u_2 \in U_{n-1}$ and $v_1, v_2 \in U_n$, then the diagram is not concentric; the vertices v_1 and v_2 must also be adjacent, as T is 3-covalent. Hence $\langle \{v_0, v_1, v_2\} \rangle$ is a cycle within $\langle U_n \rangle$, causing the Bilinski diagram to be non-concentric. However, it is possible to avoid this configuration by choosing the root of the Bilinski diagram to be either a p -valent or a q -valent vertex. When so labeled, only four face types occur, as demonstrated by the offspring diagrams in [Figure 11](#).

One sees here that if the root is taken to be a p -valent vertex, the first corona consists entirely of faces of type \mathbf{f}_1 , which produce in turn only offspring of types \mathbf{f}_2 and \mathbf{f}_3 . Similarly, given a q -valent root, the first corona consists entirely of faces of type \mathbf{f}_2 , which produce in turn only offspring of types \mathbf{f}_1 and \mathbf{f}_4 . The non-concentric configuration described above can never be produced among the descendants of faces of types \mathbf{f}_1 or \mathbf{f}_2 .

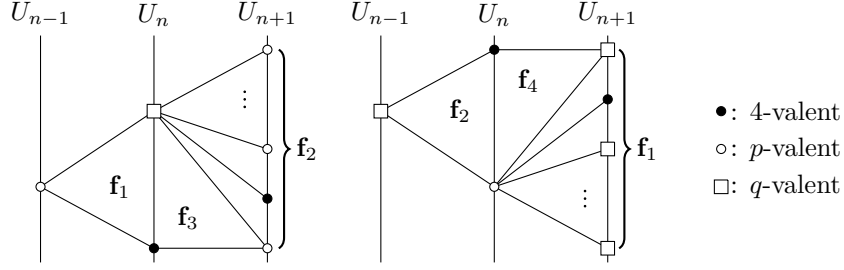


FIGURE 11. Offspring diagrams for a concentric tessellation with valence sequence $[4, p, q]$.

Inspection of [Figure 11](#) gives the first and second columns of the transition matrix M ; the third and fourth columns, corresponding to \mathbf{f}_3 and \mathbf{f}_4 , merit further explanation. A face of type \mathbf{f}_3 in F_{n+1} has a p -valent vertex in U_{n+1} ; this vertex is incident with $p - 5$ faces of type \mathbf{f}_1 in F_{n+2} . So the behavior of a face of type \mathbf{f}_3 is effectively to collapse one of the faces in U_{n+2} of type \mathbf{f}_1 begotten by the adjacent face of type \mathbf{f}_2 . Faces of type \mathbf{f}_4 behave similarly, collapsing a face of type \mathbf{f}_2 . These considerations give us

$$M = \begin{bmatrix} 0 & \frac{1}{2}(p-4) & -1 & 0 \\ \frac{1}{2}(q-4) & 0 & 0 & -1 \\ 1 & 0 & 0 & 0 \\ 0 & 1 & 0 & 0 \end{bmatrix}$$

as the transition matrix M for this accretion rule for T . As the characteristic equation for M is of degree 4, it can be solved to determine that the maximum modulus of an eigenvalue of M is

$$\Lambda = \frac{1}{4} \sqrt{[2(p-4)(q-4) - 16] + 2\sqrt{(p-4)^2(q-4)^2 - 16(p-4)(q-4)}}.$$

By [Theorem 2.3](#) and [Theorem 1.16](#), Λ is the growth rate of T . This quantity can be minimized by minimizing pq subject to the initial conditions $\frac{1}{p} + \frac{1}{q} < \frac{1}{4}$ and that p and q be even. We shall see in [Section 2.4](#) the role played by this example.

Growth rate formulas for each of the other five classes are derived in the Appendix.

Theorem 2.12. *Let σ be a valence sequence such that $\eta(\sigma) > 0$. Then σ is both monomorphic and non-concentric if and only if σ is of one of the following six forms:*

- $[3, p, p]$, with $p \geq 14$ and even;
- $[4, p, q]$, with p and q both even, $4 < p < q$, and $\frac{1}{p} + \frac{1}{q} < \frac{1}{4}$;
- $[3, p, 3, p]$, with $p \geq 7$;
- $[3, p, 4, p]$, with $p \geq 5$ and even;
- $[3, 3, p, 3, p]$, with $p \geq 5$; or
- $[3, 3, p, 3, q]$, with $p, q \geq 4$ and $\frac{1}{p} + \frac{1}{q} < \frac{1}{2}$.

Proof. The parity conditions and the inequalities bounding the parameters in each case are minimal such that σ be indeed realizable as a tessellation with $\eta(\sigma) > 0$.

As noted in [Remark 2.10](#), all valence sequences of length at least 6 are uniformly concentric. Furthermore, by [Proposition 2.5](#), all valence sequences of length 3 are monomorphic. Valence sequences $[3, p, p]$, $[4, p, q]$, and $[3, p, 3, p]$ give rise to tessellations exemplifying cases 1, 2, and 4 respectively of [Proposition 1.4](#), and hence cannot be uniformly concentric. As a face-homogeneous tessellation with valence sequence $[3, p, 3, p]$ is also edge-transitive, the sequence must be monomorphic. The proof that the sequence $[3, p, 4, p]$ is monomorphic and uniformly non-concentric is given in the Appendix, where the growth rate of a corresponding tessellation is determined.

We now prove that $[3, 3, p, 3, p]$ is monomorphic for all $p \geq 5$. As a 3-valent vertex is incident with a common face with any two of its neighbors, every 3-valent vertex must be adjacent to at least two p -valent vertices; otherwise some face would be incident with a $(3, 3, 3)$ -path. Consider a p -valent vertex v_1 . By face-homogeneity, v_1 is adjacent to some 3-valent vertex u_1 , with u_1 adjacent in turn to a 3-valent vertex u_2 which is not adjacent to v_0 . But then the other vertex adjacent to u_1 must be a p -valent vertex v_2 . This forces the pattern of valences at regional distance 1 from v_1 to be $(3, 3, p, \dots, 3, 3, p)$; as v_1 was arbitrary, this must be the pattern of valences at regional distance 1 from any p -valent vertex. As every vertex is at regional distance 1 from some p -valent vertex, $[3, 3, p, 3, p]$ must be monomorphic; the first two coronas of a tessellation with this valence sequence rooted at a p -valent vertex is depicted in [Figure 12](#). Furthermore, this local configuration to a p -valent vertex forces the local behaviors to a $(3, 3)$ -edge and a 3-valent vertex shown in [Figure 13](#). Hence when a 3-valent vertex v_0 is taken as the root of the Bilinski diagram of a tessellation with valence sequence $[3, 3, p, 3, p]$, a pendant vertex occurs in $\langle U_3 \rangle$. This is shown in [Figure 14](#). So $[3, 3, p, 3, p]$ is monomorphic but not uniformly concentric; the argument for $[3, 3, p, 3, q]$ is analogous.

We have shown these six forms to be both monomorphic and non-concentric; that these are the only such valence sequences is proved via the exhaustive examination of cases in the Appendix. □

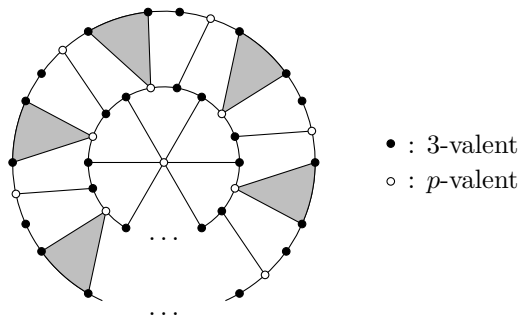


FIGURE 12. The first two coronas of a tessellation with valence sequence $[3, 3, p, 3, p]$ rooted at a p -valent vertex. Each shaded region indicates $p - 3$ faces in F_2 all having the same face type.

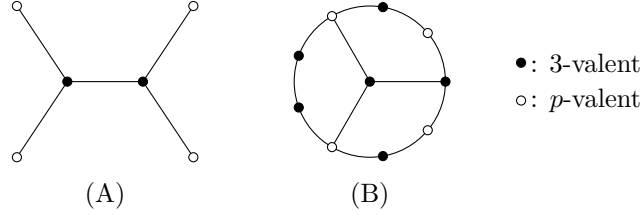


FIGURE 13. (A) Local configuration along an edge with edge-symbol $\langle 3, 3; 5, 5 \rangle$ in a face-homogeneous tessellation with valence sequence $[3, 3, p, 3, p]$. (B) Local configuration in the same tessellation when rooted at a 3-valent vertex.

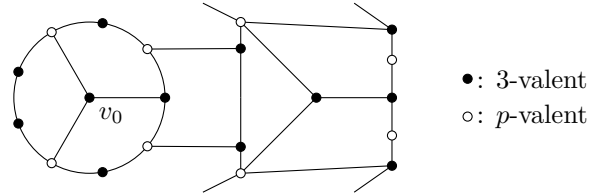


FIGURE 14. Non-concentricity of $[3, 3, p, 3, p]$ when rooted at a 3-valent vertex v_0 .

2.4. The Main Result. The following theorem establishes the so-called “golden mean” as the least rate of exponential growth for face-homogeneous tessellations with monomorphic valence sequences.

Theorem 2.13 (Least Exponential Growth Rate of Monomorphic Valence Sequences). *The least growth rate of a face-homogeneous tessellation with monomorphic valence sequence σ such that $\eta(\sigma) > 0$ is $\frac{1}{2}(1 + \sqrt{5})$ and is attained by exactly the tessellations with valence sequences $[4, 6, 14]$ and $[3, 4, 7, 4]$.*

Proof. With respect to the partial order on valence sequences, if a valence sequence σ has length at least 7, then $[3, 3, 3, 3, 3, 3, 3] \leq \sigma$. A face-homogeneous tessellation T_0 with valence sequence $[3, 3, 3, 3, 3, 3, 3]$ is edge-homogeneous with edge-symbol $\langle 3, 3; 7, 7 \rangle$ and so has growth rate $\gamma(T_0) = \frac{1}{2}(3 + \sqrt{5})$ by [Proposition 1.20](#). But then if $[3, 3, 3, 3, 3, 3, 3] < \sigma$ and T is a tessellation with monomorphic valence sequence σ , then $\gamma(T_0) \leq \gamma(T)$, by [Theorem 2.7](#). We proceed then by exhaustion: there are only finitely many forms of valence sequences of length at most 6. The Appendix contains an exhaustive classification of realizable valence sequences as monomorphic or polymorphic. For each form of monomorphic valence sequence, the least rate of growth is either determined or bounded below. The minimum growth rate of a minimal representative of each form is listed in [Table 1](#). Of these forms, $[4, 6, 14]$ and $[3, 4, 7, 4]$ have the least rate of growth, shown to be $\frac{1}{2}(1 + \sqrt{5})$ in the Appendix. \square

Remark 2.14. It is interesting to observe that the two tessellations realizing the minimum exponential growth rate are closely related. The face-homogeneous tessellation with valence sequence $[4, 6, 14]$ can be realized by the classical tiling of the

Class	σ	$\gamma(T_\sigma) \approx$	Class	σ	$\gamma(T_\sigma) \approx$
$[p, p, p]$	$[7, 7, 7]$	2.6180	$[p, p, q, r, q]$	$[4, 4, 6, 5, 6]$	6.6650
$[3, p, p]$	$[3, 14, 14]$	2.6180	$[3, p, q, q, p]$	$[3, 4, 6, 6, 4]$	4.9911
$[p, p, q]$	$[6, 6, 7]$	1.722	$[p, q, r, s, t]$	$[4, 6, 10, 12, 8]$	14.5753
$[4, \mathbf{p}, \mathbf{q}]$	$[4, \mathbf{6}, \mathbf{14}]$	1.6180	$[p, p, p, p, p, p]$	$[4, 4, 4, 4, 4, 4]$	5.8284
$[p, q, r]$	$[6, 8, 10]$	3.4789	$[p, p, q, p, p, q]$	$[4, 4, 5, 4, 4, 5]$	7.1347
$[p, p, p, p]$	$[5, 5, 5, 5]$	3.7320	$[p, q, p, q, p, q]$	$[4, 5, 4, 5, 4, 5]$	7.8729
$[p, p, q, q]$	$[4, 4, 6, 6]$	3.4081	$[p, q, q, p, r, r]$	$[6, 4, 4, 6, 8, 8]$	13.1291
$[3, p, 3, p]$	$[3, 7, 3, 7]$	2.6180	$[p, q, p, r, q, r]$	$[4, 5, 4, 6, 5, 6]$	9.8115
$[p, q, p, q]$	$[4, 5, 4, 5]$	2.6180	$[p, q, r, p, q, r]$	$[4, 6, 8, 4, 6, 8]$	13.5612
$[3, p, 4, p]$	$[3, 6, 4, 6]$	2.9655	$[p, q, p, r, s, r]$	$[4, 5, 4, 6, 7, 6]$	10.9033
$[3, \mathbf{p}, \mathbf{q}, \mathbf{p}]$	$[3, \mathbf{4}, \mathbf{7}, \mathbf{4}]$	1.6180	$[p, q, r, p, s, t]$	$[4, 6, 8, 4, 10, 12]$	18.1174
$[p, q, p, r]$	$[4, 5, 4, 6]$	3.1462	$[p, q, r, s, t, u]$	$[4, 6, 10, 14, 12, 8]$	23.9963
$[p, q, r, s]$	$[4, 6, 10, 8]$	7.0367	$[3, p, p, 3, p, p]$	$[3, 4, 4, 3, 4, 4]$	4.3306
$[p, p, p, p, p]$	$[4, 4, 4, 4, 4]$	3.7320	$[3, p, 3, p, 3, p]$	$[3, 4, 3, 4, 3, 4]$	3.7320
$[3, 3, 3, 3, p]$	$[3, 3, 3, 3, 7]$	1.7553	$[3, 3, 3, p, q, p]$	$[3, 3, 3, 4, 5, 4]$	4.0265
$[3, 3, 3, p, p]$	$[3, 3, 3, 6, 6]$	3.0217	$[3, p, q, 3, q, p]$	$[3, 4, 6, 3, 6, 4]$	6.8091
$[3, 3, p, 3, p]$	$[3, 3, 5, 3, 5]$	2.6180	$[3, p, 3, q, 3, r]$	$[3, 4, 3, 5, 3, 6]$	5.6723
$[3, 3, p, 3, q]$	$[3, 3, 4, 3, 5]$	1.9318	$[3, p, q, r, q, p]$	$[3, 4, 6, 5, 6, 4]$	8.0601

TABLE 1. Table of the least exponential growth rate within each monomorphic class of valence sequences. All rates of growth have been truncated at four decimal places rather than being rounded.

hyperbolic plane by triangles with interior angles $\frac{\pi}{2}$, $\frac{\pi}{3}$, and $\frac{\pi}{7}$. Moreover, a face-homogeneous tessellation with valence sequence $[3, 4, 7, 4]$ is the subgraph of one with valence sequence $[4, 6, 14]$ obtained by the deletion of all edges joining 6-valent and 14-valent vertices. Many artistic renderings of these tilings exist, and can be found on web sites regarding the $(2, 3, 7)$ -triangle group, the Order-7 triangular tiling, or triangular tilings of the hyperbolic plane, including Wikipedia.

3. POLYMORPHIC VALENCE SEQUENCES

3.1. Polymorphic Valence Sequences. With respect to the ordering of cyclic sequences, the least polymorphic valence sequence with positive angle excess is $[4, 4, 4, 5]$; that is to say, every cyclic sequence σ such that $\sigma < [4, 4, 4, 5]$ is either not realizable as a tessellation, is realizable only by a finite map or a Euclidean tessellation, or is monomorphic. While all valence sequence of length 3 are monomorphic, k -covalent polymorphic valence sequences abound for $k \geq 4$. The following theorem gives a simple sufficient condition under which a realizable valence sequence is polymorphic.

Proposition 3.1. *Let $\sigma = [p_0, \dots, p_{k-1}]$ be the valence sequence of a face-homogeneous tessellation $T \in \mathcal{G}_{4,4} \cup \mathcal{G}_{3+,5}$. If there exist distinct $i, j \in \{0, \dots, k-1\}$ such that $p_i, p_{i+1} \geq 4$ and either*

- (1) $p_i = p_j, p_{i+1} = p_{j+1}$, and $p_{i+2} \neq p_{j+2}$, or
- (2) $p_i = p_j, p_{i+1} = p_{j-1}$, and $p_{i+2} \neq p_{j-2}$,

then σ is polymorphic.

Proof. As the only two forms of valence sequences of length $k = 4$ that satisfy the hypothesis, namely $[p, p, p, q]$ and $[p, p, q, r]$, are polymorphic (see Appendix), we

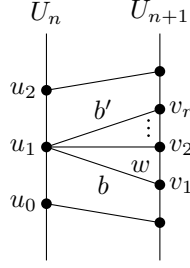


FIGURE 15. A configuration of faces demonstrating polymorphicity.

assume that $k \geq 5$. Also, since condition (2) is identical to (1) save for orientation within the cyclic sequence, it suffices to assume that there are distinct i, j such that (1) holds. Furthermore, we may assume $i = 0$ due to the rotational equivalence of valence sequences.

Since $k \geq 5$, there exists for some n a face in F_n incident with three consecutive vertices $u_0, u_1, u_2 \in U_n$ with valence $\rho(u_m) = p_m$ for $m = 0, 1, 2$. Let b be the brick in F_{n+1} incident with the edge u_0u_1 , and let b' be the brick (or perhaps notched brick if $p_2 = 3$) in F_{n+1} incident with the edge u_1u_2 . Let v_1, \dots, v_r be the vertices in U_{n+1} incident with u_1 in consecutive order, so that v_1 is incident with b and v_r is incident with b' . Thus $r = p_1 - 2 \geq 2$. If σ contains a subsequence $[q, p_1, p_2]$ with $q \neq p_0$, then $\rho(v_r)$ may equal either p_0 or q , resulting in a choice of face types for b' , and we're done. Otherwise we must have $\rho(v_r) = p_0$, which forces the vertex v_{r-2} and subsequent alternate neighbors of u_1 in U_{n+1} also to be p_0 -valent.

If p_1 is even, then $\rho(v_1)$ may equal either p_2 or p_{j+2} in which case the wedge $w \in F_{n+1}$ incident with vertices v_1, u_1, v_2 may be of either type \mathbf{w}_2 or type \mathbf{w}_{j+2} , and T is polymorphic. (See [Figure 15](#).)

If p_1 is odd, then working backward as in the even case forces $\rho(v_1) = p_0$, which implies that either $p_0 = p_2$ or $p_0 = p_{j+2}$, and without loss of generality, we assume the former. Now we may assign $\rho(v_2)$ to be either p_0 or p_{j+2} , and the argument proceeds as in the even case. \square

The existence of polymorphic valence sequences considerably complicates the computation of growth rates of face-homogeneous tessellations. The above proof suggests that, unlike in the monomorphic case, polymorphic valence sequences may admit many different accretion rules, as we illustrate in the next section.

3.2. Two non-isomorphic tessellations with the same valence sequence.

The minimal polymorphic valence sequence under the partial order on cyclic sequences, namely $[4, 4, 4, 5]$, is unfortunately not amenable to study via our methods. In fact, there is no well-defined transition matrix between coronas, and this problem is shared by all valence sequences of the form $[4, 4, 4, q]$ for $q > 4$. However, $[4, 4, 6, 8]$ provides us with the opportunity to investigate two distinct (but related) accretion rules.

The valence sequence $[4, 4, 6, 8]$ is representative of form $[p, p, q, r]$ discussed in the Appendix. As every face is incident with a pair of adjacent 4-valent vertices,

every realization of this valence sequence contains a countable infinity of pairwise-disjoint double rays, each induced exclusively by 4-valent vertices. **Figure 16** (A) shows a strip-like patch bordering a double ray of 4-valent vertices. To obtain **Figure 16** (B) from this (or vice versa), one can fix pointwise the half-plane on one side of the double ray while translating the half-plane on the other side along one edge of the double ray.

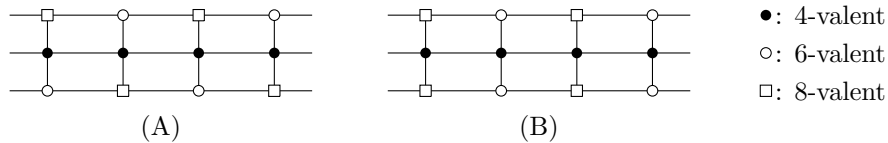


FIGURE 16. Two non-isomorphic patches of a tessellation with valence sequence $[4, 4, 6, 8]$, local to double rays of 4-valent vertices.

To construct still other such (non-isomorphic) realizations, one can choose to “translate” along any one of these double rays by leaving fixed the half-plane on one side of the double ray but translating the half-plane on the other side one edge. Since there exists a countable infinity of double rays along which one may choose to translate one or the other or neither of the adjacent half-planes, there exists an uncountable class of pairwise non-isomorphic tessellations that all have the same valence sequence $[4, 4, 6, 8]$.

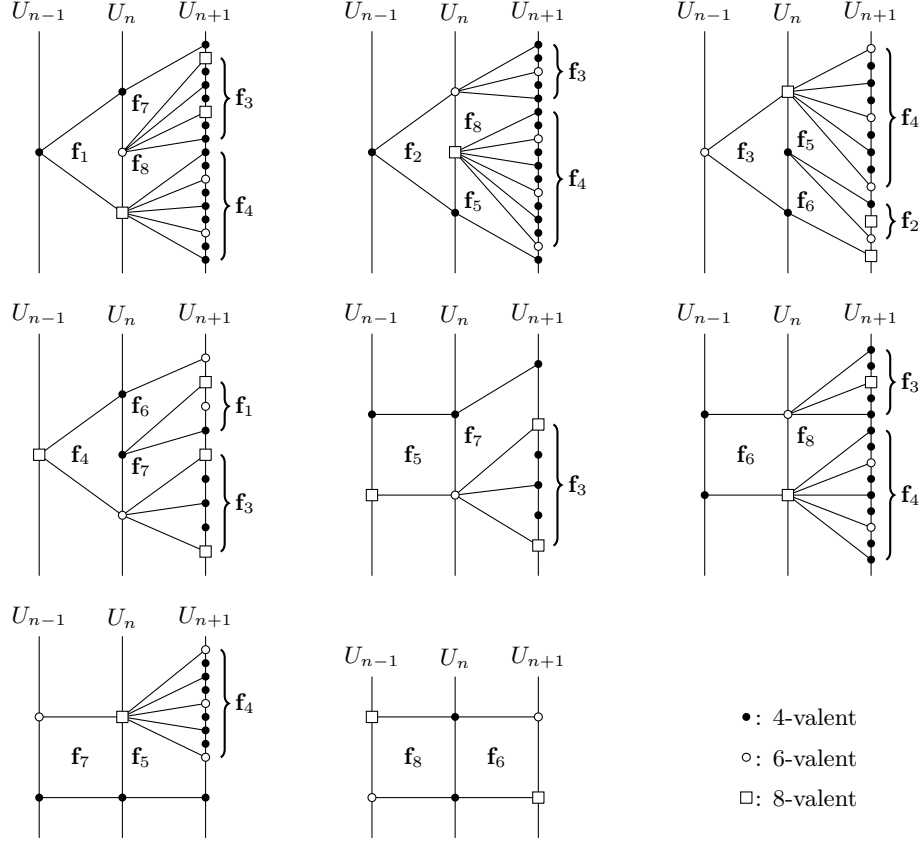
While one might expect that all tessellations having the same valence sequence always have the same growth rate, we show that this is not so.

We begin by observing that every 4-valent vertex in a face-homogeneous tessellation with valence sequence $[4, 4, 6, 8]$ is adjacent to two other 4-valent vertices and two vertices with valences 6 or 8; thus any given 4-valent vertex either has exactly one 6-valent and one 8-valent neighbor, has two 6-valent neighbors, or has two 8-valent neighbors. Furthermore, every 4-valent vertex lies on a double ray (two-way infinite path) of 4-valent vertices; if one vertex along this path has a 6-valent neighbor and an 8-valent neighbor, then so does every other vertex along the double ray. This is the behavior demonstrated in **Figure 16** (A).

If the local configuration specified in **Figure 16** (A) is enforced along every double ray of 4-valent vertices, then the tessellation obtained is unique; let this tessellation be T_1 . We can then construct offspring diagrams for T_1 as given in **Figure 17**. It is interesting to note that T_1 is the dual of the Cayley graph of the group with presentation

$$G_1 = \langle a, b, c \mid a^2 = b^2 = c^2 = (aba)^2 = (bc)^3 = (caba)^4 = 1 \rangle.$$

Encoding the offspring diagrams into a matrix, we obtain the transition matrix M_1 of T_1 given below. The four entries underlined in the matrix are the only entries

FIGURE 17. Offspring diagrams for T_1

which change between this example and the next example, T_2 , that we construct.

$$M_1 = \begin{bmatrix} 0 & 0 & 0 & 1 & 0 & 0 & 0 & 0 \\ 0 & 0 & 1 & 0 & 0 & 0 & 0 & 0 \\ 3 & 1 & 0 & 1 & 1 & 1 & 0 & 0 \\ 2 & 5 & 2 & 0 & 0 & 2 & 2 & 0 \\ 0 & 1 & 1 & 0 & 0 & 0 & 1 & 0 \\ 0 & 0 & 1 & 1 & 0 & 0 & 0 & 1 \\ 1 & 0 & 0 & 1 & 1 & 0 & 0 & 0 \\ 1 & 1 & 0 & 0 & 0 & 1 & 0 & 0 \end{bmatrix}$$

The characteristic polynomial of M_1 is

$$f_1(z) = (z - 1)(z + 1)(z^2 + 3z + 1)(z^4 - 3z^3 - 4z^2 - 3z + 1),$$

which in turn gives that the eigenvalue of maximum modulus of M_1 is

$$\lambda_1 = \frac{1}{4} \left(3 + \sqrt{33} + 2\sqrt{\frac{13}{2} + \frac{3\sqrt{33}}{2}} \right) \approx 4.13016.$$

Considering again the double-rays of 4-valent vertices, it is trivial to note that if a vertex on such a double ray has two 6-valent neighbors in the tessellation, then both vertices adjacent to it in the double-ray have two 8-valent neighbors. This local behavior is shown in Figure 16 (B).

If this pattern is extended to all such double rays we obtain the tessellation T_2 , which is also the dual of a Cayley graph. The underlying group of this Cayley graph is is

$$G_2 = \langle a, b, c, d \mid a^2 = b^2 = c^2 = d^2 = (ab)^2 = (ad)^2 = (cd)^3 = (bc)^4 \rangle.$$

The growth behavior of T_2 differs from that of T_1 only in the offspring of faces of types \mathbf{f}_3 and \mathbf{f}_4 , as shown in the offspring diagrams in Figure 18.

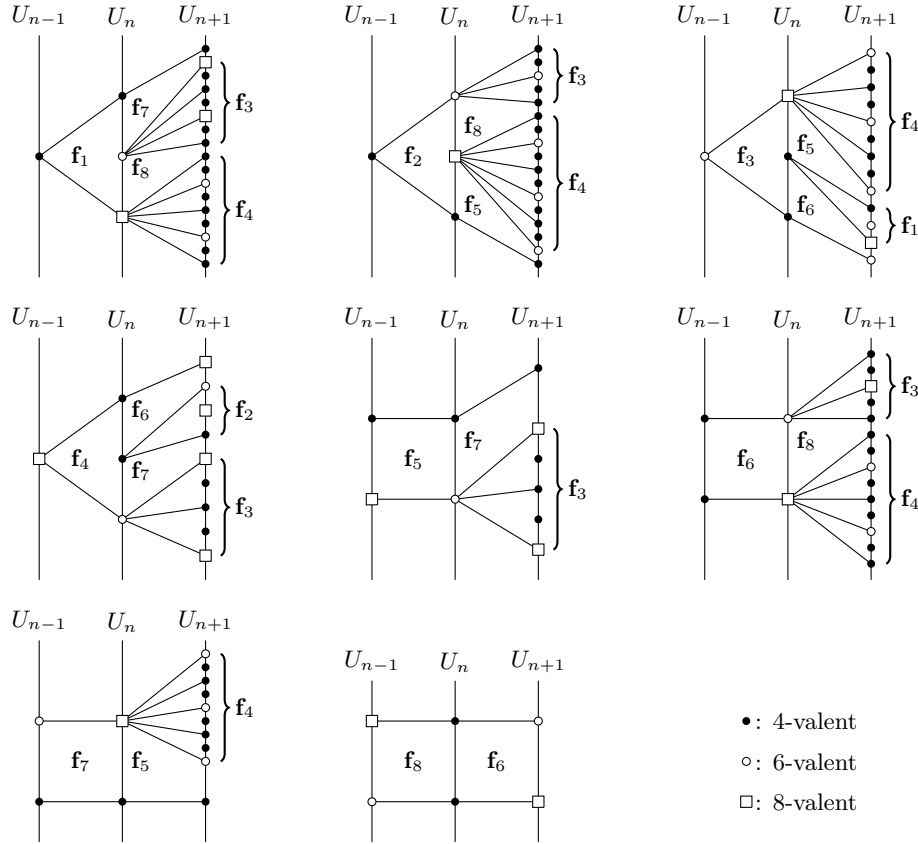


FIGURE 18. Offspring diagrams for T_2

The effect of the change of offspring of types \mathbf{f}_2 and \mathbf{f}_3 in the transition matrix of T_2 lies only in the underlined 2×2 submatrix of M_1 , while the remainder of the

matrix M_2 remains identical to M_1 . Hence we have

$$M_2 = \begin{bmatrix} 0 & 0 & \underline{1} & \underline{0} & 0 & 0 & 0 & 0 \\ 0 & 0 & \underline{0} & \underline{1} & 0 & 0 & 0 & 0 \\ 3 & 1 & 0 & 1 & 1 & 1 & 0 & 0 \\ 2 & 5 & 2 & 0 & 0 & 2 & 2 & 0 \\ 0 & 1 & 1 & 0 & 0 & 0 & 1 & 0 \\ 0 & 0 & 1 & 1 & 0 & 0 & 0 & 1 \\ 1 & 0 & 0 & 1 & 1 & 0 & 0 & 0 \\ 1 & 1 & 0 & 0 & 0 & 1 & 0 & 0 \end{bmatrix}.$$

The characteristic polynomial of M_2 is

$$f_2(z) = (z - 1)^2 (z^6 + 2z^5 - 15z^4 - 40z^3 - 15z^2 + 2z + 1).$$

As polynomials of degree 6 are unfortunately not solvable by radicals, we obtain by approximation that the root of maximum modulus is $\lambda_2 \approx 4.14659$.

As these growth rates are nearly the same, there is only a small difference in corona sizes in the first several coronas. However, the size of the coronas and distribution of face types differs greatly farther from the root. To demonstrate this, [Table 2](#) gives corona sizes in Bilinski diagrams of T_1 and of T_2 , both rooted at 4-valent vertices. Note that the sizes of the coronas of T_2 dominate those of T_1 only after the 13th corona.

3.3. Some conjectures. Ideally, all tessellations realizing the same polymorphic valence sequence would have the same growth rate. The example of valence sequence $[4, 4, 6, 8]$ illustrates that this is not so. We propose the following definitions.

Definition 3.2. Let σ be some polymorphic valence sequence, and define \mathcal{T}_σ to be the set of isomorphism classes of face-homogeneous tessellations with valence sequence σ . Let

$$(22) \quad \underline{\lambda}_\sigma = \inf\{\gamma(T) : T \in \mathcal{T}_\sigma\},$$

$$(23) \quad \bar{\lambda}_\sigma = \sup\{\gamma(T) : T \in \mathcal{T}_\sigma\},$$

$$(24) \quad \mathcal{L}_\sigma = \{T : T \in \mathcal{T}_\sigma \text{ and } \gamma(T) = \underline{\lambda}_\sigma\}, \text{ and}$$

$$(25) \quad \mathcal{H}_\sigma = \{T : T \in \mathcal{T}_\sigma \text{ and } \gamma(T) = \bar{\lambda}_\sigma\}$$

We conjecture that the lower and upper bounds $\underline{\lambda}_\sigma$ and $\bar{\lambda}_\sigma$ for any given valence sequence σ are realized.

Conjecture 3.3. *Let σ be a polymorphic valence sequence. Then \mathcal{L}_σ and \mathcal{H}_σ are nonempty.*

Bearing in mind the polymorphic valence sequence $[4, 4, 6, 8]$ analyzed in [Section 3.2](#), we propose as a conjecture the following sharper version of [Theorem 2.7](#).

Conjecture 3.4. *Let σ_1 and σ_2 be valence sequences such that $\sigma_1 < \sigma_2$. Then*

$$(26) \quad \bar{\lambda}_{\sigma_1} \leq \underline{\lambda}_{\sigma_2}.$$

In the spirit of the famous quote of the late George Pólya [\[12\]](#) (“If you can’t solve a problem, then there is an easier problem you can solve: find it.”), we offer the following (perhaps) easier conjecture.

n	$ F_{1,n} $	$ F_{2,n} $	n	$ F_{1,n} $	$ F_{2,n} $
1	4	4	29	1.20050×10^{18}	1.27748×10^{18}
2	30	28	30	4.95826×10^{18}	5.29701×10^{18}
3	110	108	31	2.04784×10^{19}	2.19652×10^{19}
4	494	468	32	8.45791×10^{19}	9.10786×10^{19}
5	1938	1900	33	3.49325×10^{20}	3.77673×10^{20}
6	8272	7956	34	1.44277×10^{21}	1.56603×10^{21}
7	33464	32868	35	5.95887×10^{21}	6.49377×10^{21}
8	140046	136380	36	2.46111×10^{22}	2.69268×10^{22}
9	573610	565956	37	1.01648×10^{23}	1.11655×10^{23}
10	2.38167×10^6	2.34358×10^6	38	4.19821×10^{23}	4.62986×10^{23}
11	9.80378×10^6	9.73259×10^6	39	1.73393×10^{24}	1.91983×10^{24}
12	4.05773×10^7	4.02988×10^7	40	7.16140×10^{24}	7.96071×10^{24}
13	1.67365×10^8	1.67318×10^8	41	2.95777×10^{25}	3.30099×10^{25}
14	6.91836×10^8	6.93034×10^8	42	1.22161×10^{26}	1.36878×10^{26}
15	2.85585×10^9	2.87639×10^9	43	5.04544×10^{26}	5.67580×10^{26}
16	1.17992×10^{10}	1.19181×10^{10}	44	2.08385×10^{27}	2.35352×10^{27}
17	4.87218×10^{10}	4.94504×10^{10}	45	8.60662×10^{27}	9.75910×10^{27}
18	2.01257×10^{11}	2.04947×10^{11}	46	3.55467×10^{28}	4.04670×10^{28}
19	8.31149×10^{11}	8.50179×10^{11}	47	1.46814×10^{29}	1.67800×10^{29}
20	3.43297×10^{12}	3.52419×10^{12}	48	6.06363×10^{29}	6.95799×10^{29}
21	1.41782×10^{13}	1.46172×10^{13}	49	2.50438×10^{30}	2.88520×10^{30}
22	5.85596×10^{13}	6.05990×10^{13}	50	1.03435×10^{31}	1.19637×10^{31}
23	2.41857×10^{14}	2.51322×10^{14}	60	1.49395×10^{37}	1.79797×10^{37}
24	9.98918×10^{14}	1.04199×10^{15}	70	2.15777×10^{43}	2.70207×10^{43}
25	4.12567×10^{15}	4.32117×10^{15}	80	3.11654×10^{49}	4.06079×10^{49}
26	1.70397×10^{16}	1.79166×10^{16}	90	4.50134×10^{55}	6.10274×10^{55}
27	7.03766×10^{16}	7.42979×10^{16}	100	6.50145×10^{61}	9.17148×10^{61}
28	2.90667×10^{17}	3.08066×10^{17}	200	2.56861×10^{123}	5.38996×10^{123}

TABLE 2. Corona sizes in T_1 and T_2 ; emphasis on the 14th corona beyond which the coronas of T_2 appear to exceed in size those of T_1 .

Conjecture 3.5. *Let σ_1 and σ_2 be valence sequences with $\sigma_1 < \sigma_2$. Then*

$$(27) \quad \Delta_{\sigma_1} \leq \Delta_{\sigma_2}.$$

If **Conjecture 3.4** holds, then one could delete the condition of monomorphicity from the hypothesis of **Theorem 2.7** and therefore from **Theorem 2.13** as well. Moreover, the Appendix could be much abbreviated. For example, one could eliminate the exhaustive consideration of the many forms of 6-covalent face-homogeneous tessellations listed and treated there by observing that the least valence sequence σ of length 6 with $\eta(\sigma) > 0$ is $[3, 3, 3, 3, 3, 4]$. Thus, if any tessellation with the polymorphic valence sequence $[3, 3, 3, 3, 3, 4]$ has growth rate greater than $\frac{1}{2}(1 + \sqrt{5})$, then so does every tessellation with valence sequence $\sigma \geq [3, 3, 3, 3, 3, 4]$.

Beyond these conjectures, there are some open questions. Consider the partially ordered set of valence sequences, and in particular, the poset consisting of the polymorphic valence sequences.

Question 3.6. *As one goes up a chain in the poset, do intervals of the form $[\Delta_\sigma, \bar{\lambda}_\sigma]$ become (asymptotically) longer?*

Question 3.7. *Do the intervals in the complement of*

$$\bigcup_{\sigma} \{[\underline{\lambda}_{\sigma}, \bar{\lambda}_{\sigma}] : \sigma \text{ is polymorphic}\}$$

become arbitrarily long?

If the answer to [Question 3.7](#) is negative, we pose the following.

Question 3.8. *If x is a sufficiently large real number, is there always some polymorphic valence sequence σ such that $\underline{\lambda}_{\sigma} \leq x \leq \bar{\lambda}_{\sigma}$?*

Or, on the other hand,

Question 3.9. *Do there exist polymorphic sequences σ, τ such that*

$$[\underline{\lambda}_{\sigma}, \bar{\lambda}_{\sigma}] \cap [\underline{\lambda}_{\tau}, \bar{\lambda}_{\tau}] \neq \emptyset?$$

REFERENCES

- [1] Stanko Bilinski, *Homogene mreže ravnine*, Rad Jugoslav. Akad. Znanosti i Umjetnosti **271** (1948), 145–255.
- [2] ———, *Homogene Netze der Eben*, Bull. Internat. Acad. Yougoslave. Cl. Sci. Math. Phys. Tech. (N.S.) **2** (1949), 63–111.
- [3] Jennifer A. Bruce and Mark E. Watkins, *Concentric bilinski diagrams*, Australasian J. Combin **30** (2004), 161–174.
- [4] Stephen J. Graves, *Growth of tessellations*, Ph.D. Thesis, 2009.
- [5] ———, *Tessellations with arbitrary growth rates*, Discrete Math **310** (2010), 2435–2439.
- [6] Stephen J. Graves, Tomaz Pisanski, and Mark E. Watkins, *Growth of edge-transitive tessellations*, SIAM J. Discrete Math **23** (2008), 1–18.
- [7] Stephen J. Graves and Mark E. Watkins, *Appendix to “Growth of face-homogeneous tessellations”*, arXiv.
- [8] Branko Grünbaum and G. C. Shephard, *Edge-transitive planar graphs*, J. Graph Theory **11** (1987), 141–155.
- [9] ———, *Tilings and Patterns*, W. H. Freeman & Company, New York, 1987.
- [10] Judith Flagg Moran, *The growth rate and balance of homogeneous tilings in the hyperbolic plane*, Discrete Math **173** (1997), 151–186.
- [11] Peter Niemeyer and Mark E. Watkins, *Geodesic rays and fibers in one-ended planar graphs*, J. Combin. Theory Ser. B **69** (1997), 142–163.
- [12] George Pólya, *Mathematical discovery on understanding, learning, and teaching problem solving, volume i*, John Wiley & Sons, 1962.
- [13] Jana Šiagiová and Mark E. Watkins, *Covalence sequences of planar vertex-homogeneous maps*, Discrete Math. **307** (2007), 599–614.

DEPARTMENT OF MATHEMATICS, UNIVERSITY OF TEXAS AT TYLER, TYLER, TX 75799

E-mail address: `sgraves@uttyler.edu`

DEPARTMENT OF MATHEMATICS, SYRACUSE UNIVERSITY, SYRACUSE, NY 13244-1150

E-mail address: `mewatkin@syr.edu`

**APPENDIX TO
“GROWTH OF FACE-HOMOGENEOUS TESSELLATIONS”**

STEPHEN J. GRAVES AND MARK E. WATKINS

1. INTRODUCTION

This article is the APPENDIX to our paper “Growth of Face-Homogeneous Tessellations” which will appear in *Ars Mathematica Contemporanea* [1]. Its purpose is to make available to the interested reader many of the details of the numerous, often routine, calculations necessary to verify some of the results in the cited article. These calculations also provide a classification of all general forms of valence sequences of lengths 3, 4, 5, and 6.

All external references in this APPENDIX are to items in [1], and are cited with [1] preceding the reference, e.g., [1]Definition 1.9. The reader should consult [1] for any unfamiliar terminology.

Notational convention. Throughout this APPENDIX, and without further mention, the symbol σ denotes a realizable valence sequence having positive angle excess, i.e., $\eta(\sigma) > 0$ (see [1]Definition 1.9). Moreover, unless explicitly stated otherwise, when σ is given, the symbol T denotes a face-homogeneous tessellation whose valence sequence is σ .

As explained in [1], when the offspring diagrams for a given valence sequence σ are determined solely by σ itself, then σ is *monomorphic*, and so the growth rates of such tessellations are explicit functions of the valence sequence. In those cases where a functional value is not computationally feasible, a lower bound for the growth rates of all tessellations of the given form is determined by comparing the growth rates of the minimal valence sequences having the given form. On the other hand, the possibility of two or more consistent offspring types of a given face type is sufficient for σ to be *polymorphic*.

Many computations throughout were obtained or verified using *Wolfram Mathematica*.

Remark 1.1. It is frequently the case that the characteristic polynomial of a transition matrix contains a factor of the form $z^4 - az^3 - bz^2 - az + 1$; these “palindromic” polynomials have a root of maximum modulus

$$\frac{1}{4} \left(\left(a + \sqrt{a^2 + 4b + 8} \right) + \sqrt{4b - 8 + a \left(a + \sqrt{a^2 + 4b + 8} \right)} \right)$$

when $a, b > 0$.

2. CLASSIFICATION OF FACE-HOMOGENEOUS TESSELLATIONS WITH VALENCE SEQUENCES OF LENGTH 3

Recall that all 3-covalent tessellations have monomorphic valence sequences by [1]Proposition 2.5. There are exactly three such forms: $[p, p, p]$, $[p, p, q]$, and $[p, q, r]$ (cf. the last paragraph of [1]Section 1.3).

Proposition 2.1. *If $\sigma = [p, p, p]$, then $p \geq 7$ and*

$$\gamma(T) = \frac{1}{2} \left[(p-4) + \sqrt{(p-4)^2 - 4} \right].$$

Proof. Since $\eta(\sigma) > 0$, we must have $p \geq 7$. Moreover, T is edge-homogeneous with edge-symbol $\langle p, p; 3, 3 \rangle$. Hence by [1]Proposition 1.17,

$$\begin{aligned} \gamma(T) &= \frac{1}{2} \left[(p-2) - 2 + \sqrt{(p-2)^2 - 4(p-2)} \right] \\ &= \frac{1}{2} \left[(p-4) + \sqrt{(p-4)^2 - 4} \right]. \end{aligned}$$

□

Often special attention is required when a term in the valence sequence equals 3.

Proposition 2.2. *If $\sigma = [p, p, 3]$, then $p \geq 14$ and is even, and*

$$\gamma(T) = \frac{1}{4} \left(p - 8 + \sqrt{(p-8)^2 - 16} \right).$$

Proof. For σ to be realizable, p must be even. By [1]Proposition 1.10, $p > 12$. Hence $p \geq 14$. Take T_0 to be a face-homogeneous tessellation with valence sequence $[p, p, 3]$ labeled as a Bilinski diagram about a p -valent root. Let v_0 be an arbitrary 3-valent vertex, and label the three p -valent vertices adjacent to v_0 by v_1, v_2 , and v_3 . Then the induced graph of $\{v_0, v_1, v_2, v_3\}$ is isomorphic to the complete graph K_4 . Since every face of T_0 is incident with exactly one 3-valent vertex, each face f lies in exactly one of these planar embeddings of K_4 .

Let T_1 be the tessellation remaining when all 3-valent vertices and their incident edges are removed from T_0 . Then T_1 is face-homogeneous with valence sequence $[\frac{p}{2}, \frac{p}{2}, \frac{p}{2}]$. (This is demonstrated for $p = 16$ in Figure 2.1.)

The corona boundaries in T_0 and T_1 are in close correspondence but are not identical, as T_1 is uniformly concentric while T_0 is not. Taking $F_{i,n}$ to be the i^{th} corona of T_i , we see from the Figure 2.1 that there are two types of faces in T_1 : those of type \mathbf{f}_1 are incident with a single vertex in U_{n-1} and two vertices in U_n ; those of type \mathbf{f}_2 are incident with two vertices in U_{n-1} and one vertex in U_n . Each face of type \mathbf{f}_1 in T_1 corresponds to exactly two faces of T_0 , and each face of type \mathbf{f}_2 in T_1 corresponds to exactly four faces of T_0 . Since the transition matrix of T_1 is

$$M = \begin{bmatrix} \frac{p}{2} - 4 & -1 \\ 1 & 0 \end{bmatrix},$$

we have that

$$|F_{0,n}| = \begin{bmatrix} 2 \\ 4 \end{bmatrix} \cdot M^{n-1} \begin{bmatrix} p/2 \\ 0 \end{bmatrix}$$

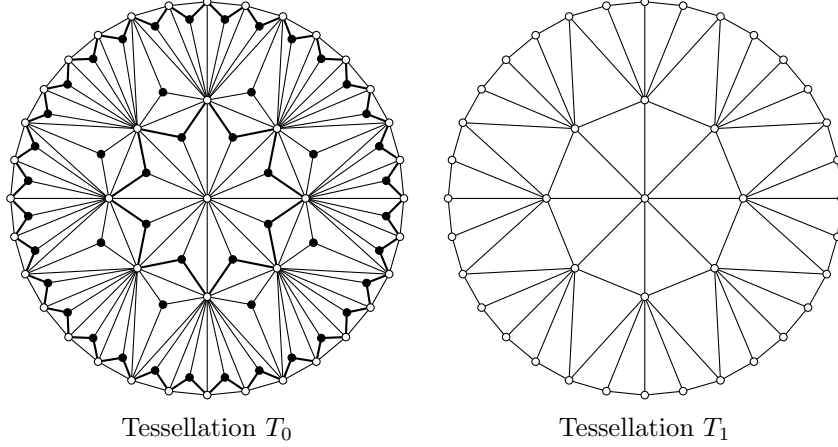


FIGURE 2.1. Tessellation T_0 is face-homogeneous with valence sequence $[16, 16, 3]$; T_1 is the tessellation remaining when all 3-valent vertices and their incident edges are removed from T_0 and is face-homogeneous with valence sequence $[8, 8, 8]$. Edges belonging to both the coronas $\langle F_{0,n} \rangle$ and $\langle F_{0,n+1} \rangle$ of T_0 are darkened.

via the standard dot product. So we have by [Proposition 2.1](#),

$$\begin{aligned} \gamma(T_0) = \gamma(T_1) &= \frac{1}{2} \left[\frac{p}{2} - 4 + \sqrt{\left(\frac{p}{2} - 4\right)^2 - 4} \right] \\ &= \frac{1}{4} \left[p - 8 + \sqrt{(p-8)^2 - 16} \right]. \end{aligned}$$

□

Proposition 2.3. *If $\sigma = [p, p, q]$ for $q \geq 4$, then $p \geq 6$ and is even, and*

$$\gamma(T) = \frac{1}{4} \left[\left(a + \sqrt{a^2 + 4b + 8} \right) + \sqrt{4b - 8 + a \left(a + \sqrt{a^2 + 4b + 8} \right)} \right]$$

where $a = \frac{p-4}{2}$ and $b = \frac{(p-4)(q-4)-4}{2}$.

Proof. Since σ is realizable, p must be even and $\frac{2}{p} + \frac{1}{q} < \frac{1}{2}$. Hence $p \geq 6$. The offspring diagrams for this vertex sequence are shown in [Figure 2.2](#).

We note that the presence of faces of types \mathbf{f}_2 or \mathbf{f}_3 in F_n decreases by one the number of faces of each of types \mathbf{f}_0 and \mathbf{f}_1 in F_{n+1} . This gives the transition matrix

$$M = \begin{bmatrix} \frac{1}{2}(p-4) & p-4 & -1 & 0 \\ \frac{1}{2}(q-4) & 0 & 0 & -1 \\ 1 & 0 & 0 & 0 \\ 0 & 1 & 0 & 0 \end{bmatrix}.$$

The characteristic polynomial of M is palindromic:

$$\chi(z) = z^4 - \left(\frac{p-4}{2}\right) z^3 - \left(\frac{(p-4)(q-4)-4}{2}\right) z^2 - \left(\frac{p-4}{2}\right) z + 1.$$

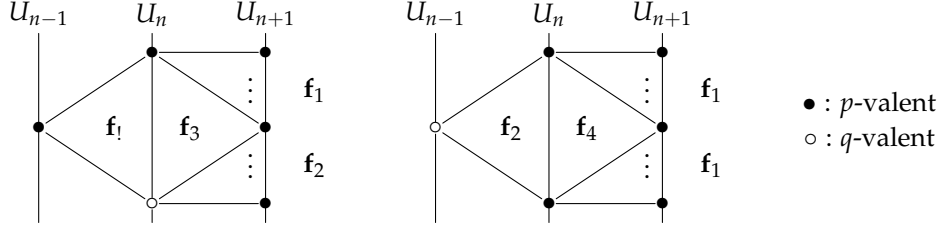


FIGURE 2.2. Offspring diagrams for a face-homogeneous tessellation with valence sequence $[p, p, q]$ and $q \geq 4$.

Hence by [Remark 1.1](#), the growth rate of T is as stated. \square

The following proposition proved in [1] as Example 2.11 is restated here for the sake of completeness.

Proposition 2.4. *If $\sigma = [4, p, q]$, then*

$$\gamma(T) = \frac{1}{4} \sqrt{[2(p-4)(q-4) - 16] + 2\sqrt{(p-4)^2(q-4)^2 - 16(p-4)(q-4)}}.$$

\square

Valence sequences of the form $[p, q, r]$ introduce a computational difficulty, since the associated characteristic polynomial has degree 6 and is not solvable by radicals. Hence we are unable to determine a general formula for the growth rate of a face-homogeneous tessellation with valence sequence $[p, q, r]$. However, subject to the condition that the angle excess be positive, the least vertex sequence (in the partial order on cyclic sequences) having this form is $[6, 8, 10]$. Thus if T_0 is a face-homogeneous tessellation with valence sequence $[6, 8, 10]$ and T is a face-homogeneous tessellation with valence sequence $[p, q, r] \geq [6, 8, 10]$, then by [1] Theorem 2.7 we have $\gamma(T_0) \leq \gamma(T)$, since realizable valence sequences of length 3 are monomorphic.

This method of determining the rate of growth of the least element of a class of valence sequences as a lower bound for growth within the class will be used throughout this Appendix whenever the characteristic polynomial of a transition matrix is not readily solvable by radicals.

Proposition 2.5. *If $\sigma = [p, q, r]$, then $\gamma(T) \geq 3.4789$.*

Proof. As the terms are presumed to be distinct, they are all even. By [Proposition 2.4](#), we may assume that they are all ≥ 6 . Then T has offspring diagrams as shown in [Figure 2.3](#).

Thus the transition matrix is

$$M = \begin{bmatrix} 0 & \frac{1}{2}(p-4) & \frac{1}{2}(p-4) & -1 & 0 & 0 \\ \frac{1}{2}(q-4) & 0 & \frac{1}{2}(q-4) & 0 & -1 & 0 \\ \frac{1}{2}(r-4) & \frac{1}{2}(r-4) & 0 & 0 & 0 & -1 \\ 1 & 0 & 0 & 0 & 0 & 0 \\ 0 & 1 & 0 & 0 & 0 & 0 \\ 0 & 0 & 1 & 0 & 0 & 0 \end{bmatrix}$$

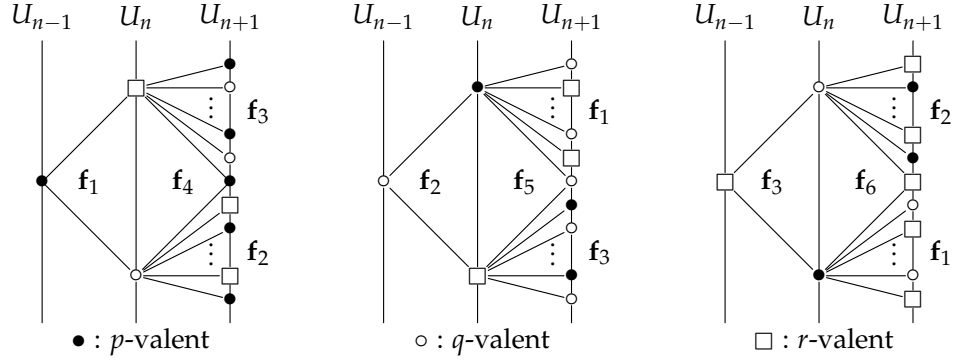


FIGURE 2.3. Offspring diagrams for a face-homogeneous tessellation with valence sequence $[p, q, r]$.

giving characteristic polynomial

$$\chi(z) = z^6 - az^4 - bz^3 - az^2 + 1,$$

with

$$a = \frac{1}{4}(pq + pr + qr - 8p - 8q - 8r + 36) \text{ and}$$

$$b = \frac{1}{4}(p-4)(q-4)(r-4).$$

The least valence sequence in this class is $\sigma_1 = [6, 8, 10]$. If T_1 has valence sequence σ_1 , then numerical approximation of eigenvalues of M gives that $\gamma(T_1) \approx 3.4789$. The argument in the paragraph preceding this proposition gives that, if T is a tessellation with valence sequence $\sigma \geq \sigma_1$, then $\gamma(T) \geq 3.4789$. \square

3. CLASSIFICATION OF FACE-HOMOGENEOUS TESSELLATIONS WITH VALENCE SEQUENCES OF LENGTH 4

The ten forms of valence sequences of length 4 are the following: $[p, p, p, q]$ and $[p, p, q, r]$, which are polymorphic, and $[p, p, p, p]$, $[p, p, q, q]$, $[3, p, 3, p]$, $[p, q, p, q]$, $[p, 3, p, 4]$, $[p, 3, p, r]$, $[p, q, p, r]$, and $[p, q, r, s]$, which are monomorphic.

Proposition 3.1. *The valence sequences $\sigma_1 = [p, p, p, q]$ and $\sigma_2 = [p, p, q, r]$ are polymorphic for all permitted distinct values of p, q, r for which $\eta(\sigma_1), \eta(\sigma_2) > 0$.*

Proof. If $p, q \geq 4$, then $[p, p, p, q]$ is polymorphic by [1]Proposition 3.1. If $\sigma_2 = [p, p, q, r]$ is realizable and $\eta(\sigma_2) > 0$, then the neighbors of an r -valent vertex must be alternately p -valent and q -valent; hence r must be even. Similarly, q must be even. The valences of neighbors of a p -valent vertex must be alternately p and either q or r . So p is also even, and thus $p, q, r \geq 4$ as well. By [1]Proposition 3.1, σ_2 is polymorphic.

The valence sequence $[p, p, p, 3]$ is not subject to [1]Proposition 3.1. In this case, we must have $p \geq 5$, and we refer to Figure 3.1. Since the types of the faces indicated in the figure with a question mark (?) are dependent upon the particular embedding rule chosen for T , $[p, p, p, 3]$ is polymorphic. \square

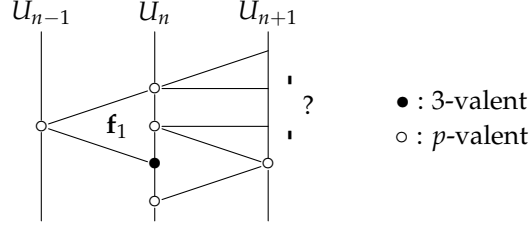


FIGURE 3.1. Offspring of a wedge of type \mathbf{f}_0 in a face-homogeneous tessellation with valence sequence $[p, p, p, 3]$.

Proposition 3.2. *If $\sigma = [p, p, p, p]$, then σ is monomorphic, and*

$$\gamma(T) = (p-3) + \sqrt{(p-3)^2 - 1}.$$

Proof. Clearly $p \geq 5$. Since T is edge-homogeneous with edge-symbol $\langle p, p; 4, 4 \rangle$, we apply [1]Proposition 1.17(1). \square

Proposition 3.3. *If $\sigma = [p, p, q, q]$, then σ is monomorphic, p and q are even, and*

$$\gamma(T) = \frac{1}{8} + \left(p + q + a - 8 + \sqrt{2(p^2 + q^2) + 36pq - 112(p + q) + 2a(p + q - 8)} \right),$$

where $a = \sqrt{p^2 + 34pq + q^2 - 96p - 96q + 256}$.

Proof. The argument that p and q are even is similar to that of Proposition 3.1 above. We see from the offspring diagrams in Figure 3.2 that σ is monomorphic, yielding the transition matrix

$$M = \begin{bmatrix} \frac{p-4}{2} & \frac{3p-10}{2} & \frac{p-4}{2} & 0 & p-4 \\ \frac{3q-10}{2} & \frac{q-4}{2} & \frac{q-4}{2} & q-4 & 0 \\ 1 & 1 & 1 & 0 & 0 \\ 0 & 1 & 0 & 0 & 1 \\ 1 & 0 & 0 & 1 & 0 \end{bmatrix}.$$

The characteristic polynomial of M is

$$\chi(z) = \frac{1}{2}(z-1)(2z^4 - az^3 - bz^2 - az + 2),$$

where $a = p + q - 8$ and $b = 4pq - 10p - 10q + 20$. Thus the growth rate of T is as stated. \square

Proposition 3.4. *If $\sigma = [p, q, p, q]$, then σ is monomorphic, and*

$$\gamma(T) = \frac{1}{2} \left(p - 4 + \sqrt{(p-4)^2 - 4} \right)$$

if $p = 3$, while

$$\gamma(T) = \frac{1}{2} \left(p + q - 6 + \sqrt{(p+q-6)^2 - 4} \right)$$

if $p, q \geq 4$.

Proof. Since $\eta(\sigma) > 0$, we have $q \geq 7$ when $p = 3$. Otherwise we may assume $q > p \geq 4$. Since T is edge-homogeneous with edge-symbol $\langle p, q; 4, 4 \rangle$, we apply [1]Proposition 1.17(2) when $q = 3$ and apply [1]Proposition 1.17(1) $p, q \geq 4$. \square

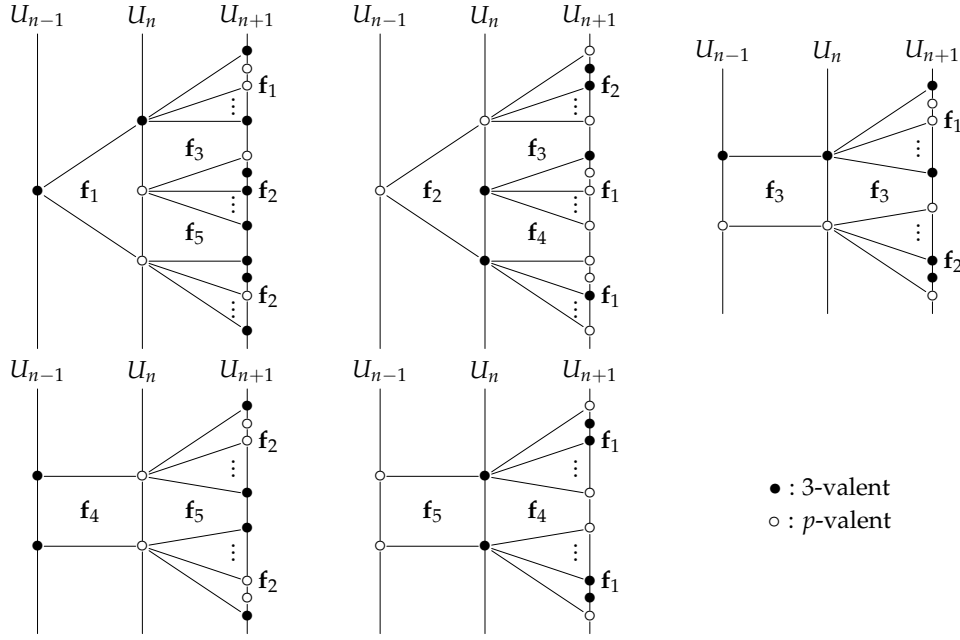


FIGURE 3.2. Offspring diagrams for a face-homogeneous tessellation with valence sequence $[p, p, q]$.

Proposition 3.5. *If $\sigma = [3, p, 4, p]$, then σ is monomorphic with $p \geq 5$ but not uniformly concentric, and*

$$\gamma(T) = \frac{1}{4} \left[p - 3 + \sqrt{p^2 - 4p + 1} + \sqrt{2p^2 - 10p - 6 + 2(p - 3)\sqrt{p^2 - 4p + 1}} \right].$$

Proof. The valence sequence $\sigma = [3, p, 4, p]$ is not uniformly concentric, as seen in the offspring diagrams in [Figure 3.3](#) by the existence of type \mathbf{f}_6 faces. (This valence sequence shows that the sufficient conditions for non-concentricity in [\[1\]](#)Theorem 1.4 are not necessary.) Two faces of type \mathbf{f}_1 in F_n are incident with a common 4-valent vertex in U_n whenever they are both adjacent to a face of type \mathbf{f}_6 in F_n ; the effect of this is that the 4-valent vertex is adjacent to no vertex in U_{n+1} . Hence the induced graph $\langle U_{n+1} \rangle$ must contain a pendant vertex whenever F_n contains a face of type \mathbf{f}_6 . The inclusion of an \mathbf{f}_6 face then removes two \mathbf{f}_4 faces from F_{n+1} to be replaced with an \mathbf{f}_7 face, and converts two \mathbf{f}_1 faces into \mathbf{f}_5 faces. The faces of type \mathbf{f}_7 in F_n generate no offspring in F_{n+1} .

Subject to these considerations, the transition matrix M of T is

$$M = \begin{bmatrix} p-3 & p-4 & p-4 & \frac{1}{2}(p-4) & \frac{1}{2}(p-4) & -2 & 0 \\ 0 & 0 & 0 & 0 & 0 & 0 & 0 \\ 0 & 1 & 0 & 0 & 0 & 0 & 0 \\ 1 & 2 & 0 & 0 & 1 & -2 & 0 \\ 0 & 0 & 2 & 0 & 0 & 2 & 0 \\ \frac{1}{2} & 0 & 0 & \frac{1}{2} & 0 & 0 & 0 \\ 0 & 0 & 0 & 0 & 0 & 1 & 0 \end{bmatrix}.$$

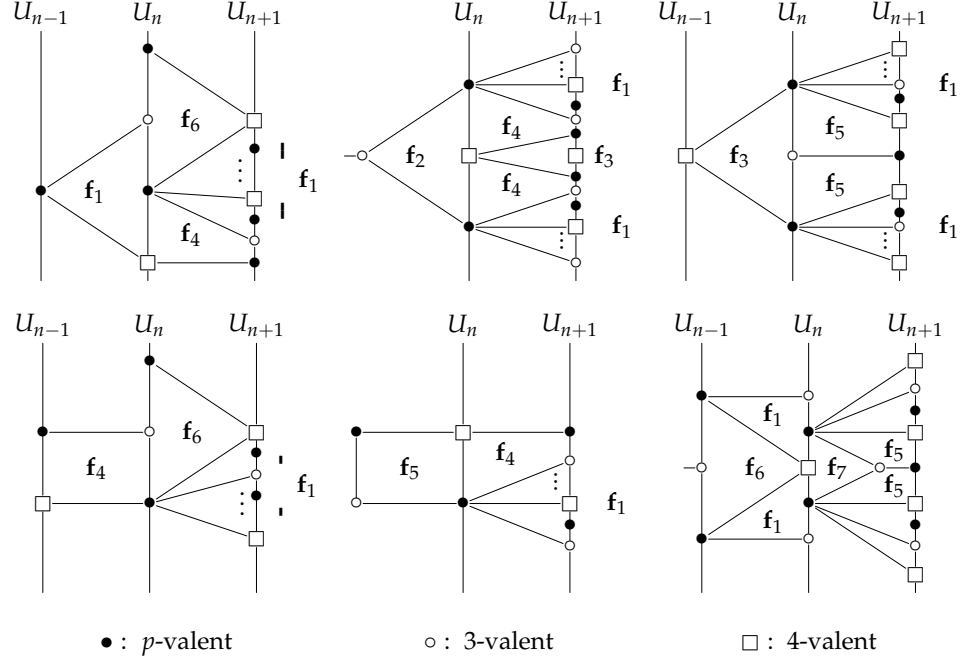


FIGURE 3.3. Offspring diagrams for a tessellation with valence sequence $[3, p, 4, p]$.

The characteristic polynomial of M has the factorization

$$\chi(z) = z^3 \left(z^4 - (p-3)z^3 - \frac{1}{2}(p-8)z^2 - (p-3)z + 1 \right).$$

As the quartic factor is palindromic, we apply Remark 1.1; the maximum modulus of an eigenvalue of M can be computed by radicals and is given by

$$\Lambda = \frac{1}{4} \left[p - 3 + \sqrt{p^2 - 4p + 1} + \sqrt{2p^2 - 10p - 6 + 2(p-3)\sqrt{p^2 - 4p + 1}} \right].$$

By [1]Theorem 2.3 and [1]Proposition 1.14, the result holds. \square

Proposition 3.6. *If $\sigma = [3, p, q, p]$ with $q \geq 5$, then σ is monomorphic and*

$$\gamma(T) = \frac{1}{4} \left(p - 4 + a + \sqrt{2p^2 + 2pq - 18p - 4q + 16 + a(2p - 8)} \right),$$

where $a = \sqrt{p^2 + 2pq - 10p - 4q + 16}$.

Proof. The offspring diagrams given in Figure 3.4 show that σ is monomorphic. Although \mathbf{f}_6 faces exhibit the “collapsing” behavior common to non-concentric tessellations, we note that the unique vertex in F_{n+1} incident with an \mathbf{f}_6 face in F_n has valence $q \geq 5$. The effect of the \mathbf{f}_6 face is to decrease the number of \mathbf{f}_3 faces in

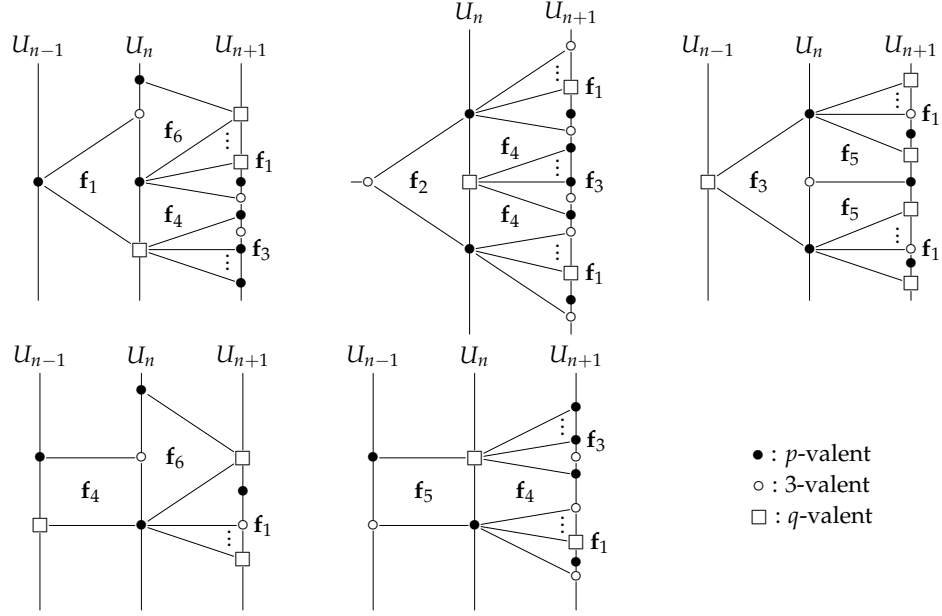


FIGURE 3.4. Offspring diagrams for a face-homogeneous tessellation with valence sequence $[3, p, q, p]$ with $q \geq 5$.

F_{n+1} by one. Hence the transition matrix of T is

$$M = \begin{bmatrix} p-3 & p-4 & p-4 & \frac{p-4}{2} & \frac{p-4}{2} & 0 \\ 0 & 0 & 0 & 0 & 0 & 0 \\ \frac{q-4}{2} & q-3 & 0 & 0 & \frac{q-4}{2} & -1 \\ 1 & 2 & 0 & 0 & 1 & 0 \\ 0 & 0 & 2 & 0 & 0 & 0 \\ \frac{1}{2} & 0 & 0 & \frac{1}{2} & 0 & 0 \end{bmatrix},$$

the characteristic polynomial of which is

$$\chi(z) = z(z-1) \left[z^4 - (p-4)z^3 - \frac{1}{2}(pq - p - 2q - 4)z^2 - (p-4)z + 1 \right].$$

As the factor of degree 4 is palindromic, [Remark 1.1](#) gives the desired result. \square

The following proposition, as compared with the previous one, illustrates how much easier these calculations become when all valences are at least 4.

Proposition 3.7. *If $\sigma = [p, q, p, r]$ and $q, r \geq 4$, then σ is monomorphic and*

$$\gamma(T) = \frac{1}{4} \left[p-4 + a + \sqrt{2p^2 + 2pq + 2pr + 4qr - 24p - 16q - 16r + 64 + a(2p-8)} \right],$$

where $a = \sqrt{p^2 + 2pq + 2pr + 4qr - 16p - 16q - 16r + 64}$.

Proof. Since $q \neq r$, it must be that p is even for σ to be realizable. As the distribution of offspring shown in [Figure 3.5](#) is determined, σ is monomorphic. From these

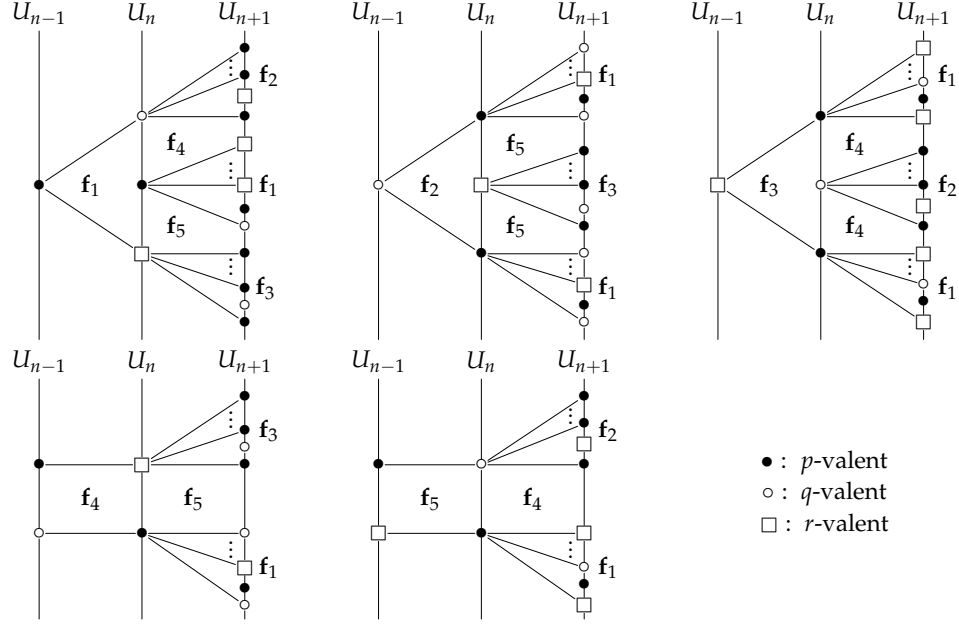


FIGURE 3.5. Offspring diagrams for a face-homogeneous tessellation with valence sequence $[p, q, p, r]$ with $q, r \geq 4$.

diagrams we produce the transition matrix

$$M = \begin{bmatrix} p-3 & p-4 & p-4 & \frac{p-4}{2} & \frac{p-4}{2} \\ \frac{q-4}{2} & 0 & q-3 & 0 & \frac{q-4}{2} \\ \frac{r-4}{2} & r-3 & 0 & \frac{r-4}{2} & 0 \\ 1 & 0 & 2 & 0 & 1 \\ 1 & 2 & 0 & 1 & 0 \end{bmatrix}.$$

The characteristic polynomial of M is

$$\chi(z) = \frac{1}{2}(z-1)(2z^4 - bz^3 - cz^2 - bz + 2),$$

where

$$\begin{aligned} b &= 2p - 8 \text{ and} \\ c &= pq + pr + 2qr - 4p - 8q - 8r + 20. \end{aligned}$$

As in the previous proof, the fourth degree factor is palindromic, and we apply [Remark 1.1](#). \square

Proposition 3.8. *If $\sigma = [p, q, r, s]$, then σ is monomorphic, all terms are even, and $\gamma(T) \geq 7.0367$.*

Proof. Since p, q, r and s are all distinct, they must be even by previous arguments. We apply [1]Lemma 2.9 to obtain the transition matrix

$$M = \begin{bmatrix} 0 & \frac{p-4}{2} & p-3 & \frac{p-4}{2} & 0 & 0 & \frac{p-4}{2} & \frac{p-4}{2} \\ \frac{q-4}{2} & 0 & \frac{q-4}{2} & q-3 & \frac{q-4}{2} & 0 & 0 & \frac{q-4}{2} \\ r-3 & \frac{r-4}{2} & 0 & \frac{r-4}{2} & \frac{r-4}{2} & \frac{r-4}{2} & 0 & 0 \\ \frac{s-4}{2} & s-3 & \frac{s-4}{2} & 0 & 0 & \frac{s-4}{2} & \frac{s-4}{2} & 0 \\ 0 & 1 & 1 & 0 & 0 & 0 & 1 & 0 \\ 0 & 0 & 1 & 1 & 0 & 0 & 0 & 1 \\ 1 & 0 & 0 & 1 & 1 & 0 & 0 & 0 \\ 1 & 1 & 0 & 0 & 0 & 1 & 0 & 0 \end{bmatrix}.$$

This matrix has characteristic polynomial

$$f(z) = (z-1)^2(z^6 + 2z^5 - bz^4 - cz^3 - bz^2 + 2z + 1),$$

with

$$b = \frac{1}{4}[(p+r)(q+s) + 4(pr+qs) - 16(p+q+r+s) + 68] \text{ and}$$

$$c = \frac{1}{4}[2(pr(q+s) + qs(p+r)) - 10(p+r)(q+s) - 8(pr+qs) + 32(p+q+r+s) - 112].$$

As this polynomial cannot be factored further by elementary methods, we determine the least possible rate of growth of T rather than attempt to calculate the growth rate in the general case.

There are three minimal valence sequences of the form $[p, q, r, s]$, all pairwise incomparable under the partial order on cyclic sequences, namely: $\sigma_1 = [4, 6, 8, 10]$, $\sigma_2 = [4, 6, 10, 8]$, and $[4, 8, 6, 10]$. If T_i is a tessellation with valence sequence σ_i for $i = 1, 2, 3$, then the approximate growth rates of the three tessellations are

$$\begin{aligned} \gamma(T_1) &\approx 7.2091, \\ \gamma(T_2) &\approx 7.0367, \text{ and} \\ \gamma(T_3) &\approx 7.7106. \end{aligned}$$

Hence $\gamma(T) \geq \gamma(T_2) \approx 7.0367$. \square

4. CLASSIFICATION OF FACE-HOMOGENEOUS TESSELLATIONS WITH VALENCE SEQUENCES OF LENGTH 5

Theorem 4.1. *Suppose that σ has length 5. Then σ is polymorphic if and only if it is one of the following, where $p, q, r, s \geq 4$:*

- (1) $[p, p, p, p, q]$ with $\frac{4}{p} + \frac{1}{q} < \frac{3}{2}$;
- (2) $[p, p, p, p, 3]$ for any integer $p \geq 4$;
- (3) $[p, p, p, q, q]$ with q even and $\frac{3}{p} + \frac{2}{q} < \frac{3}{2}$;
- (4) $[p, p, q, p, q]$ with $\frac{3}{p} + \frac{2}{q} < \frac{3}{2}$;
- (5) $[p, p, 3, p, 3]$ for any integer $p \geq 4$;
- (6) $[p, p, p, q, r]$ with q and r both even, and $\frac{3}{p} + \frac{1}{q} + \frac{1}{r} < \frac{3}{2}$;
- (7) $[3, 3, 3, p, q]$ with p and q both even, and $\frac{1}{p} + \frac{1}{q} < \frac{1}{2}$;
- (8) $[p, p, q, p, r]$ with $\frac{3}{p} + \frac{1}{q} + \frac{1}{r} < \frac{3}{2}$;
- (9) $[p, p, 3, p, q]$ with $\frac{3}{p} + \frac{1}{q} < \frac{7}{6}$;

- (10) $[p, p, q, q, r]$ with p, q , and r even, and $\frac{2}{p} + \frac{2}{q} + \frac{1}{r} < \frac{3}{2}$;
(11) $[p, q, p, q, r]$ with r even, and $\frac{2}{p} + \frac{2}{q} + \frac{1}{r} < \frac{3}{2}$;
(12) $[3, p, 3, p, q]$ with q even and $\frac{2}{p} + \frac{1}{q} < \frac{5}{6}$;
(13) $[p, p, q, r, s]$ with p, q, r , and s all even and $\frac{2}{p} + \frac{1}{q} + \frac{1}{r} + \frac{1}{s} < \frac{3}{2}$;
(14) $[p, q, p, r, s]$ with p, r and s all even and $\frac{2}{p} + \frac{1}{q} + \frac{1}{r} + \frac{1}{s} < \frac{3}{2}$.

Proof. We establish by this theorem that each of these fourteen cases is polymorphic. That they are the only polymorphic valence sequences of length 5 is determined by the eight propositions which follow.

Except for Case (7), all of these valence sequences are realized by tessellations in $\mathcal{G}_{3^+,5}$; as one sees by inspection, except for Cases (5), (7), and (12), all satisfy the further hypotheses of [1]Theorem 3.1 and hence are polymorphic.

Case (5) If $\sigma = [p, p, 3, p, 3]$, then there are two distinct offspring diagrams for a face of type \mathbf{f}_1 as shown in Figure 4.1. Thus, as in the previous case, σ is polymorphic.

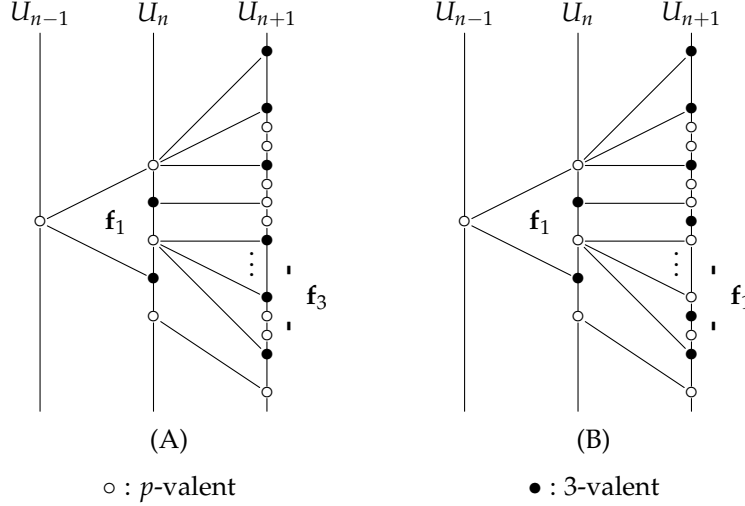


FIGURE 4.1. Two distinct offspring diagrams for a face of type \mathbf{f}_1 in a tessellation with valence sequence $[p, p, 3, p, 3]$.

Case (7) If $\sigma = [3, 3, 3, p, q]$, then both p and q are even, and $\frac{1}{p} + \frac{1}{q} < \frac{1}{2}$ holds. Without loss of generality assume that $q \geq 6$. Then there are two sets of possible offspring for a face of type \mathbf{f}_5 , as shown in Figure 4.2. When adjacent faces of type \mathbf{f}_5 occur in F_n both incident to a common 3-valent vertex in U_n , one must have offspring as specified in Figure 4.2(A) and the other must have offspring as specified in Figure 4.2(B). However, the configuration (as read clockwise about the common q -valent vertex in U_{n-1}) could be either (A)-(B) or (B)-(A). As these are non-isomorphic configurations, σ is polymorphic.

Case (12) If $\sigma = [3, p, 3, p, q]$, then q is even and $\frac{2}{p} + \frac{1}{q} < \frac{5}{6}$ holds. The faces of type \mathbf{f}_1 have at least two distinct offspring diagrams, depending partly upon one of the faces with which they are adjacent in F_n , as demonstrated in Figure 4.3. The faces labeled $\mathbf{f}_1, \mathbf{f}_2$ can be of either type, thus demonstrating polymorphicity; also, the face labeled \mathbf{f}_{10} could have two distinct orientations. \square

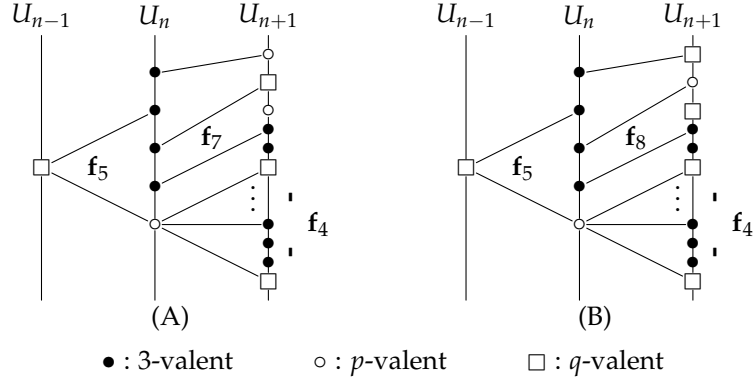


FIGURE 4.2. Two distinct offspring diagrams for a face of type f_5 in a tessellation with valence sequence $[3, 3, 3, p, q]$.

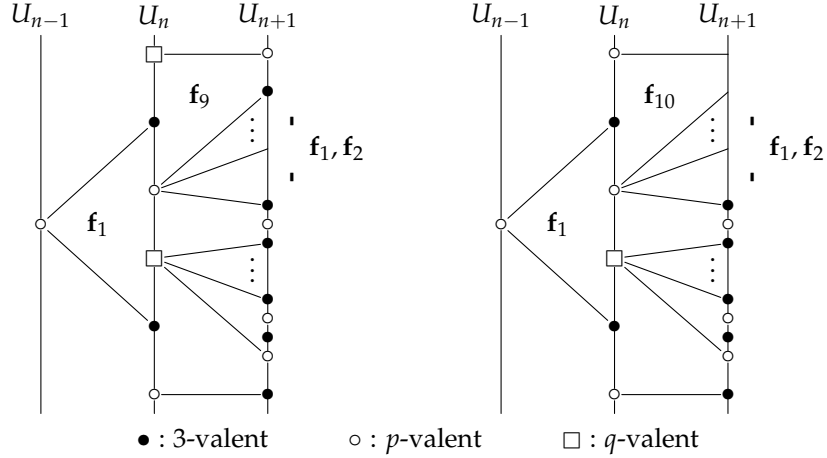


FIGURE 4.3. Two distinct offspring diagrams for a face of type f_1 in a tessellation with valence sequence $[3, p, 3, p, q]$.

Having shown that these 14 valence sequences are polymorphic, we prove exhaustively via Propositions 4.2 to 4.9 that all other valence sequences of length 5 are monomorphic. In these eight cases, we also calculate the exact growth rates in terms of the valences wherever feasible; otherwise we demonstrate a lower bound for the growth rate of tessellations within the class as per the method of Proposition 2.5.

Proposition 4.2. *Let $\sigma = [p, p, p, p, p]$. Then $p \geq 4$, σ is monomorphic, and*

$$\gamma(T) = \frac{1}{2} \left(3p - 8 + \sqrt{9p^2 - 48p + 60} \right).$$

Proof. As T is edge-homogeneous with edge-symbol $\langle p, p; 5, 5 \rangle$, [1] Proposition 1.17 gives the stated growth rate. \square

Proposition 4.3. *If $\sigma = [3, 3, 3, 3, p]$, then σ is monomorphic with $p \geq 7$ and*

$$\gamma(T) = \frac{1}{2} \sqrt{2(p-4) + 2\sqrt{(p-5)(p-2)}}.$$

Proof. To show that σ is monomorphic, let v_0 be a p -valent root. The first two coronas of T must be as shown in [Figure 4.4](#) (up to isomorphism). As the configura-

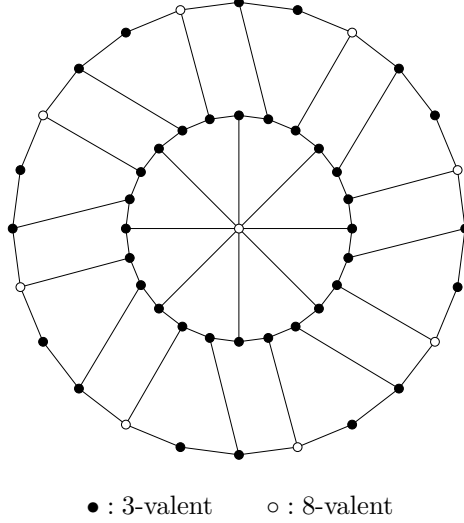


FIGURE 4.4. First two coronas of a tessellation with valence sequence $[3, 3, 3, 3, 8]$ when rooted at an 8-valent vertex, exemplifying the pattern of valences at regional distance 1 from a p -valent vertex in $[3, 3, 3, 3, p]$.

tion of vertices at regional distance 2 from any p -valent vertex is known, and every face is incident with exactly one p -valent vertex, we have fixed the configuration of the entire tessellation up to isomorphism; thus σ is monomorphic.

The offspring diagrams for $[3, 3, 3, 3, p]$ appear in [Figure 4.5](#), and give the matrix

$$M = \begin{bmatrix} 0 & 0 & \frac{1}{2}(p-4) & 0 & \frac{1}{2}(p-4) & -1 \\ 0 & 0 & 1 & 0 & 0 & 0 \\ 1 & 0 & 0 & 0 & 0 & 0 \\ 0 & 0 & \frac{1}{2} & 0 & \frac{1}{2} & 0 \\ 1 & \frac{1}{2} & 0 & 0 & 0 & 0 \\ 0 & \frac{1}{2} & 0 & 0 & 0 & 0 \end{bmatrix}.$$

This matrix has characteristic polynomial

$$\chi(z) = \frac{1}{4}z^2(4z^4 - 4(p-4)z^2 + (p-6)),$$

and so the growth rate of a tessellation T with valence sequence $[3, 3, 3, 3, p]$ is

$$\gamma(T) = \frac{1}{2} \sqrt{2(p-4) + 2\sqrt{(p-5)(p-2)}}.$$

□

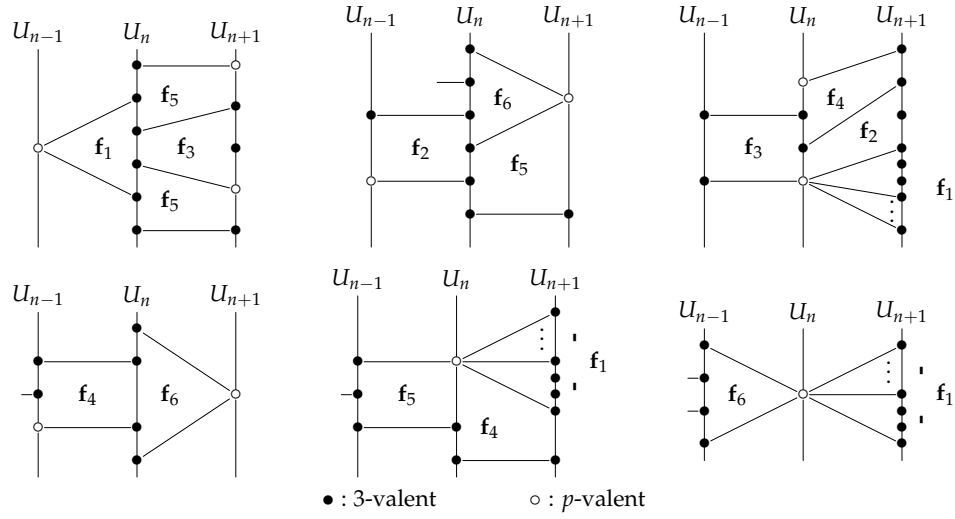


FIGURE 4.5. Face types and offspring in $[3, 3, 3, 3, p]$.

Proposition 4.4. *If $\sigma = [3, 3, 3, p, p]$ with even $p \geq 6$, then σ is monomorphic and*

$$\gamma(T) = \frac{1}{8} \left[p - 4 + \sqrt{p^2 + 32p - 80} + \sqrt{2(p - 4)(p + 16 + \sqrt{p^2 + 32p - 80})} \right].$$

Proof. We again have that the faces within two coronas of a p -valent root vertex must be configured as shown (exemplified by $[3, 3, 3, 8, 8]$ in [Figure 4.6](#)). Since every face is incident with two adjacent p -valent vertices, this determines the accretion rule for the tessellation; hence σ is monomorphic. Offspring diagrams for the tessellation appear in [Figure 4.7](#).

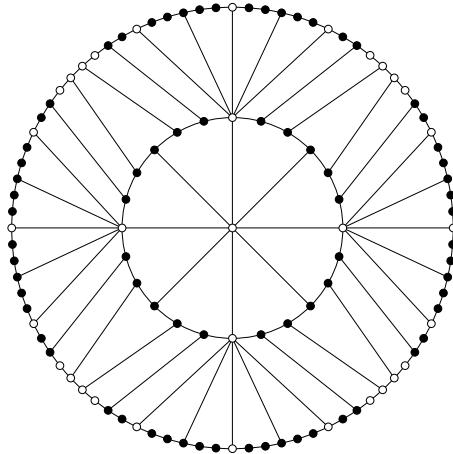


FIGURE 4.6. First two coronas of a tessellation with valence sequence $[3, 3, 3, 8, 8]$ when rooted at an 8-valent vertex.

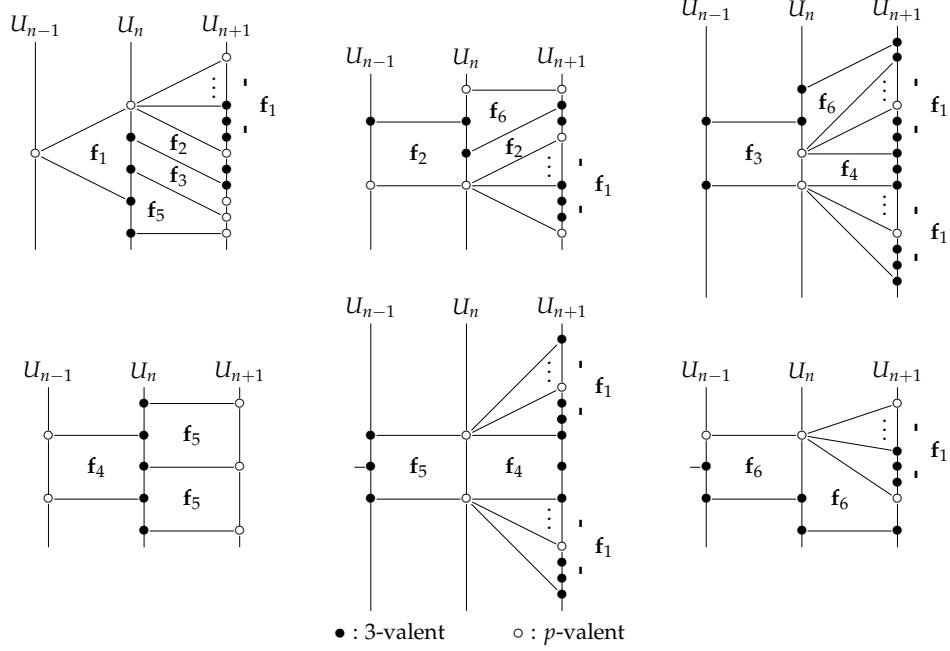


FIGURE 4.7. Offspring diagrams for a tessellation with valence sequence $[3, 3, 3, p, p]$.

We may assume by [1] Proposition 1.14 that the Bilinski diagram of a tessellation T with valence sequence σ is rooted at a p -valent vertex, and thereby is concentric. The offspring diagrams determine the transition matrix

$$M = \begin{bmatrix} \frac{p-4}{2} & \frac{p-4}{2} & \frac{3p-10}{2} & 0 & p-4 & \frac{p-4}{2} \\ 1 & 1 & 0 & 0 & 0 & 0 \\ 1 & 0 & 0 & 0 & 0 & 0 \\ 0 & 0 & 1 & 0 & 1 & 0 \\ \frac{1}{2} & 0 & 0 & 1 & 0 & 0 \\ 0 & \frac{1}{2} & \frac{1}{2} & 0 & 0 & \frac{1}{2} \end{bmatrix},$$

which has characteristic polynomial

$$\chi(z) = \frac{1}{4}(2z-1)(z-1)(2z^4 - (p-4)z^3 - (5p-16)z^2 - (p-4)z + 2).$$

Solving for the eigenvalue of maximum modulus gives

$$\gamma(T) = \frac{1}{8} \left[p-4 + \sqrt{p^2 + 32p - 80} + \sqrt{2(p-4)(p+16 + \sqrt{p^2 + 32p - 80})} \right].$$

□

Proposition 4.5. *If $\sigma = [3, 3, p, 3, p]$, then σ is monomorphic with $p \geq 5$ and*

$$\gamma(T) = \frac{1}{2} \left(p-2 + \sqrt{(p-2)^2 - 4} \right).$$

Proof. While σ is not uniformly concentric, choosing a p -valent root produces a concentric Bilinski diagram with exactly three face types, the offspring diagrams for which are shown in [Figure 4.8](#). The transition matrix

$$M = \begin{bmatrix} p-3 & \frac{p-4}{2} & \frac{p-4}{2} \\ 1 & 1 & 0 \\ 1 & \frac{1}{2} & \frac{1}{2} \end{bmatrix}$$

has a cubic characteristic polynomial with factorization

$$\chi(z) = \frac{1}{2}(2z - 1)(z^2 - (p - 2)z + 1).$$

By [\[1\]Theorem 2.3](#) and [\[1\]Proposition 1.14](#),

$$\gamma(T) = \frac{1}{2} \left((p - 2) + \sqrt{(p - 2)^2 - 4} \right).$$

□

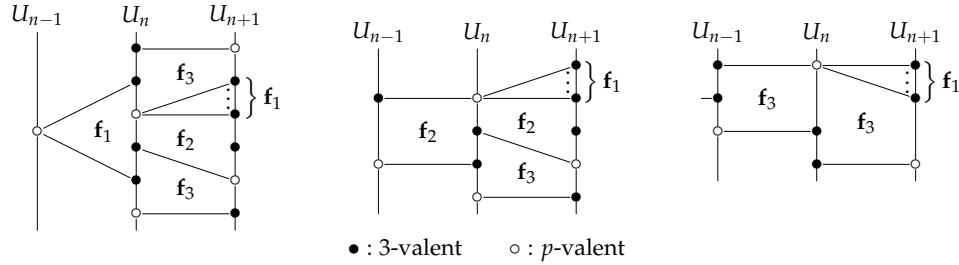


FIGURE 4.8. Offspring diagrams for a tessellation with valence sequence $[3, 3, p, 3, p]$ when rooted at a p -valent vertex.

Proposition 4.6. *If $\sigma = [3, 3, p, 3, q]$, then σ is monomorphic with $p, q \geq 4$ and*

$$\gamma(T) = \frac{1}{2} \sqrt{2(p - 2)(q - 2) - 4 + 2\sqrt{(p - 2)^2(q - 2)^2 - 4(p - 2)(q - 2)}}.$$

Proof. Suppose a 3-valent vertex in $V(T)$ is adjacent to at least two other 3-valent vertices. These three consecutive 3-valent vertices must all be incident with a common face f ; but then f does not have valence sequence σ . By contradiction, each 3-valent vertex in $V(T)$ must be adjacent to at most one other 3-valent vertex.

On the other hand, assume that v_1 is a 3-valent vertex adjacent to no other 3-valent vertices. Then there is a face f incident with v_1 which is incident with consecutive vertices with valences $(p, 3, p)$ or $(q, 3, q)$. In neither case does f have valence sequence σ . Thus each 3-valent vertex in $V(T)$ must be adjacent to exactly one other 3-valent vertex. This forces all edges with edge-symbol $\langle 3, 3; 5, 5 \rangle$ to have the configuration shown in [Figure 4.9](#).

As with $[3, 3, p, 3, p]$, this configuration determines the entire tessellation, and so σ is monomorphic. Taking a p -valent vertex to be the root of the Bilinski diagram gives face types and offspring diagrams as shown in [Figure 4.10](#).

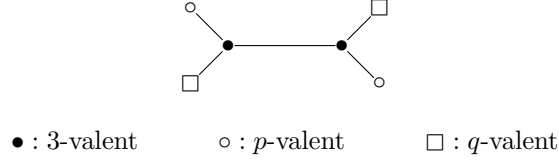


FIGURE 4.9. The local configuration in a tessellation with valence sequence $[3, 3, p, 3, q]$ at an edge with symbol $\langle 3, 3; 5, 5 \rangle$.

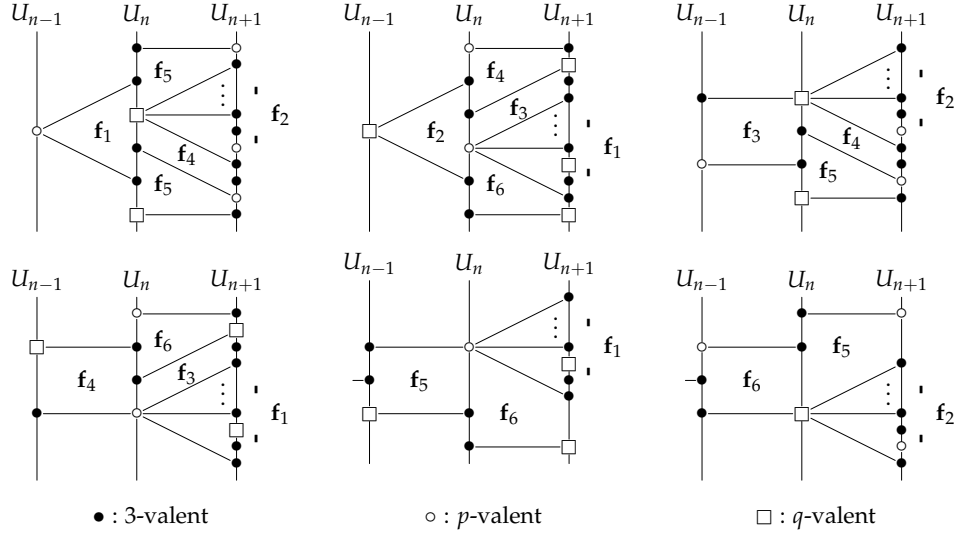


FIGURE 4.10. Offspring diagrams for a tessellation with valence sequence $[3, 3, p, 3, q]$.

In turn these give the transition matrix

$$M = \begin{bmatrix} 0 & p-3 & 0 & \frac{p-4}{2} & \frac{p-4}{2} & 0 \\ q-3 & 0 & \frac{q-4}{2} & 0 & 0 & \frac{q-4}{2} \\ 0 & 1 & 0 & 1 & 0 & 0 \\ 1 & 0 & 1 & 0 & 0 & 0 \\ 1 & 0 & \frac{1}{2} & 0 & 0 & \frac{1}{2} \\ 0 & 1 & 0 & \frac{1}{2} & \frac{1}{2} & 0 \end{bmatrix},$$

which has characteristic polynomial

$$\begin{aligned} \chi(z) &= z^6 - \left(pq - 2p - 2q + \frac{9}{4}\right) z^4 + \frac{1}{4}(pq - 2p - 2q + 6) z^2 - \frac{1}{4} \\ &= \frac{1}{4}(2z-1)(2z+1)(z^4 + (pq - 2p - 2q + 2)z^2 - 1). \end{aligned}$$

Thus the growth rate of T is

$$\gamma(T) = \frac{1}{2} \sqrt{2(p-2)(q-2) - 4 + 2\sqrt{(p-2)^2(q-2)^2 - 4(p-2)(q-2)}}.$$

□

Proposition 4.7. *Let $\sigma = [p, p, q, r, q]$ with $p, q, r \geq 4$. Then p and q are even and*

$$\gamma(T) \geq \frac{1}{4} \left(3 + \sqrt{113} + \sqrt{106 + 6\sqrt{113}} \right) \approx 6.6650.$$

Proof. Assuming that T is labeled as a Bilinski diagram rooted at a p -valent vertex, the offspring diagrams and face types are as shown in [Figure 4.11](#) and yield the transition matrix

$$M = \begin{bmatrix} \frac{p-4}{2} & \frac{3p-10}{2} & 2p-6 & \frac{p-4}{2} & 0 & \frac{3p-10}{2} \\ \frac{3q-10}{2} & q-3 & q-4 & q-3 & q-4 & \frac{q-4}{2} \\ r-3 & \frac{r-4}{2} & 0 & \frac{r-4}{2} & r-3 & 0 \\ 1 & 1 & 2 & 1 & 0 & 1 \\ 0 & 1 & 1 & 0 & 0 & 1 \\ 2 & 1 & 0 & 1 & 2 & 0 \end{bmatrix},$$

which has characteristic polynomial

$$\begin{aligned} \chi(z) &= z^6 - \left(\frac{1}{2}p + q - 4 \right) z^5 - \left(\frac{7}{4}pq + 2pr + \frac{1}{2}qr - 9p - 6p - 6r + 25 \right) z^4 \\ &\quad - \left(\frac{3}{4}pqr - 4pq - 5pr - 2qr + 17p + 10q + 12r - 40 \right) z^3 \\ &\quad - \left(\frac{7}{4}pq + 2pr + \frac{1}{2}qr - 9p - 6p - 6r + 25 \right) z^2 - \left(\frac{1}{2}p + q - 4 \right) z + 1. \end{aligned}$$

There are four valence sequences in this class which are minimal under the partial order on valence sequences: $\sigma_1 = [4, 4, 6, 5, 6]$, $\sigma_2 = [6, 6, 4, 5, 4]$, $\sigma_3 = [6, 6, 8, 4, 8]$, and $\sigma_4 = [8, 8, 6, 4, 6]$. If T_i is a face-homogeneous tessellation with valence sequence σ_i , then the growth rates of T_i for $i = 1, 2, 3, 4$ are

$$\begin{aligned} \gamma(T_1) &= \frac{1}{4} \left(3 + \sqrt{113} + \sqrt{106 + 6\sqrt{113}} \right) \approx 6.6650 \\ \gamma(T_2) &= 2 + \sqrt{2} + \sqrt{5 + 4\sqrt{2}} \approx 6.6786 \\ \gamma(T_3) &= \frac{1}{2} \left(3 + \sqrt{65} + \sqrt{70 + 6\sqrt{65}} \right) \approx 10.9711 \\ \gamma(T_4) &\approx 10.5872 \end{aligned}$$

Thus by [\[1\]Theorem 2.7](#), if $\sigma \geq \sigma_i$ for some $i \in \{1, 2, 3, 4\}$, then $\gamma(T) \geq 6.6650$. \square

Proposition 4.8. *Let $\sigma = [p, p, q, 3, q]$ where $p, q \geq 4$. Then both p and q are even, $\frac{1}{p} + \frac{1}{q} < \frac{7}{12}$, σ is monomorphic, and $\gamma(T) \geq 4.9911$.*

Proof. Suppose T is labeled as a Bilinski diagram with a p -valent root. Then the face types and offspring diagrams for T are described in [Figure 4.12](#). These offspring diagrams give us the transition matrix

$$M = \begin{bmatrix} \frac{p-4}{2} & \frac{3p-10}{2} & \frac{p-4}{2} & 0 & \frac{3p-10}{2} & p-4 \\ \frac{3q-10}{2} & q-3 & q-3 & q-4 & \frac{q-4}{2} & 0 \\ 1 & 1 & 1 & 0 & 1 & 0 \\ 0 & 1 & 0 & 0 & 1 & 1 \\ 2 & 0 & 0 & 2 & 0 & 0 \\ 0 & \frac{1}{2} & \frac{1}{2} & 0 & 0 & 0 \end{bmatrix}.$$

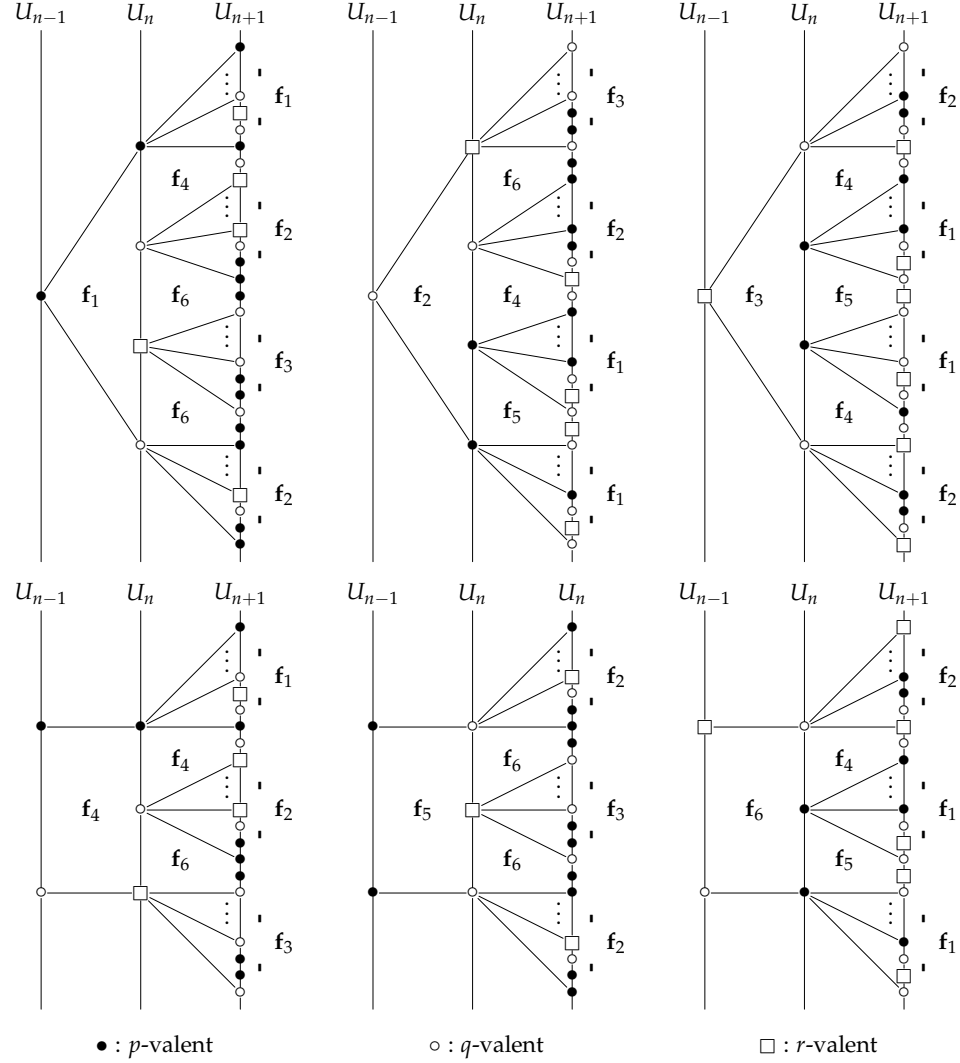


FIGURE 4.11. Offspring diagrams for a tessellation with valence sequence $[p, p, q, r, q]$.

So we have the characteristic polynomial

$$\begin{aligned}
 \chi(z) = & z^6 - \left(\frac{1}{2}p + q - 4\right) z^5 - \left(\frac{7}{4}pq - 3p - \frac{9}{2}q + 7\right) z^4 \\
 & + \left(\frac{7}{4}pq - 2p - 4q + 4\right) z^3 - \left(\frac{7}{4}pq - 3p - \frac{9}{2}q + 7\right) z^2 \\
 & - \left(\frac{1}{2}p + q - 4\right) z + 1.
 \end{aligned}$$

We again reduce to the minimal sequences in this class, namely $\sigma_1 = [4, 4, 6, 3, 6]$ and $\sigma_2 = [6, 6, 4, 3, 4]$. If T_i is a tessellation with valence sequence σ_i for $i = 1, 2$,

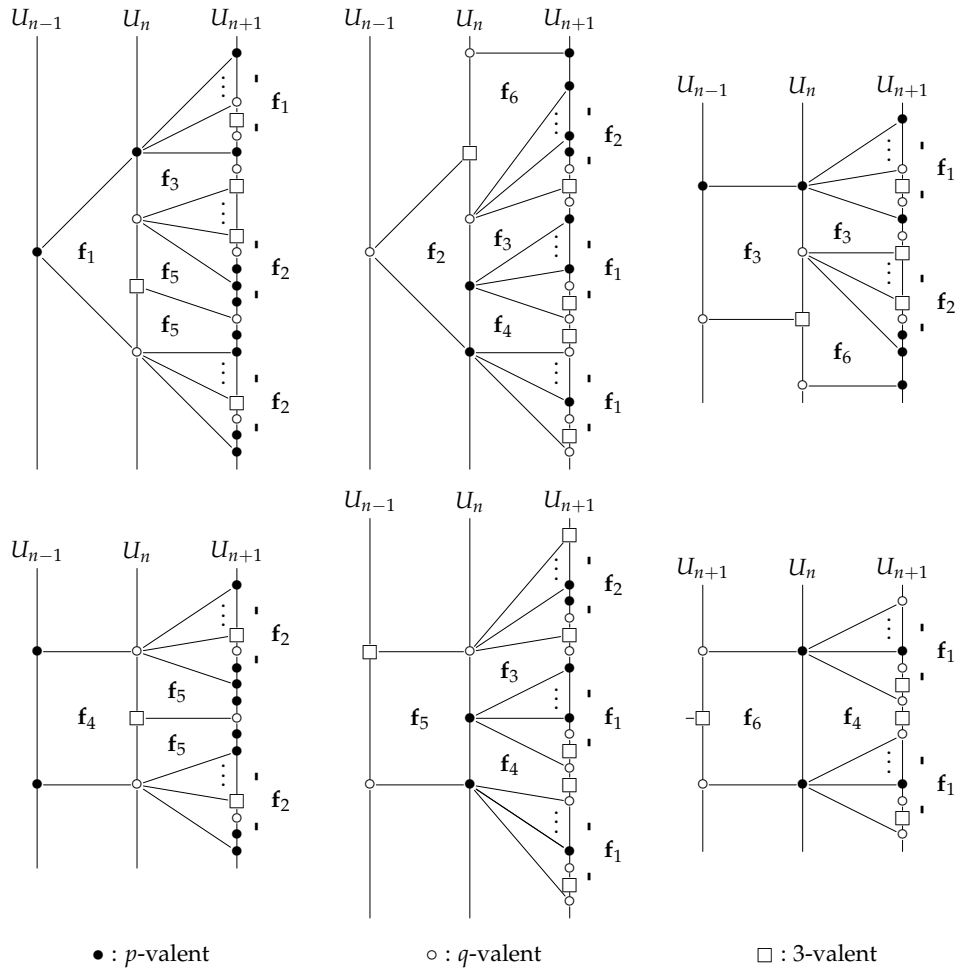


FIGURE 4.12. Offspring diagrams for a tessellation with valence sequence $[p, p, q, 3, q]$.

then numerical approximation of the eigenvalues of the transition matrices gives that

$$\begin{aligned} \gamma(T_1) &\approx 5.4330 \text{ and} \\ \gamma(T_2) &\approx 4.9911, \end{aligned}$$

so $\gamma(T) \geq 4.9911$ by [1]Theorem 2.7 whenever $\sigma \geq \sigma_1$ or $\sigma \geq \sigma_2$. □

Proposition 4.9. *If $\sigma = [p, q, r, s, t]$, then all terms are even, $\frac{1}{p} + \frac{1}{q} + \frac{1}{r} + \frac{1}{s} + \frac{1}{t} < \frac{3}{2}$ holds, σ is monomorphic, and $\gamma(T) \geq 14.5753$.*

σ_i	$\gamma(T_i)$
[4, 6, 8, 10, 12]	14.8673
[4, 6, 8, 12, 10]	14.6868
[4, 6, 10, 8, 12]	15.1157
[4, 6, 10, 12, 8]	14.5753
[4, 6, 12, 8, 10]	15.0199
[4, 6, 12, 10, 8]	14.6594
[4, 8, 6, 10, 12]	15.1938
[4, 8, 6, 12, 10]	15.0988
[4, 8, 10, 6, 12]	15.5192
[4, 8, 12, 6, 10]	15.3442
[4, 10, 6, 8, 12]	15.5443
[4, 10, 8, 6, 12]	15.6248

TABLE 1. Table of minimal sequences in class $[p, q, r, s, t]$ and their approximate growth rates.

Proof. Applying Lemma 2.9, we calculate the transition matrix for a tessellation T with valence sequence σ to be

$$M = \begin{bmatrix} 0 & \frac{p-4}{2} & p-3 & p-3 & \frac{p-4}{2} & 0 & 0 & \frac{p-4}{2} & p-3 & \frac{p-4}{2} \\ \frac{q-4}{2} & 0 & \frac{q-4}{2} & q-3 & \frac{q-4}{2} & 0 & 0 & 0 & \frac{q-4}{2} & q-3 \\ r-3 & \frac{r-4}{2} & 0 & \frac{r-4}{2} & r-3 & r-3 & \frac{r-4}{2} & 0 & 0 & \frac{r-4}{2} \\ s-3 & s-3 & \frac{s-4}{2} & 0 & \frac{s-4}{2} & \frac{s-4}{2} & s-3 & \frac{s-4}{2} & 0 & 0 \\ \frac{t-4}{2} & t-3 & t-3 & \frac{t-4}{2} & 0 & 0 & \frac{t-4}{2} & t-3 & \frac{t-4}{2} & 0 \\ 0 & 1 & 1 & 1 & 0 & 0 & 0 & 1 & 1 & 0 \\ 0 & 0 & 1 & 1 & 1 & 0 & 0 & 0 & 1 & 1 \\ 1 & 0 & 0 & 1 & 1 & 1 & 0 & 0 & 0 & 1 \\ 1 & 1 & 0 & 0 & 1 & 1 & 1 & 0 & 0 & 0 \\ 1 & 1 & 1 & 0 & 0 & 0 & 1 & 1 & 0 & 0 \end{bmatrix}.$$

There are $\frac{1}{2}(5-1)! = 12$ distinct valences sequences in this class which are minimal under the partial order on cyclic sequences. These sequences together with the approximate growth rates of associated tessellations are tabulated in [Table 1](#). An arbitrary valence sequence σ in this class dominates at least one of these 12 minimal valence sequences, and so $\gamma(T) \geq 14.5753$ by [\[1\]Theorem 2.7](#). □

5. CLASSIFICATION OF FACE-HOMOGENEOUS TESSELLATIONS WITH VALENCE SEQUENCES OF LENGTH 6

There are 32 distinct classes of valence sequences of length 6, and every face-homogeneous tessellation with covalence at least 6 is uniformly concentric by [\[1\]Proposition 1.3](#). However, the inclusion of 3-valent vertices and their concomitant notched bricks warrant a separate treatment in [Section 5.2](#). We further extend the convention in [\[1\]](#) (following [Definition 1.7](#)) that all letters such as p, q , etc. appearing in valence sequences (not numerals such as 3, 4, etc.) represent integers ≥ 4 .

5.1. Valence sequences of length 6 with all vertices of valence at least 4.
The first result is an immediate consequence of [\[1\]Proposition 3.1](#).

Corollary 5.1. *Let $\sigma = [p_0, \dots, p_5]$ with all terms at least 4. If any of the following conditions holds, then σ is polymorphic.*

- (1) $\sigma = [p, p, p, p, p, q]$, with $\frac{5}{p} + \frac{1}{q} < 2$;
- (2) $\sigma = [p, p, p, p, q, q]$, with q even and $\frac{2}{p} - \frac{1}{q} < 1$;
- (3) $\sigma = [p, p, p, q, p, q]$, with $\frac{2}{p} + \frac{1}{q} < 1$;
- (4) $\sigma = [p, p, p, q, q, q]$, with $\frac{1}{p} + \frac{1}{q} < \frac{2}{3}$;
- (5) $\sigma = [p, p, q, p, q, q]$, with $\frac{1}{p} + \frac{1}{q} < \frac{2}{3}$;
- (6) $\sigma = [p, p, p, p, q, r]$, with $\frac{4}{p} + \frac{1}{q} + \frac{1}{r} < 2$;
- (7) $\sigma = [p, p, p, q, p, r]$, with $\frac{4}{p} + \frac{1}{q} + \frac{1}{r} < 2$;
- (8) $\sigma = [p, p, q, p, p, r]$, with p even and $\frac{4}{p} + \frac{1}{q} + \frac{1}{r} < 2$;
- (9) $\sigma = [p, p, p, q, q, r]$, with q and r even and $\frac{3}{p} + \frac{2}{q} + \frac{1}{r} < 2$;
- (10) $\sigma = [p, p, p, q, r, q]$, with q even and $\frac{3}{p} + \frac{2}{q} + \frac{1}{r} < 2$;
- (11) $\sigma = [p, p, q, p, q, r]$, with r even and $\frac{3}{p} + \frac{2}{q} + \frac{1}{r} < 2$;
- (12) $\sigma = [p, q, p, p, q, r]$, with r even and $\frac{3}{p} + \frac{2}{q} + \frac{1}{r} < 2$;
- (13) $\sigma = [p, p, q, q, p, r]$, with q even and $\frac{3}{p} + \frac{2}{q} + \frac{1}{r} < 2$;
- (14) $\sigma = [p, p, q, q, r, r]$, with $p, q,$ and r all even and $\frac{1}{p} + \frac{1}{q} + \frac{1}{r} < 1$;
- (15) $\sigma = [p, p, q, r, q, r]$, with p even and $\frac{1}{p} + \frac{1}{q} + \frac{1}{r} < 1$;
- (16) $\sigma = [p, p, p, q, r, s]$, with $q, r,$ and s all even and $\frac{3}{p} + \frac{1}{q} + \frac{1}{r} + \frac{1}{s} < 2$;
- (17) $\sigma = [p, p, q, p, r, s]$, with r and s even and $\frac{3}{p} + \frac{1}{q} + \frac{1}{r} + \frac{1}{s} < 2$;
- (18) $\sigma = [p, q, p, r, p, s]$, with $\frac{3}{p} + \frac{1}{q} + \frac{1}{r} + \frac{1}{s} < 2$;
- (19) $\sigma = [p, p, q, q, r, s]$, with $p, q, r,$ and s all even and $\frac{2}{p} + \frac{2}{q} + \frac{1}{r} + \frac{1}{s} < 2$;
- (20) $\sigma = [p, p, q, r, r, s]$, with $p, q, r,$ and s all even and $\frac{2}{p} + \frac{2}{q} + \frac{1}{r} + \frac{1}{s} < 2$;
- (21) $\sigma = [p, q, r, p, q, s]$, with $p, q, r,$ and s all even and $\frac{2}{p} + \frac{2}{q} + \frac{1}{r} + \frac{1}{s} < 2$;
- (22) $\sigma = [p, p, q, r, s, t]$, with $p, q, r, s,$ and t all even and $\frac{2}{p} + \frac{1}{q} + \frac{1}{r} + \frac{1}{s} + \frac{1}{t} < 2$;
- (23) $\sigma = [p, q, p, r, s, t]$ with $p, r, s,$ and t all even and $\frac{2}{p} + \frac{1}{q} + \frac{1}{r} + \frac{1}{s} + \frac{1}{t} < 2$;

The following propositions give the rate of growth of the nine monomorphic valence sequences of length 6 all of whose terms are at least 4.

Proposition 5.2. *If $\sigma = [p, p, p, p, p, p]$ with $p \geq 4$, then σ is monomorphic and*

$$\gamma(T) = 2p - 5 + 2\sqrt{p^2 - 5p + 6}.$$

Proof. Clearly T is edge-homogeneous with edge-symbol $\langle p, p; 6, 6 \rangle$, and so one may apply [1]Proposition 1.17. \square

Proposition 5.3. *If $\sigma = [p, p, q, p, p, q]$, then $\frac{2}{p} + \frac{1}{q} < 1$ holds, σ is monomorphic with p even, and*

$$\gamma(T) = \frac{1}{8} \left(a + b + \sqrt{2ab + 2b^2 + 32pq - 112p - 96q + 256} \right)$$

where $a = \sqrt{(p + 2q - 8)(25p + 2q - 72)}$ and $b = 5p + 2q - 16$.

Proof. This valence sequence gives rise to only four face types, as shown in [Figure 5.1](#), which in turn yields the transition matrix

$$M = \begin{bmatrix} \frac{5p-16}{2} & 3p-10 & 2p-7 & 2p-6 \\ \frac{3q-10}{2} & q-3 & q-3 & q-4 \\ 3 & 2 & 2 & 2 \\ 1 & 2 & 1 & 1 \end{bmatrix}.$$

The characteristic polynomial of M is

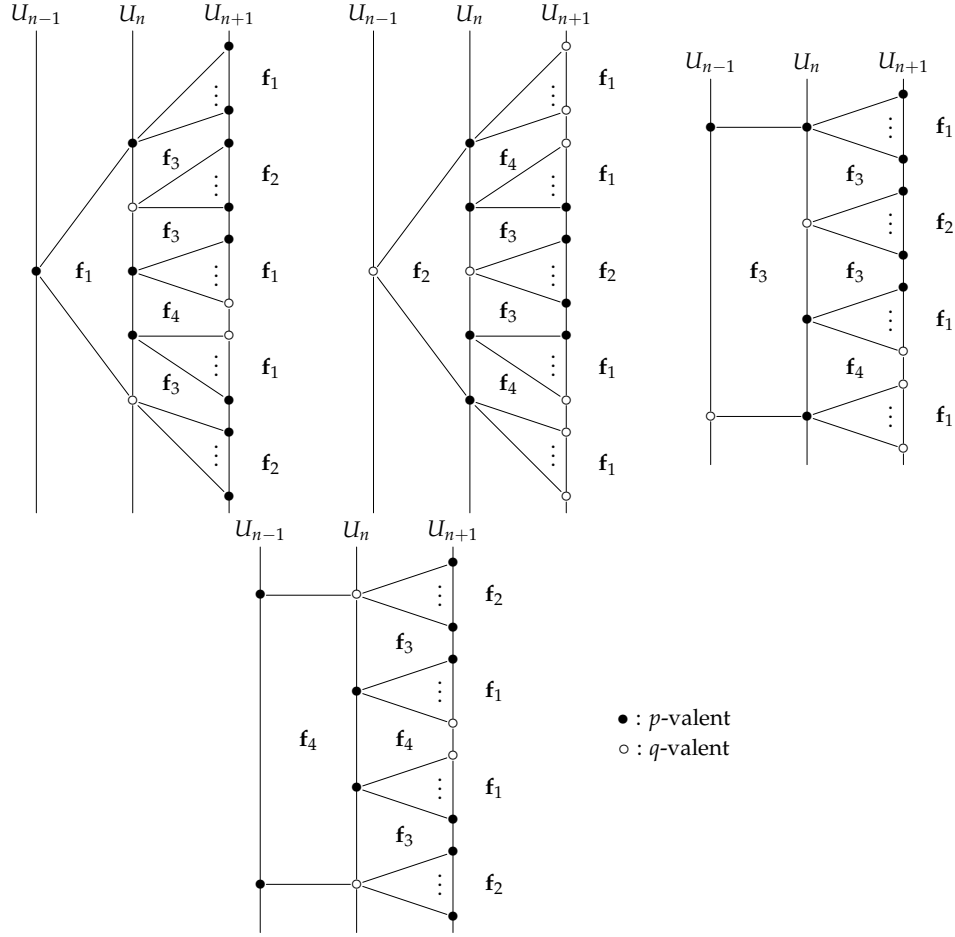


FIGURE 5.1. Offspring diagrams for a face-homogeneous tessellation with valence sequence $[p, p, q, p, p, q]$.

$$\chi(z) = z^4 - \left(\frac{5}{2}p + q - 8\right) z^3 - (2pq - 7p - 6q + 18) z^2 - \left(\frac{5}{2}p + q - 8\right) z + 1,$$

which is palindromic, and so [Remark 1.1](#) applies. □

Proposition 5.4. *If $\sigma = [p, q, p, q, p, q]$, then $\frac{1}{p} + \frac{1}{q} < \frac{2}{3}$ holds, σ is monomorphic, and*

$$\gamma(T) = p + q - 5 + \sqrt{(p + q - 4)(p + q - 6)}.$$

Proof. Again T is edge-homogeneous with edge-symbol $\langle p, q; 6, 6 \rangle$, and so one again applies [1] Proposition 1.17. \square

Proposition 5.5. *If $\sigma = [p, q, q, p, r, r]$, then $\frac{1}{p} + \frac{1}{q} + \frac{1}{r} < 1$ holds, σ is monomorphic with p, q , and r all even, and the following hold:*

- (1) $\sigma_1 = [4, 6, 6, 4, 8, 8]$, $\sigma_2 = [6, 4, 4, 6, 8, 8]$, and $\sigma_3 = [8, 4, 4, 8, 6, 6]$ are pairwise incomparable minimal elements in this class. Their transition matrices yield, respectively, the characteristic polynomials

$$\begin{aligned}\chi_1(z) &= (z^6 - 5z^5 - 111z^4 - 34z^3 - 111z^2 - 5z + 1)(z - 1), \\ \chi_2(z) &= (z^6 - 6z^5 - 87z^4 - 80z^3 - 87z^2 - 6z + 1)(z - 1),\end{aligned}$$

and

$$\chi_3(z) = (z^6 - 7z^5 - 79z^4 - 94z^3 - 79z^2 - 7z + 1)(z - 1).$$

- (2) If σ_i is the valence sequence of the tessellation T_i , ($i = 1, 2, 3$), then

$$\gamma(T_1) \approx 13.4721, \quad \gamma(T_2) \approx 13.1291, \quad \gamma(T_3) \approx 13.4341$$

- (3) For any tessellation T with valence sequence $\sigma = [p, q, q, p, r, r]$, we have $\gamma(T) \geq 13.1291$.

Proof. The offspring diagrams given in Figure 5.2 demonstrate that σ is monomorphic with transition matrix

$$M = \begin{bmatrix} p-3 & \frac{3p-10}{2} & \frac{3p-10}{2} & p-3 & p-3 & p-4 & p-4 \\ \frac{3q-10}{2} & \frac{q-4}{2} & 2q-6 & \frac{3q-10}{2} & \frac{q-4}{2} & 0 & 2q-6 \\ \frac{3r-10}{2} & 2r-6 & \frac{r-4}{2} & \frac{r-4}{2} & \frac{3r-10}{2} & 2r-6 & 0 \\ 1 & 2 & 1 & 1 & 1 & 2 & 0 \\ 1 & 1 & 2 & 1 & 1 & 0 & 2 \\ 1 & 0 & 1 & 1 & 0 & 0 & 1 \\ 1 & 1 & 0 & 0 & 1 & 1 & 0 \end{bmatrix}.$$

The characteristic polynomial of M (which is palindromic in $-z$) is

$$\chi(z) = z^7 - az^6 - bz^5 - cz^4 + cz^3 + bz^2 + az - 1,$$

where

$$\begin{aligned}a &= \frac{1}{2}(2p + q + r - 10), \\ b &= \frac{1}{4}(7pq + 7pr - 36p + 15qr - 50q - 50r + 156), \text{ and} \\ c &= \frac{1}{4}(12pqr - 33pq - 33pr + 88p - 57qr + 140q + 140r - 340)\end{aligned}$$

The minimal valence sequences in this class are as given; numerical approximation of eigenvalues provides the desired result. \square

Proposition 5.6. *If $\sigma = [p, q, p, r, q, r]$, then σ is monomorphic with p and r even, $\frac{1}{p} + \frac{1}{q} + \frac{1}{r} < 1$ holds, and $\gamma(T) \geq 9.8115$.*

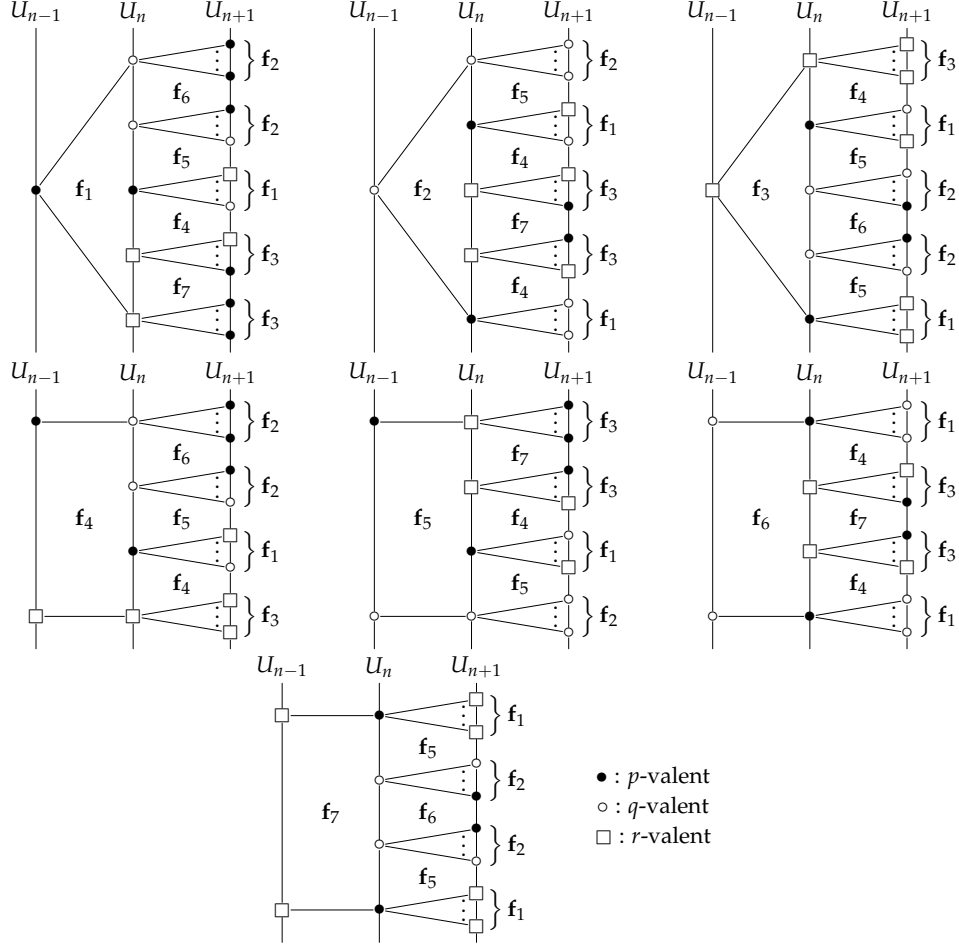


FIGURE 5.2. Offspring diagrams for a face-homogeneous tessellation with valences sequence $[p, q, q, p, r, r]$.

Proof. The offspring diagrams for σ appear in [Figure 5.3](#). They in turn give the transition matrix

$$M = \begin{bmatrix} p-3 & p-4 & \frac{3p-10}{2} & 2p-6 & p-3 & \frac{p-4}{2} & \frac{3p-10}{2} \\ \frac{q-4}{2} & 0 & q-3 & q-3 & \frac{q-4}{2} & 0 & q-3 \\ \frac{3r-10}{2} & 2r-6 & r-3 & r-4 & r-3 & \frac{3r-10}{2} & \frac{r-4}{2} \\ q-3 & q-3 & \frac{q-4}{2} & 0 & \frac{q-4}{2} & q-3 & 0 \\ 1 & 2 & 1 & 2 & 1 & 1 & 1 \\ 1 & 0 & 2 & 2 & 1 & 0 & 2 \\ 2 & 2 & 1 & 0 & 1 & 2 & 0 \end{bmatrix}.$$

The characteristic polynomial is

$$\chi(z) = z^7 - az^6 - bz^5 - cz^4 + cz^3 + bz^2 + az - 1,$$

with

$$\begin{aligned}
 a &= p + r - 5, \\
 b &= \frac{1}{4}(10pq + 5pr - 36p + 4q^2 + 10qr - 64q - 36r + 156), \text{ and} \\
 c &= \frac{1}{4}(4pq^2 + 4qr^2 + 4pqr - 38pq - 19pr - 38qr \\
 &\quad + 88p + 192q + 88r - 340).
 \end{aligned}$$

There are two minimal valence sequences in this class, namely $\sigma_1 = [4, 5, 4, 6, 5, 6]$

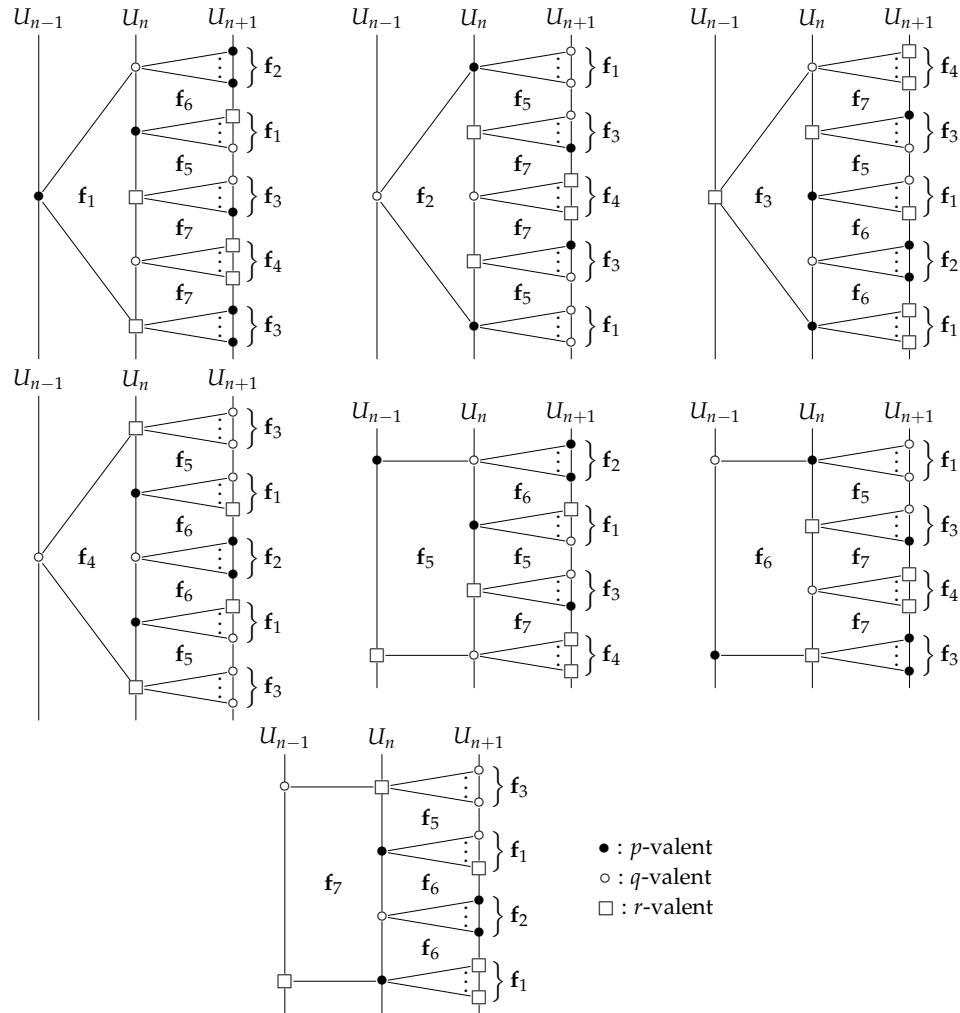


FIGURE 5.3. Offspring diagrams for a face-homogeneous tessellation with valence sequence $[p, q, p, r, q, r]$.

and $\sigma_2 = [6, 4, 6, 8, 4, 8]$. As $\chi(z)$ does not factor, numerical approximation of the eigenvalues in the respective cases of T_1 and T_2 yields $\gamma(T_1) \approx 9.8115$ and $\gamma(T_2) \approx$

13.5789 Thus for any tessellation T with valence sequence $\sigma \geq \sigma_1$ and $\sigma \geq \sigma_2$, we have $\gamma(T) \geq 9.8115$. \square

Proposition 5.7. *If $\sigma = [p, q, r, p, q, r]$, then $\frac{1}{p} + \frac{1}{q} + \frac{1}{r} < 1$ holds, σ is monomorphic with all valences even, and $\gamma(T) \geq 13.5612$.*

Proof. The offspring diagrams in Figure 5.4 show that σ is monomorphic and give the transition matrix

$$M = \begin{bmatrix} p-3 & \frac{3p-10}{2} & \frac{3p-10}{2} & p-3 & p-3 & p-4 \\ \frac{3q-10}{2} & q-3 & \frac{3q-10}{2} & q-4 & q-3 & q-3 \\ \frac{3r-10}{2} & \frac{3r-10}{2} & r-3 & r-3 & r-4 & r-3 \\ 1 & 2 & 1 & 1 & 1 & 1 \\ 1 & 1 & 2 & 1 & 1 & 1 \\ 2 & 1 & 1 & 1 & 1 & 1 \end{bmatrix}.$$

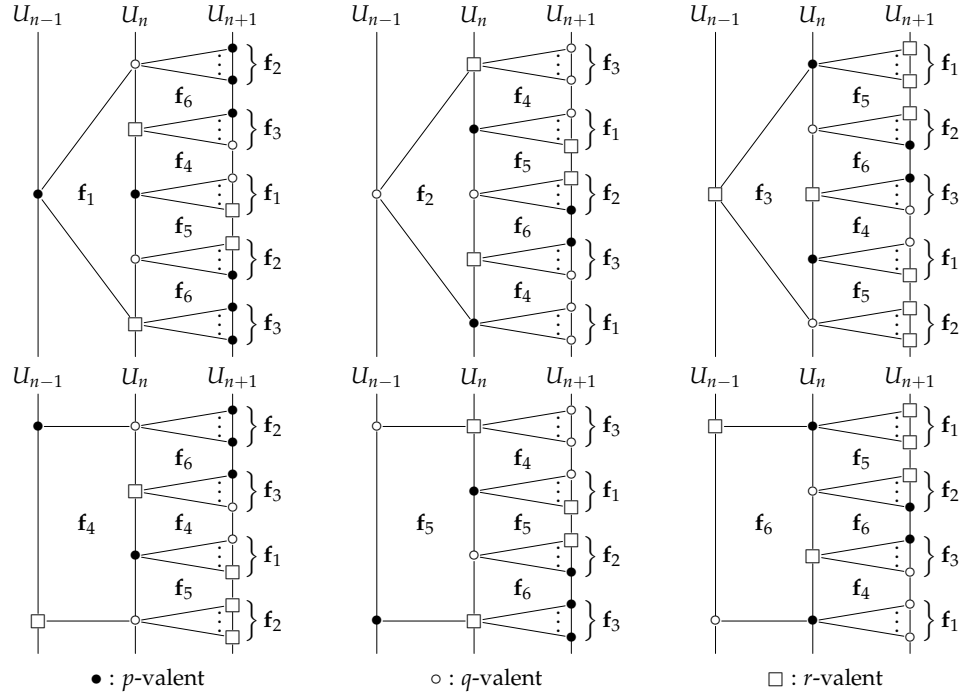


FIGURE 5.4. Offspring diagrams for a face-homogeneous tessellation with valence sequence $[p, q, r, p, q, r]$.

The characteristic polynomial of M is

$$\chi(z) = z^6 - az^5 - bz^4 - cz^3 - bz^2 - az + 1,$$

where

$$\begin{aligned} a &= p + q + r - 6, \\ b &= \frac{1}{4}(5(pq + pr + qr) - 32(p + q + r) + 132), \text{ and} \\ c &= \frac{1}{2}(2pqr - 7(pq + pr + qr) + 28(p + q + r) - 104). \end{aligned}$$

Since $p, q,$ and r must all be even, the unique minimal valence sequence in this class is $\sigma' = [4, 6, 8, 4, 6, 8]$. If T' is a face-homogeneous tessellation with valence sequence σ' , then numerical approximation of eigenvalues gives that $\gamma(T') \approx 13.5612$. By arguments similar to those above, we have $\gamma(T) \geq 13.5612$. \square

Proposition 5.8. *If $\sigma = [p, q, p, r, s, r]$, then $\frac{2}{p} + \frac{1}{q} + \frac{2}{r} + \frac{1}{s} < 2$ holds, σ is monomorphic with p and r even, and $\gamma(T) \geq 10.9033$.*

Proof. That σ is monomorphic is shown by the offspring diagrams in [Figure 5.5](#), which in turn yield the transition matrix

$$M = \begin{bmatrix} p-3 & p-4 & \frac{3p-10}{2} & 2p-6 & p-3 & \frac{p-4}{2} & \frac{3p-10}{2} \\ \frac{q-4}{2} & 0 & q-3 & q-3 & \frac{q-4}{2} & 0 & q-3 \\ \frac{3r-10}{2} & 2r-6 & r-3 & r-4 & r-3 & \frac{3r-10}{2} & \frac{r-4}{2} \\ s-3 & s-3 & \frac{s-4}{2} & 0 & \frac{s-4}{2} & s-3 & 0 \\ 1 & 2 & 1 & 2 & 1 & 1 & 1 \\ 1 & 0 & 2 & 2 & 1 & 0 & 2 \\ 2 & 2 & 1 & 0 & 1 & 2 & 0 \end{bmatrix}.$$

The characteristic polynomial of M is

$$\chi(z) = z^7 - az^6 - bz^5 - cz^4 + cz^3 + bz^2 + az - 1,$$

where

$$\begin{aligned} a &= p + r - 5, \\ b &= \frac{1}{2}pq + \frac{5}{4}pr + 2ps + 2qr + qs + \frac{1}{2}rs - 9p - 8q - 9r - 8s + 39, \text{ and} \\ c &= \frac{1}{2}pqr + pqs + \frac{1}{2}prs + qrs - \frac{7}{2}pq - \frac{19}{4}pr - 6ps - 6qr - 7qs - \frac{7}{2}rs \\ &\quad + 22p + 24q + 22r + 24s - 85. \end{aligned}$$

The four minimal valence sequences in this class are $\sigma_1 = [4, 5, 4, 6, 7, 6]$, $\sigma_2 = [4, 7, 4, 6, 5, 6]$, $\sigma_3 = [6, 4, 6, 8, 5, 8]$, and $\sigma_4 = [6, 5, 6, 8, 4, 8]$. Numerical approximation of eigenvalues of their respective transition matrices gives the following growth rates, where T_i is a face-homogeneous tessellation with valence sequence σ_i :

$$\begin{aligned} \gamma(T_1) &\approx 10.9033; \\ \gamma(T_2) &\approx 11.2073; \\ \gamma(T_3) &\approx 14.2638; \text{ and} \\ \gamma(T_4) &\approx 14.4008. \end{aligned}$$

By [\[1\]](#)Theorem 2.7, we have $\gamma(T) \geq 10.9033$. \square

Proposition 5.9. *If $\sigma = [p, q, r, p, s, t]$, then $\frac{2}{p} + \frac{1}{q} + \frac{1}{r} + \frac{1}{s} + \frac{1}{t} < 2$ holds, σ is monomorphic with all terms even, and $\gamma(T) \geq 18.1174$.*

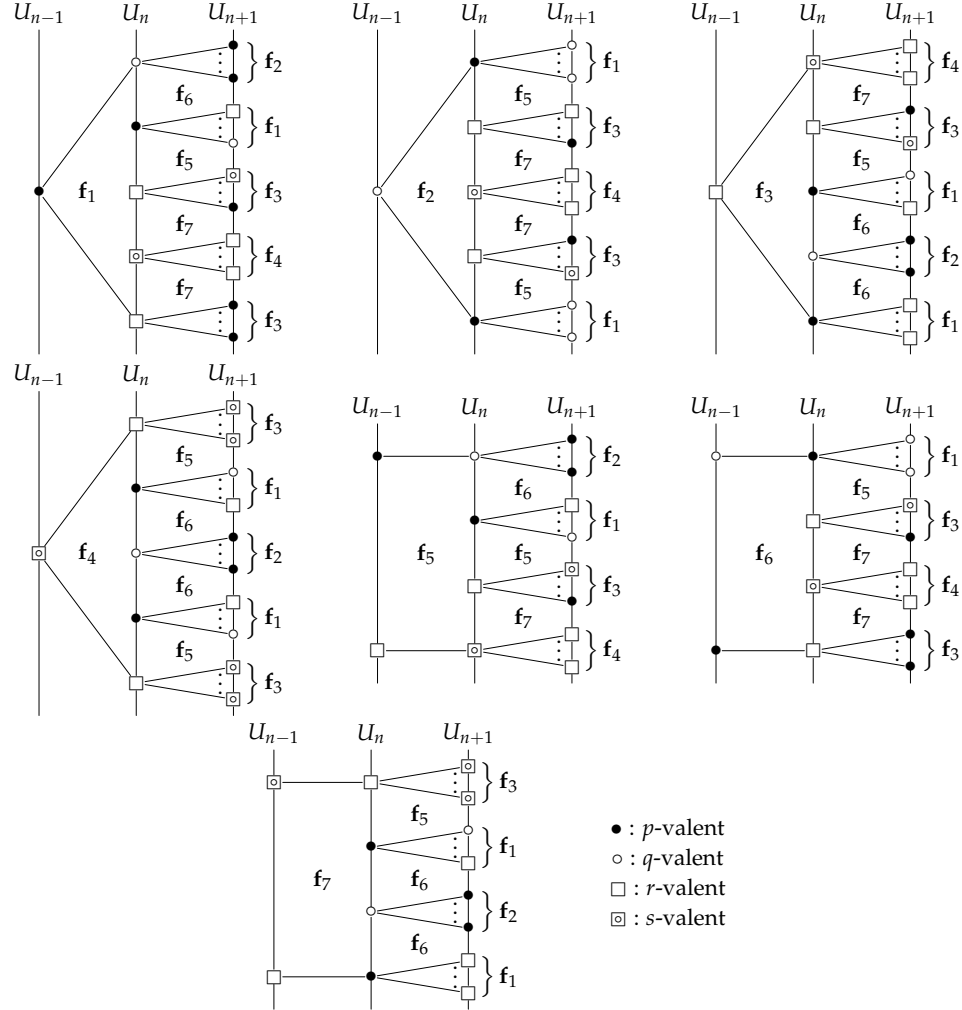


FIGURE 5.5. Offspring diagrams for a face-homogeneous tessellation with valence sequence $[p, q, p, r, s, r]$.

Proof. As T is monomorphic and belongs to $\mathcal{G}_{4,4}$, we again appeal to [1]Lemma 2.9 to obtain the 12×12 transition matrix

$$M = \begin{bmatrix}
 0 & \frac{p-4}{2} & p-3 & p-3 & p-3 & \frac{p-4}{2} & 0 & 0 & \frac{p-4}{2} & p-3 & p-3 & \frac{p-4}{2} \\
 \frac{q-4}{2} & 0 & \frac{q-4}{2} & q-3 & q-3 & q-3 & \frac{q-4}{2} & 0 & 0 & \frac{q-4}{2} & q-3 & q-3 \\
 r-3 & \frac{r-4}{2} & 0 & \frac{r-4}{2} & r-3 & r-3 & r-3 & \frac{r-4}{2} & 0 & 0 & \frac{r-4}{2} & r-3 \\
 p-3 & p-3 & \frac{p-4}{2} & 0 & \frac{p-4}{2} & p-3 & p-3 & p-3 & \frac{p-4}{2} & 0 & 0 & \frac{p-4}{2} \\
 s-3 & s-3 & s-3 & \frac{s-4}{2} & 0 & \frac{s-4}{2} & \frac{s-4}{2} & s-3 & s-3 & \frac{s-4}{2} & 0 & 0 \\
 \frac{t-4}{2} & t-3 & t-3 & t-3 & \frac{t-4}{2} & 0 & 0 & \frac{t-4}{2} & t-3 & t-3 & \frac{t-4}{2} & 0 \\
 0 & 0 & 1 & 1 & 1 & 1 & 0 & 0 & 1 & 1 & 1 & 0 \\
 1 & 0 & 0 & 1 & 1 & 1 & 0 & 0 & 0 & 1 & 1 & 1 \\
 1 & 1 & 0 & 0 & 1 & 1 & 1 & 0 & 0 & 0 & 1 & 1 \\
 1 & 1 & 1 & 0 & 0 & 1 & 1 & 1 & 0 & 0 & 0 & 1 \\
 1 & 1 & 1 & 1 & 0 & 0 & 1 & 1 & 1 & 0 & 0 & 0 \\
 0 & 1 & 1 & 1 & 1 & 0 & 0 & 1 & 1 & 1 & 0 & 0
 \end{bmatrix}.$$

The minimal valence sequences in this class are $\sigma_1 = [4, 6, 8, 4, 10, 12]$ and $\sigma_2 = [6, 4, 8, 6, 10, 12]$. Continuing previous notational convention, we have by numerical approximation

$$\gamma(T_1) \approx 18.1174 \quad \text{and} \quad \gamma(T_2) \approx 19.4819.$$

Thus by [1]Theorem 2.7, we have $\gamma(T) \geq 18.1174$. □

Proposition 5.10. *If $\sigma = [p, q, r, s, t, u]$, then $\frac{1}{p} + \frac{1}{q} + \frac{1}{r} + \frac{1}{s} + \frac{1}{t} + \frac{1}{u} < 2$ holds, σ is monomorphic with all terms even, and $\gamma(T) \geq 23.9963$.*

Proof. As all the valences are distinct, σ is monomorphic, and so [1]Lemma 2.9 applies to determine directly the transition matrix

$$M = \begin{bmatrix} 0 & \frac{p-4}{2} & p-3 & p-3 & p-3 & \frac{p-4}{2} & 0 & 0 & \frac{p-4}{2} & p-3 & p-3 & \frac{p-4}{2} \\ \frac{q-4}{2} & 0 & \frac{q-4}{2} & q-3 & q-3 & \frac{q-4}{2} & 0 & 0 & \frac{q-4}{2} & q-3 & q-3 & \frac{q-4}{2} \\ r-3 & \frac{r-4}{2} & 0 & \frac{r-4}{2} & r-3 & r-3 & r-3 & \frac{r-4}{2} & 0 & 0 & \frac{r-4}{2} & r-3 \\ s-3 & s-3 & \frac{s-4}{2} & 0 & \frac{s-4}{2} & s-3 & s-3 & s-3 & \frac{s-4}{2} & 0 & 0 & \frac{s-4}{2} \\ t-3 & t-3 & t-3 & \frac{t-4}{2} & 0 & \frac{t-4}{2} & \frac{t-4}{2} & t-3 & t-3 & \frac{t-4}{2} & 0 & 0 \\ \frac{u-4}{2} & u-3 & u-3 & u-3 & \frac{u-4}{2} & 0 & 0 & \frac{u-4}{2} & u-3 & u-3 & \frac{u-4}{2} & 0 \\ 0 & 1 & 1 & 1 & 1 & 0 & 0 & 0 & 1 & 1 & 1 & 0 \\ 0 & 0 & 1 & 1 & 1 & 1 & 0 & 0 & 0 & 1 & 1 & 1 \\ 1 & 0 & 0 & 1 & 1 & 1 & 1 & 0 & 0 & 0 & 1 & 1 \\ 1 & 1 & 0 & 0 & 1 & 1 & 1 & 1 & 0 & 0 & 0 & 1 \\ 1 & 1 & 1 & 0 & 0 & 1 & 1 & 1 & 1 & 0 & 0 & 0 \\ 1 & 1 & 1 & 1 & 0 & 0 & 0 & 1 & 1 & 1 & 0 & 0 \end{bmatrix}.$$

As all the valences must also be even, all the minimal valence sequences in this class are permutations on $(4, 6, 8, 10, 12, 14)$, of which there are exactly $\frac{1}{2}(6-1)! = 60$. Among these, the valence sequence in this class with the least rate of growth is $[4, 6, 10, 14, 12, 8]$, as shown in Table 2, with growth rate approximately 23.9963.

Thus by [1]Theorem 2.7, we have $\gamma(T) \geq 23.9963$. □

5.2. Valence sequences of length 6 with at least one 3-valent vertex.

We first classify those valence sequences which are polymorphic. Complete sets of offspring diagrams are generally not needed and hence not provided, as polymorphicity becomes evident by considering offspring of only some of the face types.

Theorem 5.11. *If σ is one of the following 23 valence sequences where $p, q, r, s \geq 4$, then σ is polymorphic:*

Case	Sequence	Case	Sequence	Case	Sequence
(1)	$[3, 3, 3, 3, 3, p]$	(9)	$[3, 3, 3, p, 3, q]$	(17)	$[p, p, q, q, p, 3]$
(2)	$[p, p, p, p, p, 3]$	(10)	$[p, p, p, 3, p, q]$	(18)	$[p, p, 3, q, 3, q]$
(3)	$[3, 3, 3, 3, p, p]$	(11)	$[p, p, 3, p, p, q]$	(19)	$[3, 3, 3, p, q, r]$
(4)	$[3, 3, 3, p, 3, p]$	(12)	$[3, 3, 3, p, p, q]$	(20)	$[p, p, 3, p, q, r]$
(5)	$[p, p, p, 3, p, 3]$	(13)	$[p, p, p, q, 3, q]$	(21)	$[p, 3, p, q, p, r]$
(6)	$[3, 3, 3, p, p, p]$	(14)	$[p, p, 3, p, 3, q]$	(22)	$[p, 3, p, q, r, s]$
(7)	$[3, 3, p, 3, p, p]$	(15)	$[p, 3, p, p, 3, q]$		
(8)	$[3, 3, 3, 3, p, q]$	(16)	$[3, 3, p, p, 3, q]$		

Proof. Exactly twelve of the 23 listed cases satisfy the hypothesis of [1]Proposition 3.1, including belonging to $\mathcal{G}_{3+,5}$. For these cases it suffices to identify the triples satisfying the proposition’s hypotheses. Valence sequences (2), (5), (6), and (10) contain triples $(p, p, 3)$ as well as (p, p, p) ; valence sequences (11), (12), (14), (17), and (18) contain both $(p, p, 3)$ and (p, p, q) ; sequence (13) contains both (p, p, p)

σ_i	$\gamma(T_i)$	σ_i	$\gamma(T_i)$
[4, 6, 8, 10, 12, 14]	24.41712251	[4, 8, 10, 6, 12, 14]	24.87880785
[4, 6, 8, 10, 14, 12]	24.21960545	[4, 8, 10, 6, 14, 12]	24.80899840
[4, 6, 8, 12, 10, 14]	24.61270141	[4, 8, 10, 12, 6, 14]	25.35303706
[4, 6, 8, 12, 14, 10]	24.08285752	[4, 8, 10, 14, 6, 12]	25.18185562
[4, 6, 8, 14, 10, 12]	24.48957224	[4, 8, 12, 6, 10, 14]	25.03584620
[4, 6, 8, 14, 12, 10]	24.15679180	[4, 8, 12, 6, 14, 10]	24.90132812
[4, 6, 10, 8, 12, 14]	24.58261968	[4, 8, 12, 10, 6, 14]	25.23325447
[4, 6, 10, 8, 14, 12]	24.45332058	[4, 8, 12, 14, 6, 10]	24.77199967
[4, 6, 10, 12, 8, 14]	24.85506399	[4, 8, 14, 6, 10, 12]	25.01874720
[4, 6, 10, 12, 14, 8]	24.04416760	[4, 8, 14, 6, 12, 10]	24.95377767
[4, 6, 10, 14, 8, 12]	24.68019759	[4, 8, 14, 10, 6, 12]	24.96611444
★ [4, 6, 10, 14, 12, 8]	23.99630569	[4, 8, 14, 12, 6, 10]	24.67581103
[4, 6, 12, 8, 10, 14]	24.80458415	[4, 10, 6, 8, 12, 14]	24.98236812
[4, 6, 12, 8, 14, 10]	24.54658791	[4, 10, 6, 8, 14, 12]	24.82334169
[4, 6, 12, 10, 8, 14]	24.88247982	[4, 10, 6, 12, 8, 14]	25.58786488
[4, 6, 12, 10, 14, 8]	24.27525170	[4, 10, 6, 14, 8, 12]	25.52589967
[4, 6, 12, 14, 8, 10]	24.41387775	[4, 10, 8, 6, 12, 14]	24.98070079
[4, 6, 12, 14, 10, 8]	24.06126298	[4, 10, 8, 6, 14, 12]	24.89788355
[4, 6, 14, 8, 10, 12]	24.78717089	[4, 10, 8, 12, 6, 14]	25.70437512
[4, 6, 14, 8, 12, 10]	24.65801011	[4, 10, 8, 14, 6, 12]	25.58679602
[4, 6, 14, 10, 8, 12]	24.74623904	[4, 10, 12, 6, 8, 14]	25.18902550
[4, 6, 14, 10, 12, 8]	24.33423320	[4, 10, 12, 8, 6, 14]	25.30889683
[4, 6, 14, 12, 8, 10]	24.45269393	[4, 10, 14, 6, 8, 12]	25.05471909
[4, 6, 14, 12, 10, 8]	24.16830858	[4, 10, 14, 8, 6, 12]	25.04268293
[4, 8, 6, 10, 12, 14]	24.71739812	[4, 12, 6, 8, 10, 14]	25.38856036
[4, 8, 6, 10, 14, 12]	24.50356321	[4, 12, 6, 10, 8, 14]	25.71589810
[4, 8, 6, 12, 10, 14]	24.99665188	[4, 12, 8, 6, 10, 14]	25.24072240
[4, 8, 6, 12, 14, 10]	24.43259325	[4, 12, 8, 10, 6, 14]	25.77151261
[4, 8, 6, 14, 10, 12]	24.93312365	[4, 12, 10, 6, 8, 14]	25.29247408
[4, 8, 6, 14, 12, 10]	24.58265856	[4, 12, 10, 8, 6, 14]	25.49621988

TABLE 2. Table of minimal sequences in the class $[p, q, r, s, t, u]$, with approximate growth rates. See [Proposition 5.10](#).

and (p, p, q) ; sequence (20) contains both $(p, p, 3)$ and (p, p, r) ; finally, sequence (21) contains both $(q, p, 3)$ and (q, p, r) . We treat the remaining eight cases in turn.

- (1) $[3, 3, 3, 3, 3, p]$: We have distinct possible sets of offspring of a face of type \mathbf{f}_5 as shown in [Figure 5.6](#). Thus σ is polymorphic.
- (3) $[3, 3, 3, 3, p, p]$: Thus p is even. The 3-valent vertices fall into two classes: those adjacent only to other 3-valent vertices, and those adjacent to two 3-valent vertices and one p -valent vertex. Once the neighbors of an arbitrary 3-valent vertex are determined, the vertices at regional distance 2 from that 3-valent vertex can be identified by the configurations given in [Figure 5.7](#).

Both of these configurations admit wedges in F_2 incident with a p -valent vertex in U_1 . The configuration of descendants of wedges in F_n with a p -valent

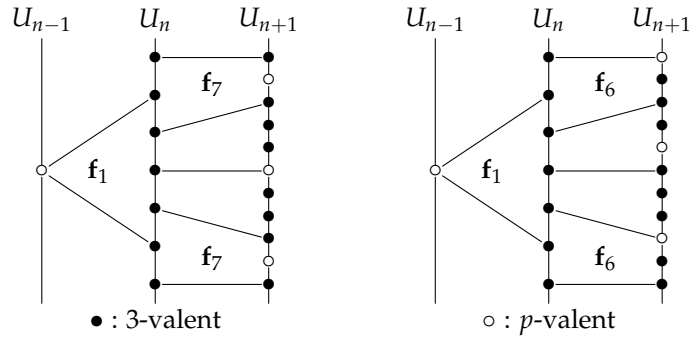


FIGURE 5.6. Distinct possible offspring diagrams for a face of type f_1 in tessellations with valence sequence $[3, 3, 3, 3, 3, p]$.

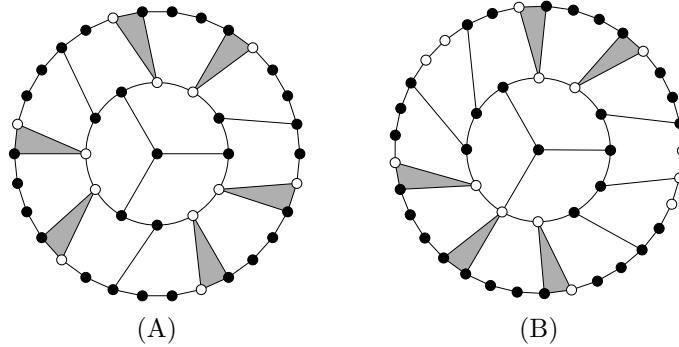


FIGURE 5.7. First two coronas of tessellations with valence sequence $[3, 3, 3, 3, p, p]$ when rooted at a 3-valent vertex. Figure (A) depicts the root as a 3-valent vertex adjacent only to 3-valent vertices; figure (B) depicts the root as a 3-valent vertex adjacent to two 3-valent vertices and one p -valent vertex. Shaded regions represent $p - 3$ or $p - 4$ adjacent wedges all of the same type.

vertex in U_{n-1} is not uniquely determined. Let these faces be denoted as of type f_3 .

Faces of type f_3 in F_n have two distinct possible sets of offspring, as shown in Figure 5.8. When adjacent faces of type f_3 occur in F_n , both incident to a common 3-valent vertex in U_n , one must have offspring as specified in Figure 5.8(A) and the other must have offspring as specified in Figure 5.8(B). However, the arrangement (in clockwise order about the common p -valent vertex in U_{n-1}) may be (A)-(B) or (B)-(A). The choice of one arrangement at one point in the tessellation in no way restricts the choices of the other arrangement elsewhere; hence the valence sequence is polymorphic.

- (4) $[3, 3, 3, p, 3, p]$: Wedges in F_n with a p -valent vertex in U_{n-1} have four possible configurations, partially determined by the vertices incident with the face, as shown in Figure 5.9. Face types f_1 and f_2 have their offspring completely determined by these neighboring vertices. However, a face in F_n which has as

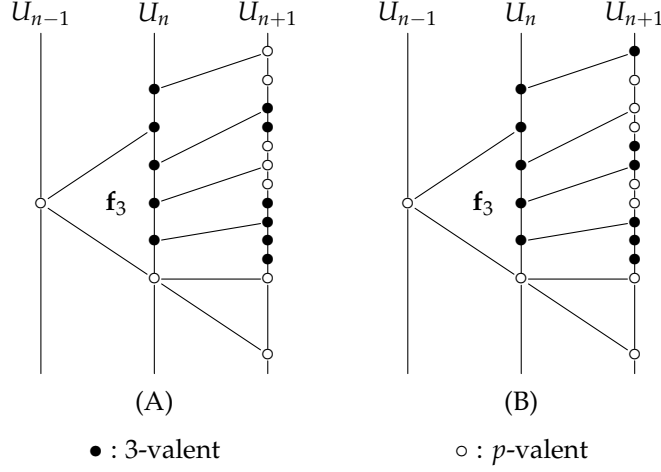


FIGURE 5.8. Distinct sets of offspring for a face of type \mathbf{f}_3 in a tessellation with valence sequence $[3, 3, 3, 3, p, p]$.

offspring wedges each incident with a p -valent vertex in U_n admits multiple distinct sets of offspring, as various accretion rules can specify varying numbers of faces of types \mathbf{f}_1 , \mathbf{f}_2 , \mathbf{f}_3 , and \mathbf{f}_4 as offspring. Therefore σ is polymorphic.

- (7) $[3, 3, p, 3, p, p]$: As shown in Figure 5.10, there are at least two distinct types of wedges which occur in F_n incident with a p -valent vertex in U_{n-1} : types \mathbf{f}_1 and \mathbf{f}_2 . Pairs of adjacent wedges occurring as offspring of a face in F_n may thus be $\mathbf{f}_1\mathbf{f}_1$ -pairs or $\mathbf{f}_2, \mathbf{f}_2$ -pairs with no effect on the surrounding offspring. When $p = 4$, these adjacent wedges occur only in F_1 ; if $p \geq 5$, the pairs occur in F_n for all $n > 1$. Therefore σ is polymorphic.
- (8) $[3, 3, 3, 3, p, q]$: Both p and q are even, and $\frac{1}{p} + \frac{1}{q} < \frac{2}{3}$ holds. The wedge type \mathbf{f}_1 in a tessellation with valence sequence σ has the configuration shown in Figure 5.11. In the figure, the only vertices drawn in U_{n+1} are those which are explicitly determined by σ as offspring of an \mathbf{f}_1 face; all other vertices incident with the offspring of an \mathbf{f}_1 face in F_n are dependent upon the choice of accretion rule.
- (9) $[3, 3, 3, p, 3, q]$: Thus $\frac{1}{p} + \frac{1}{q} < \frac{2}{3}$ holds. Wedges of type \mathbf{f}_1 have the configuration shown in Figure 5.12, where the only vertices drawn in U_{n+1} are those which are explicitly determined by the valence sequence in the offspring of a \mathbf{f}_1 face; all other vertices incident with the offspring of an \mathbf{f}_3 face in F_n are determined by the choice of accretion rule.
- (15) $[p, 3, p, p, 3, q]$: p and q both even and $\frac{3}{p} + \frac{1}{q} < \frac{4}{3}$ holds. The wedge type \mathbf{f}_1 shown in Figure 5.13 has distinct sets of offspring dependent upon the chosen accretion rule, so $[p, 3, p, p, 3, q]$ is polymorphic.
- (16) $[3, 3, p, p, 3, q]$: Thus p is even and $\frac{2}{p} + \frac{1}{q} < 1$ holds. The wedge of type \mathbf{f}_1 illustrated in Figure 5.14 admits multiple distinct offspring diagrams depending upon the choice of accretion rule. Hence $[3, 3, p, p, 3, q]$ is polymorphic.
- (19) $[3, 3, 3, p, q, r]$: p , q , and r all even, $\frac{1}{p} + \frac{1}{q} + \frac{1}{r} < 1$. Wedges of type \mathbf{f}_1 have one of two configurations of offspring in a tessellation with valence sequence $[3, 3, 3, p, q, r]$, as shown in Figure 5.15. The two diagrams differ in the face

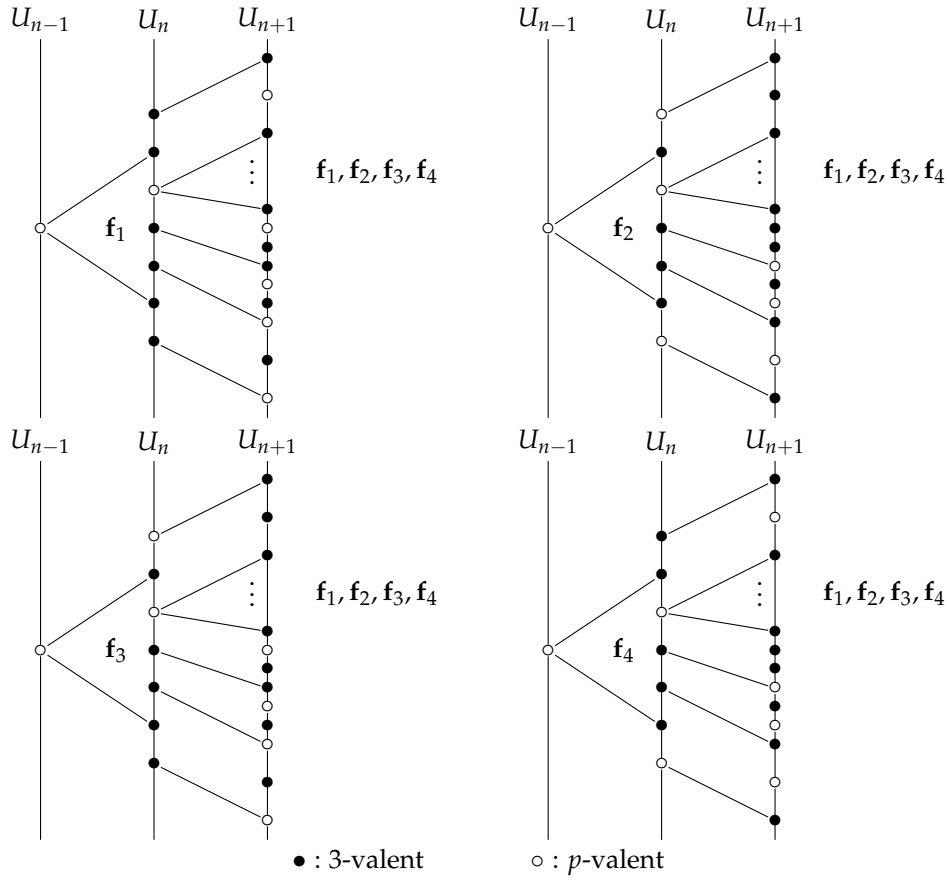


FIGURE 5.9. Offspring diagrams for wedges in F_n of a face-homogeneous tessellation with valence sequence $[3, 3, 3, p, 3, p]$, with p -valent vertex in U_{n-1} .

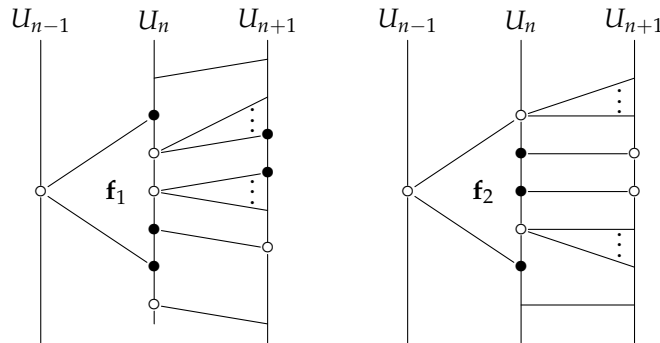


FIGURE 5.10. Wedges of types \mathbf{f}_1 and \mathbf{f}_2 in a face-homogeneous tessellation with valence sequence $[3, 3, p, 3, p, p]$.

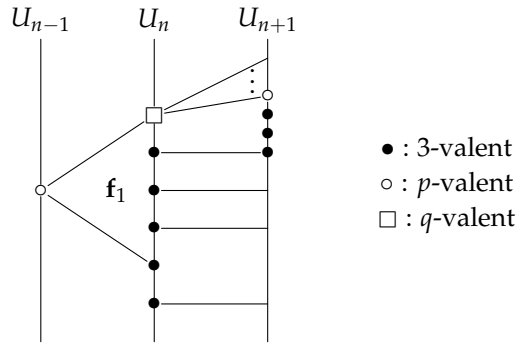


FIGURE 5.11. Offspring of a wedge of type \mathbf{f}_1 in a face-homogeneous tessellation with valence sequence $[3, 3, 3, 3, p, q]$.

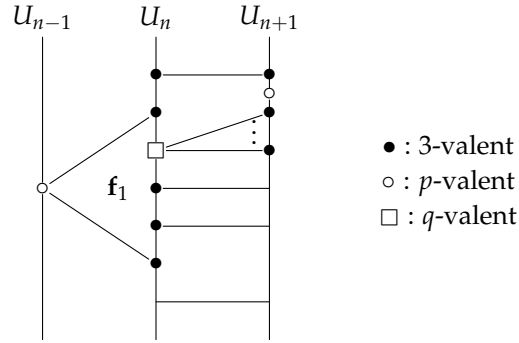


FIGURE 5.12. Offspring of a wedge of type \mathbf{f}_1 in a face-homogeneous tessellation with valence sequence $[3, 3, 3, p, 3, q]$.

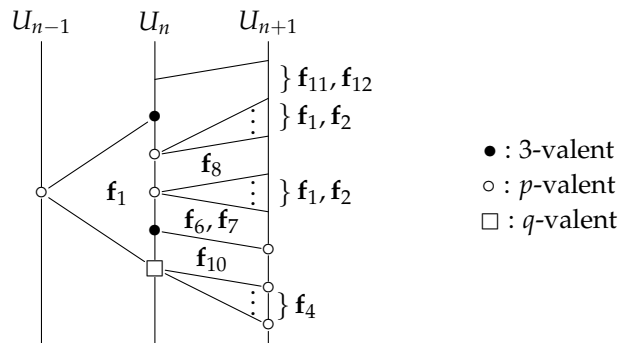


FIGURE 5.13. Offspring diagram for wedge of type \mathbf{f}_1 in a face-homogeneous tessellation with valence sequence $[p, 3, p, p, 3, q]$.

type marked with an arrow. Whenever two faces of type \mathbf{f}_1 are incident with a common edge with edge-symbol $\langle 3, p; 6, 6 \rangle$, the two configurations (A) and

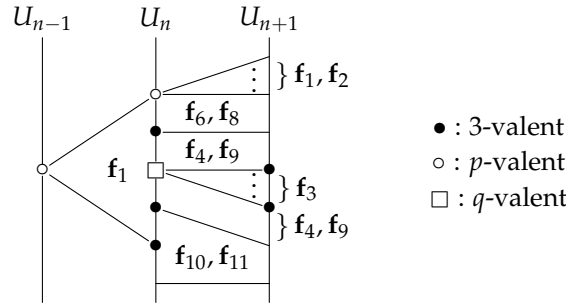


FIGURE 5.14. Offspring diagram for a wedge of type f_1 in a face-homogeneous tessellation with valence sequence $[3, 3, p, p, 3, q]$.

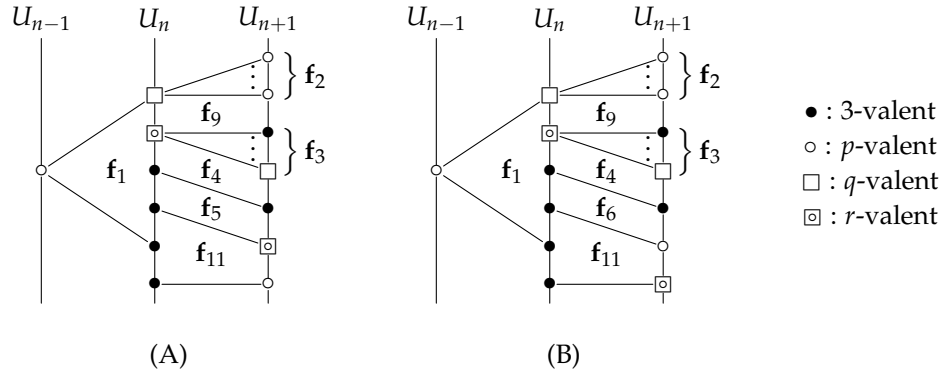


FIGURE 5.15. Distinct offspring diagrams for a wedge of type f_1 in a face-homogeneous tessellation with valence sequence $[3, 3, 3, p, q, r]$.

- (B) shown in the figure will be paired; the choice of clockwise orientation of “(A) then (B)” versus “(B) then (A)” demonstrates that σ is polymorphic.
- (22) $[p, 3, p, q, r, s]$: p, q, r , and s even. There are two distinct sets of offspring for a wedge of type f_1 , as shown in Figure 5.16. Once again, the choice of clockwise orientation about a p -valent vertex in U_{n-1} determines the pattern “(A) then (B)” versus “(B) then (A),” and gives that σ is polymorphic.

This concludes the proof of the theorem. □

Proposition 5.12. *If $\sigma = [p, p, 3, p, p, 3]$, then σ is monomorphic with p even, and*

$$\gamma(T) = \frac{1}{8} \left[5p - 10 + a + \sqrt{50p^2 + (10a - 216)p - 20a + 168} \right],$$

where $a = \sqrt{25p^2 - 116 + 132}$.

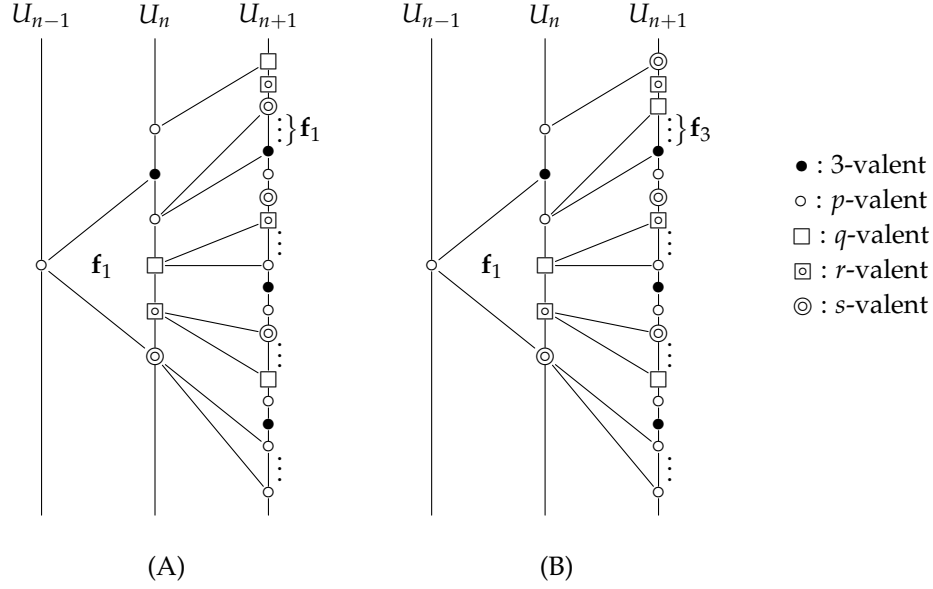


FIGURE 5.16. Offspring diagram for a wedge of type \mathbf{f}_1 in a face-homogeneous tessellation with valence sequence $[p, 3, p, q, r, s]$. Only those offspring which may vary in type are labeled.

Proof. The offspring diagrams shown in [Figure 5.17](#) demonstrate that σ is monomorphic with transition matrix

$$M = \begin{bmatrix} \frac{5p-16}{2} & 3p-10 & 2p-7 & 2p-6 & p-4 \\ 0 & 0 & 0 & 0 & 0 \\ 2 & 2 & 2 & 0 & 2 \\ 1 & 0 & 1 & 1 & 0 \\ \frac{1}{2} & 0 & 0 & 1 & 0 \end{bmatrix}.$$

Its characteristic polynomial is

$$\chi(z) = z^5 + \left(5 - \frac{5}{2}p\right)z^4 + pz^3 + \left(5 - \frac{5}{2}p\right)z^2 + z,$$

which has a palindromic quartic factor, and we apply [Remark 1.1](#). \square

Proposition 5.13. *If $\sigma = [3, p, 3, p, 3, p]$, then σ is monomorphic and*

$$\gamma(T) = p - 2 + \sqrt{(p-2)^2 - 1}.$$

Proof. As T is edge-homogeneous with edge-symbol $\langle 3, p; 6, 6 \rangle$, the result follows from [\[1\]Proposition 1.17](#). \square

Proposition 5.14. *If $\sigma = [3, 3, 3, p, q, p]$, then p is even, σ is monomorphic, and*

$$\gamma(T) \geq \frac{1}{4} \left(1 + \sqrt{57} + \sqrt{42 + 2\sqrt{57}} \right) \approx 4.0265.$$

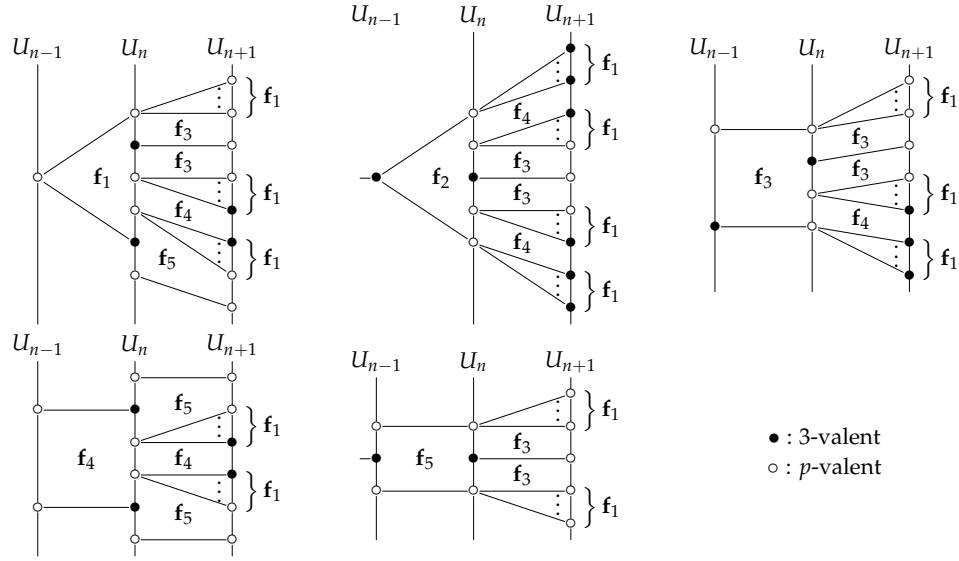


FIGURE 5.17. Offspring diagrams for a face-homogeneous tessellation with valence sequence $[p, p, 3, p, p, 3]$.

Proof. Clearly $p, q \geq 4$. The unique set of offspring diagrams for σ is depicted in Figure 5.18. Taking

$$M = \begin{bmatrix} p-3 & p-4 & p-3 & \frac{3p-10}{2} & \frac{p-4}{2} & p-3 & p-4 \\ \frac{q-4}{2} & 0 & \frac{q-4}{2} & q-3 & 0 & \frac{q-4}{2} & q-3 \\ 1 & 2 & 1 & 0 & 1 & 0 & 0 \\ 1 & 0 & 0 & 0 & 1 & 0 & 0 \\ 1 & 0 & 1 & 2 & 0 & 1 & 2 \\ 0 & 0 & \frac{1}{2} & \frac{1}{2} & 0 & \frac{1}{2} & 0 \\ \frac{1}{2} & 0 & 0 & 0 & \frac{1}{2} & 0 & 0 \end{bmatrix}$$

to be the transition matrix, we obtain

$$\chi(z) = \frac{1}{4}(2z-1)(2z^6 - az^5 - bz^4 - cz^3 - bz^2 - az + 2),$$

where

$$\begin{aligned} a &= 2p - 4, \\ b &= pq + p + 2q - 14, \text{ and} \\ c &= 2pq - 10p - 12q + 40. \end{aligned}$$

The minimal valence sequences in this class are $\sigma_1 = [3, 3, 3, 4, 5, 4]$ and $\sigma_2 = [3, 3, 3, 6, 4, 6]$; respectively, tessellations T_1 and T_2 with these valence sequences have growth rates

$$\begin{aligned} \gamma(T_1) &= \frac{1}{4} \left(1 + \sqrt{57} + \sqrt{42 + 2\sqrt{57}} \right) \approx 4.0265 \quad \text{and} \\ \gamma(T_2) &= 3 + 2\sqrt{2} \approx 5.8284. \end{aligned}$$

By [1]Theorem 2.7, the growth rate of a face-homogeneous tessellation T with valence sequence σ such that $\sigma \geq \sigma_1$ or $\sigma \geq \sigma_2$ satisfies the stated inequality. \square

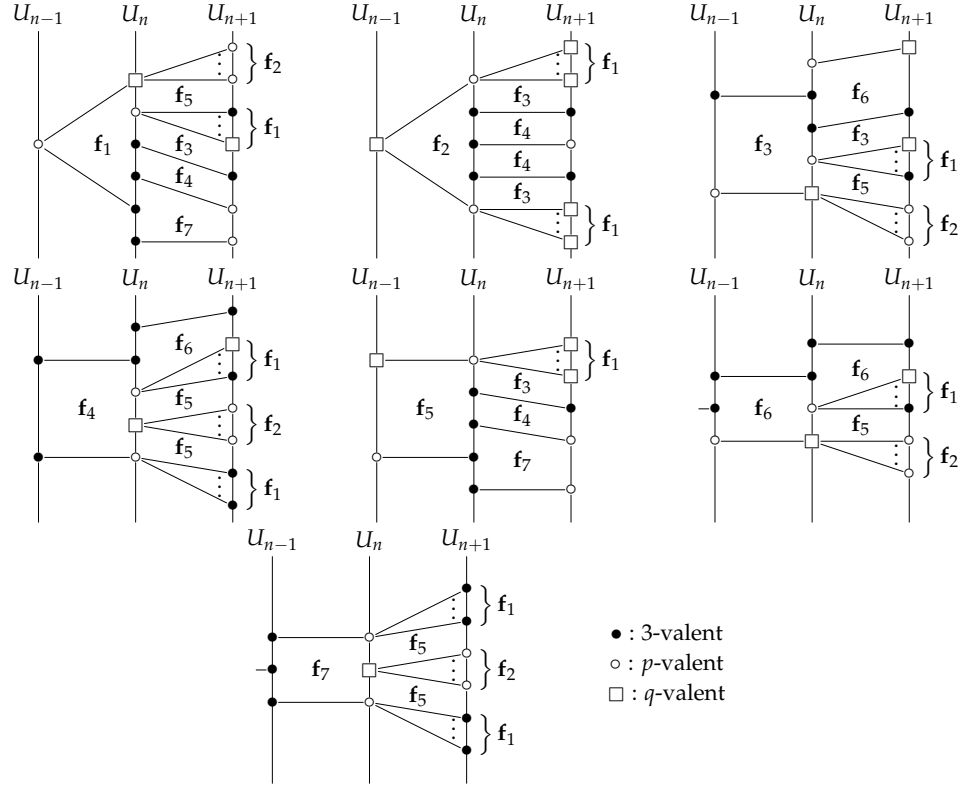


FIGURE 5.18. Offspring diagrams for a face-homogeneous tessellation with valence sequence $[3, 3, 3, p, q, p]$. See Proposition 5.14.

Proposition 5.15. *If $\sigma = [p, 3, p, q, 3, q]$, then σ is monomorphic with both p and q even, and $\gamma(T) \geq 6.8091$.*

Proof. The offspring diagrams for a tessellation T with valence sequence σ are shown in Figure 5.19. Hence σ is monomorphic, with

$$M = \begin{bmatrix} p-3 & \frac{3p-10}{2} & p-3 & \frac{p-4}{2} & \frac{3p-10}{2} & 0 & p-4 \\ \frac{3q-10}{2} & q-3 & q-3 & \frac{3q-10}{2} & \frac{q-4}{2} & q-4 & 0 \\ 1 & 1 & 1 & 1 & 1 & 0 & 0 \\ 0 & 2 & 0 & 0 & 2 & 0 & 2 \\ 2 & 0 & 0 & 2 & 0 & 2 & 0 \\ \frac{1}{2} & 0 & \frac{1}{2} & 0 & 0 & 0 & 0 \\ 0 & \frac{1}{2} & \frac{1}{2} & 0 & 0 & 0 & 0 \end{bmatrix}.$$

This transition matrix has the characteristic polynomial

$$\chi(z) = \frac{1}{4}(z-1)(4z^6 - az^5 - bz^4 + cz^3 - bz^2 - az + 4),$$

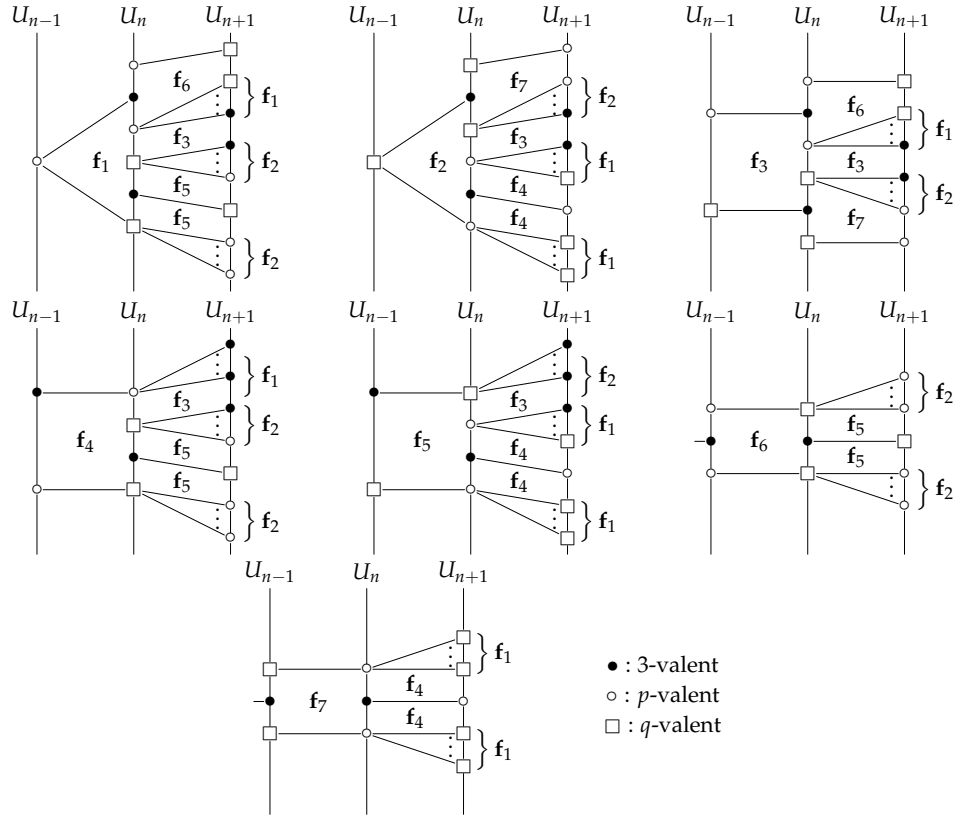


FIGURE 5.19. Offspring diagrams for a face-homogeneous tessellation with valence sequence $[p, 3, p, q, 3, q]$.

where

$$\begin{aligned}
 a &= 4p + 4q - 24, \\
 b &= 5pq - 2p - 2q - 24, \text{ and} \\
 c &= 2pq - 8p - 8q + 40.
 \end{aligned}$$

As the characteristic polynomial is not solvable, we consider the minimal valence sequence in this class, $\sigma_1 = [4, 3, 4, 6, 3, 6]$. If T_1 is a face-homogeneous tessellation with valence sequence σ_1 , we have by numerical approximation of eigenvalues that $\gamma(T_1) \approx 6.8091$. Hence by Theorem 2.7, if T is a face-homogeneous tessellation with valence sequence $\sigma \geq \sigma_1$, then $\gamma(T) \geq 6.8091$. \square

Proposition 5.16. *If $\sigma = [3, p, 3, q, 3, r]$, then σ is monomorphic and $\gamma(T) \geq 5.6429$.*

Proof. Clearly each 3-valent vertex of T has a neighbor of each other valence. This yields the offspring diagrams shown in Figure 5.20 showing σ to be monomorphic

with transition matrix

$$M = \begin{bmatrix} 0 & p-3 & p-3 & \frac{p-4}{2} & 0 & 0 & \frac{p-4}{2} & p-3 & p-3 & 0 & 0 & p-3 \\ q-3 & 0 & q-3 & q-3 & q-3 & \frac{q-4}{2} & 0 & 0 & \frac{q-4}{2} & q-3 & 0 & 0 \\ r-3 & r-3 & 0 & 0 & \frac{r-4}{2} & r-3 & r-3 & \frac{r-4}{2} & 0 & 0 & r-3 & 0 \\ \hline 0 & 0 & 1 & 1 & 0 & 0 & 0 & 0 & 1 & 0 & 0 & 0 \\ 1 & 0 & 0 & 0 & 1 & 1 & 0 & 0 & 0 & 0 & 0 & 0 \\ 0 & 1 & 0 & 0 & 0 & 0 & 1 & 1 & 0 & 0 & 0 & 0 \\ \hline 0 & 0 & 1 & 1 & 0 & 0 & 0 & 0 & 1 & 0 & 0 & 0 \\ 1 & 0 & 0 & 0 & 1 & 1 & 0 & 0 & 0 & 0 & 0 & 0 \\ 0 & 1 & 0 & 0 & 0 & 0 & 1 & 1 & 0 & 0 & 0 & 0 \\ \hline 0 & 1 & 0 & 0 & 0 & 0 & \frac{1}{2} & \frac{1}{2} & 0 & 0 & \frac{1}{2} & \frac{1}{2} \\ 0 & 0 & 1 & \frac{1}{2} & 0 & 0 & 0 & 0 & \frac{1}{2} & \frac{1}{2} & 0 & \frac{1}{2} \\ 1 & 0 & 0 & 0 & \frac{1}{2} & \frac{1}{2} & 0 & 0 & 0 & \frac{1}{2} & \frac{1}{2} & 0 \end{bmatrix}$$

The characteristic polynomial of M is

$$\chi(z) = \frac{1}{4}z^3(z-1)(2z+1)^2(z^6 - az^4 - bz^3 - az^2 + 1),$$

with

$$\begin{aligned} a &= pq + pr + qr - 4p - 4q - 4r + 9 \text{ and} \\ b &= 2pqr - 4pq - 4pr - 4qr + 8p + 8q + 8r - 16. \end{aligned}$$

The unique minimal member is $\sigma_1 = [3, 4, 3, 5, 3, 6]$. By numerical approximation of eigenvalues, if T_1 is a tessellation with valence sequence σ_1 , then $\gamma(T_1) \approx 5.6723$. Hence $\gamma(T) \geq \gamma(T_1) \approx 5.6723$ by [1]Theorem 2.7. \square

Proposition 5.17. *If $\sigma = [p, 3, p, q, r, q]$, then σ is monomorphic with p and q even and $\gamma(T) \geq 8.0601$.*

Proof. The offspring diagrams given in Figure 5.21 show that σ is monomorphic. Using those diagrams to compute the transition matrix, we obtain

$$M = \begin{bmatrix} p-3 & \frac{3p-10}{2} & 2p-6 & p-3 & \frac{p-4}{2} & \frac{3p-10}{2} & 0 \\ \frac{3q-10}{2} & q-3 & q-4 & q-3 & \frac{3q-10}{2} & \frac{q-4}{2} & q-4 \\ r-3 & \frac{r-4}{2} & 0 & \frac{r-4}{2} & r-3 & 0 & r-3 \\ \hline 1 & 1 & 2 & 1 & 1 & 1 & 0 \\ 0 & 2 & 2 & 0 & 0 & 2 & 0 \\ 2 & 1 & 0 & 1 & 2 & 0 & 2 \\ \hline \frac{1}{2} & 0 & 0 & \frac{1}{2} & 0 & 0 & 0 \end{bmatrix}.$$

In this class are four minimal valence sequences: $\sigma_1 = [4, 3, 4, 6, 5, 6]$, $\sigma_2 = [6, 3, 6, 4, 5, 4]$, $\sigma_3 = [6, 3, 6, 8, 4, 8]$, and $\sigma_4 = [8, 3, 8, 6, 4, 6]$. If T_i is a tessellation with valence sequence σ_i for $i = 1, 2, 3, 4$, then numerical approximation of eigenvalues gives

$$\begin{aligned} \gamma(T_1) &\approx 8.0601, \\ \gamma(T_2) &\approx 8.4980, \\ \gamma(T_3) &\approx 12.6691, \text{ and} \\ \gamma(T_4) &\approx 12.8316. \end{aligned}$$

If T is a tessellation with valence sequence $\sigma \geq \sigma_i$, for some $i \in \{1, 2, 3, 4\}$, then $\gamma(T) \geq 8.0601$ by [1]Theorem 2.7. \square

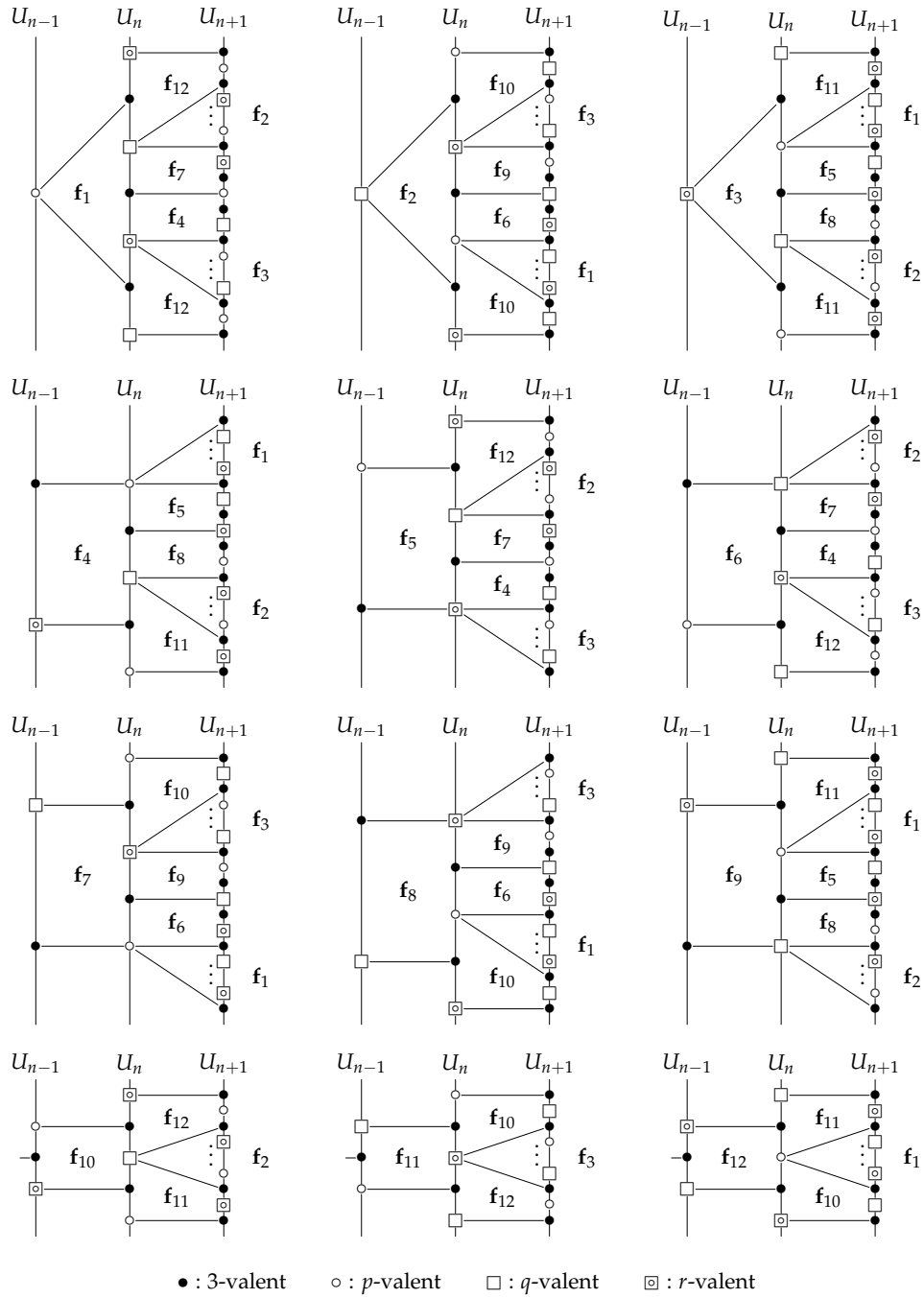


FIGURE 5.20. Offspring diagrams for a face-homogeneous tessellation with valence sequence $[3, p, 3, q, 3, r]$. See [Proposition 5.16](#).

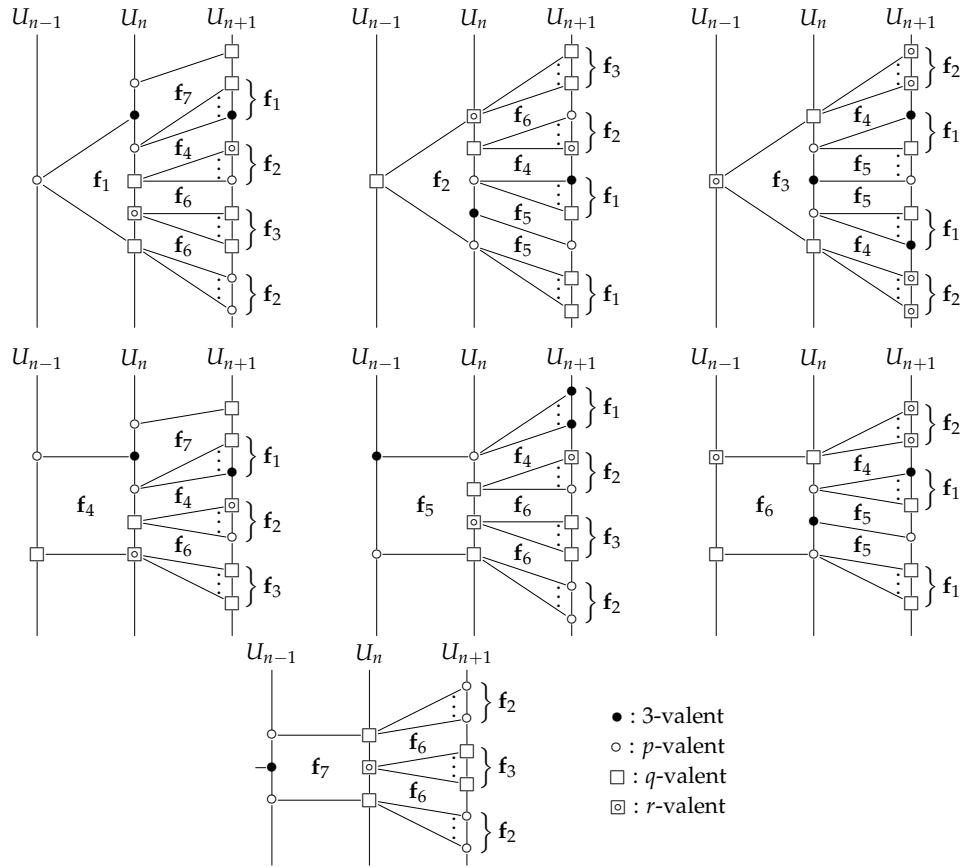


FIGURE 5.21. Offspring diagrams for a face-homogeneous tessellation with valence sequence $[p, 3, p, q, r]$.

REFERENCES

1. Stephen J. Graves and Mark E. Watkins, *Growth of face-homogeneous tessellations*, To appear in *Ars Mathematica Contemporanea* (2017).

DEPARTMENT OF MATHEMATICS, UNIVERSITY OF TEXAS AT TYLER, TYLER, TX 75799
 E-mail address: sgraves@uttyler.edu

DEPARTMENT OF MATHEMATICS, SYRACUSE UNIVERSITY, SYRACUSE, NY 13244-1150
 E-mail address: mewatkin@syr.edu